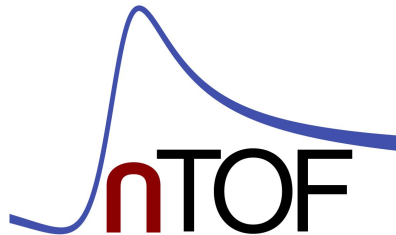


First measurement of the s-process branching $^{79}\text{Se}(n,\gamma)$

*V. Babiano¹, J. Balibrea-Correa¹, L. Caballero¹, F. Calviño², D. Cano-Ott³, A. Casanovas²,
N. Colonna⁴, S. Cristallo^{5,6}, C. Domingo-Pardo¹, R. Dressler⁷, E. González³, C. Guerrero^{8,9},
S. Heinitz⁷, U. Köster¹⁰, I. Ladarescu¹, C. Lederer-Woods¹¹, J. Lerendegui-Marco¹,
E. A. Mauger⁷, E. Mendoza³, A. Mengoni^{12,13}, I. Moench, T. Rauscher^{14,15}, N. Sosnin¹¹, D. Schumann⁷,
A. Tarifeño-Saldivia², and the n_TOF Collaboration*



65th Meeting of the INTC, 3rd November 2020



European
Research
Council



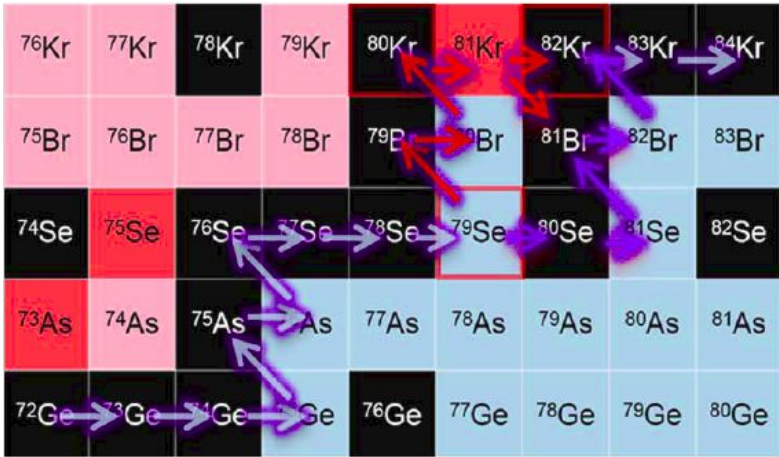
VNIVERSITAT
ID VALÈNCIA



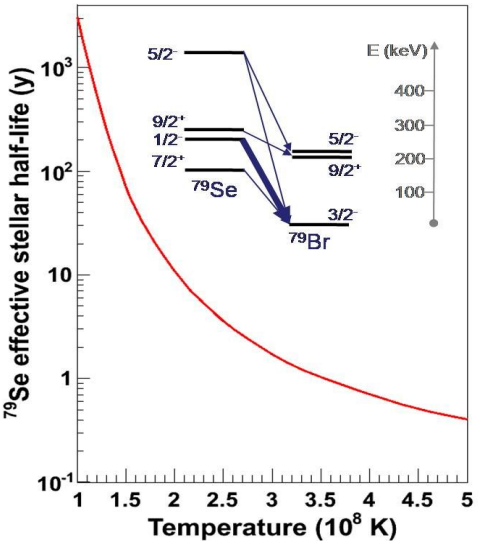
CSIC

CONSEJO SUPERIOR DE INVESTIGACIONES CIENTÍFICAS

- Motivation
- Status of the evaluations and MACS values
- Sample preparation
- Detection systems and experimental areas: combined proposal
- Counting rate estimates, feasibility and expected results
- Astrophysical impact: constraining the MACS
- Summary



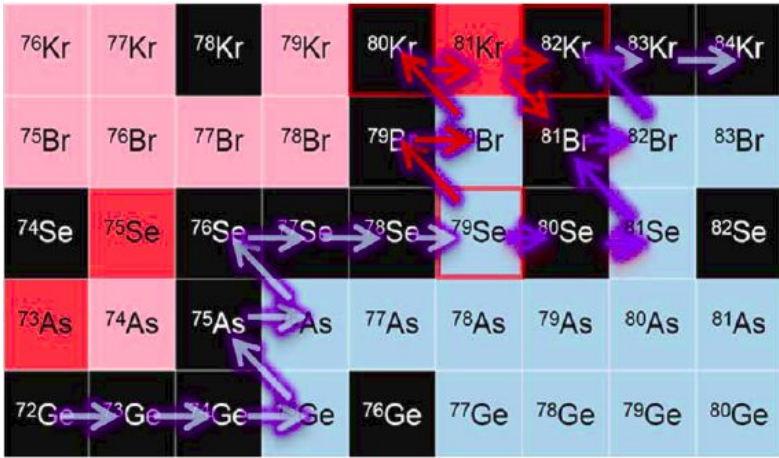
$^{79}\text{Se}(n,\gamma)$: suited for thermal conditions stellar medium→ strong thermal dependence of the beta decay rate



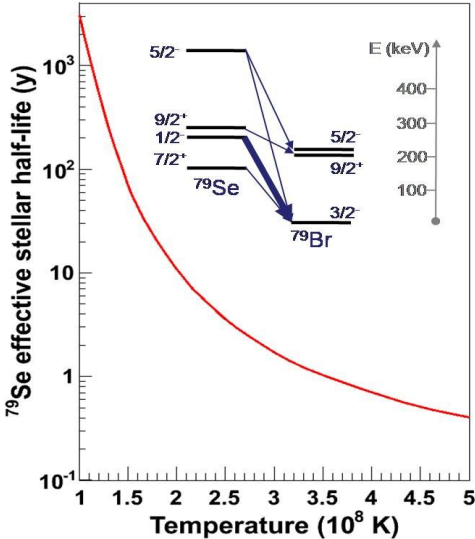
Branching at ^{79}Se : direct impact on the s-only $^{80}\text{Kr}/^{82}\text{Kr}$ abundance ratio, well characterized in presolar grains

→ One of the **21 key s-nuclei** listed in: Kaeppler, *Rev. Mod. Phys* 83, 157 (2011)

→ Listed as **1st-level priority** (two times) in the sensitivity study: Cescutti et al., *MNRS* 478 (2018)



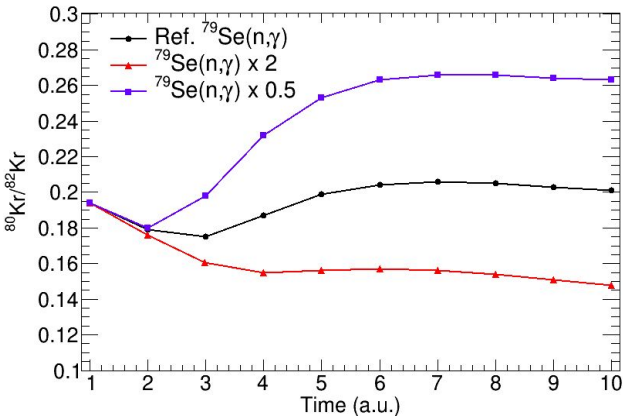
$^{79}\text{Se}(n,\gamma)$: suited for
thermal conditions
stellar medium→
strong thermal
dependence of the
beta decay rate



Branching at ^{79}Se : direct impact on the s-only $^{80}\text{Kr}/^{82}\text{Kr}$ abundance ratio, well characterized in presolar grains

→ One of the **21 key s-nuclei** listed in: *Kaeppler, Rev. Mod. Phys* 83, 157 (2011)

→ Listed as **1st-level priority** (two times) in the sensitivity study: *Cescutti et al., MNRS* 478 (2018)



Sensitivity calculations
(S. Cristallo, FUN's code):
Current unc. ~ 2 in $^{79}\text{Se}(n,\gamma)$ →
 $\pm 30\%$ $^{80}\text{Kr}/^{82}\text{Kr}$ ratio →
High impact of $^{79}\text{Se}(n,\gamma)$

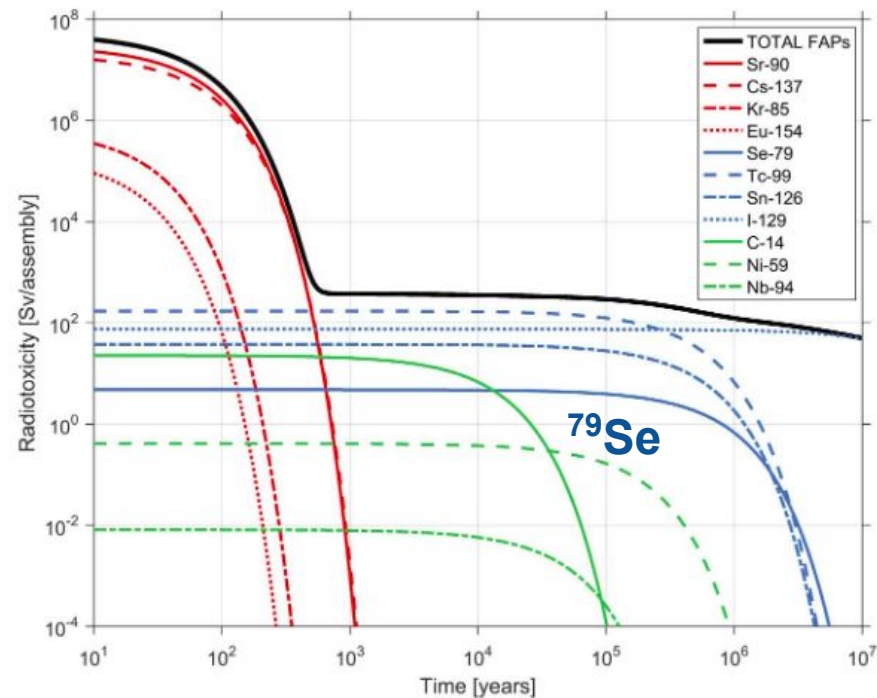
Motivation (II): nuclear waste

In terms of **long-term radiotoxicity**, however, **long-lived** fission products like Tc-99 and I-129, together with **Se-79** and Cs-135, are the main contributors in addition to the above-mentioned actinides, and dominate the potential hazard in the case of HLW not containing actinides. Figure 13.2 compares

Handbook of advanced radioactive waste conditioning technologies

^{79}Se is one of the main contributors to the long-term radiotoxicity among fission products

$^{79}\text{Se}(n,\gamma)$: relevant for nuclear waste disposal and transmutation



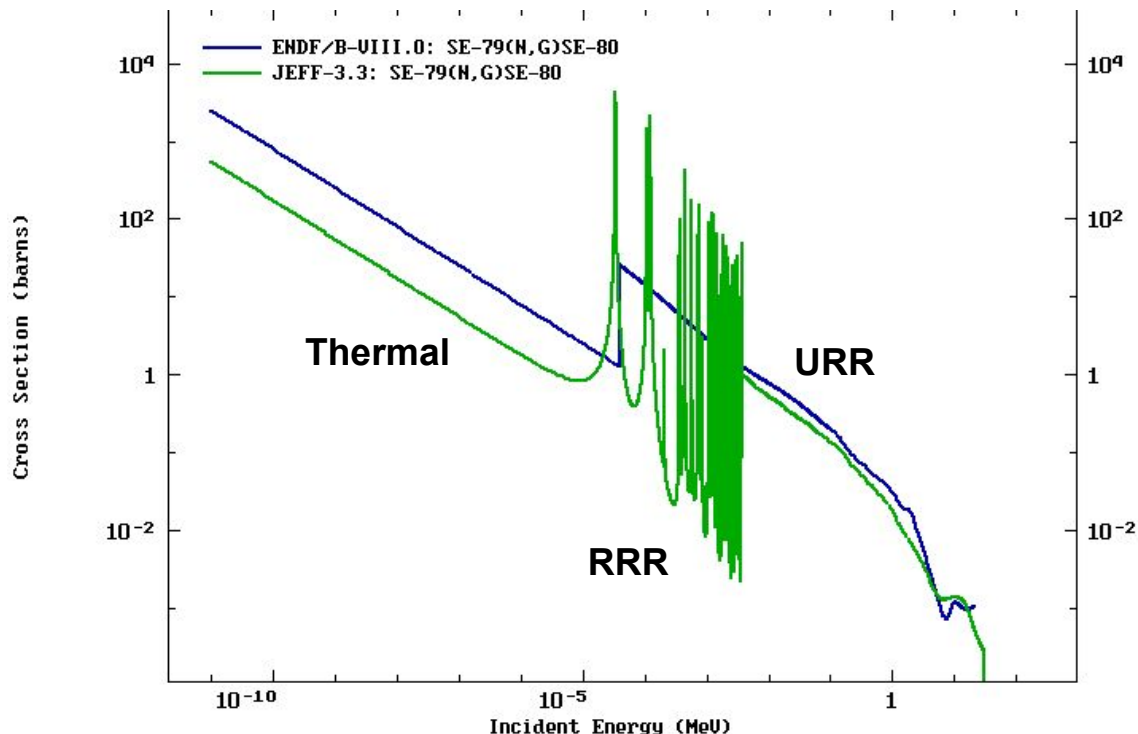
Status of the $^{79}\text{Se}(n,\gamma)$ data

EXPERIMENTAL DATA

- No data available in EXFOR
- First measurement of this cross section
- MACS via activation not possible (^{80}Se stable)

EVALUATIONS & MACS

- **JEFF-3.3:** TALYS Calculation \rightarrow Provides Resonance parameters
- **ENDF/B- VIII.0:** Systematics for the thermal point + $1/v$ dependence & OM for the URR



Status of the $^{79}\text{Se}(n,\gamma)$ data

EXPERIMENTAL DATA

- No data available in EXFOR
- First measurement of this cross section
- MACS via activation not possible (^{80}Se stable)

EVALUATIONS & MACS

- **JEFF-3.3:** TALYS Calculation → Provides Resonance parameters
- **ENDF/B- VIII.0:** Systematics for the thermal point + $1/v$ dependence & OM for the URR
- **KADoNiS:** Theoretical calculations of the MACS → factor >2 deviation

▼ Recommended MACS30 (Maxwellian Averaged Cross Section @ 30keV)

$$^{79}\text{Se} (n,\gamma) ^{80}\text{Se}$$

Total MACS at 30keV: **263 ± 46*** mb

Cross sections do not include stellar enhancement factors!
* only theoretical data available

▼ History

Version	Total MACS [mb]	Partial to gs [mb]	Partial to isomer [mb]
0.0	263 ± 46*	-	-

(Version 0.0 corresponds to Bao et al.)

▼ Comment

Last review: 1999

▼ List of all available values

original	renorm.	year	type	Comment	Ref
233		2000	t		RaT99
218 ± 50		1982	t		Ref82
514		1981	t		Har81
260		1978	t		WFH78
572		2002	t	MOST 2002	Gor02
415		2005	t	MOST 2005	Gor05

Status of the $^{79}\text{Se}(n,\gamma)$ data

EXPERIMENTAL DATA

- No data available in EXFOR
- First measurement of this cross section
- MACS via activation not possible (^{80}Se stable)

EVALUATIONS & MACS

- **JEFF-3.3:** TALYS Calculation → Provides Resonance parameters
- **ENDF/B- VIII.0:** Systematics for the thermal point + $1/v$ dependence & OM for the URR
- **KADoNiS:** Theoretical calculations of the MACS → factor >2 deviation

▼ Recommended MACS30 (Maxwellian Averaged Cross Section @ 30keV)

$$^{79}\text{Se} (n,\gamma) ^{80}\text{Se}$$

Total MACS at 30keV: **263 ± 46*** mb

Cross sections do not include stellar enhancement factors!
* only theoretical data available

▼ History

Version	Total MACS [mb]	Partial to gs [mb]	Partial to isomer [mb]
0.0	263 ± 46*	-	-

(Version 0.0 corresponds to Bao et al.)

▼ Comment

Last review: 1999

▼ List of all available values

original	renorm.	year	type	Comment	Ref
233		2000	t		RaT99
218 ± 50		1982	t		Ref82
514		1981	t		Har81
260		1978	t		WFH78
572		2002	t	MOST 2002	Gor02
415		2005	t	MOST 2005	Gor05

Despite the relevance
NO DATA → HIGH IMPACT

Low mass + radioactive + no
activation : n_TOF unique





NEUTRONS
FOR SCIENCE

$^{78}\text{Se}(n,\gamma)$ @ ILL

0.5 mm thick 6N Al casing (laser-welded)

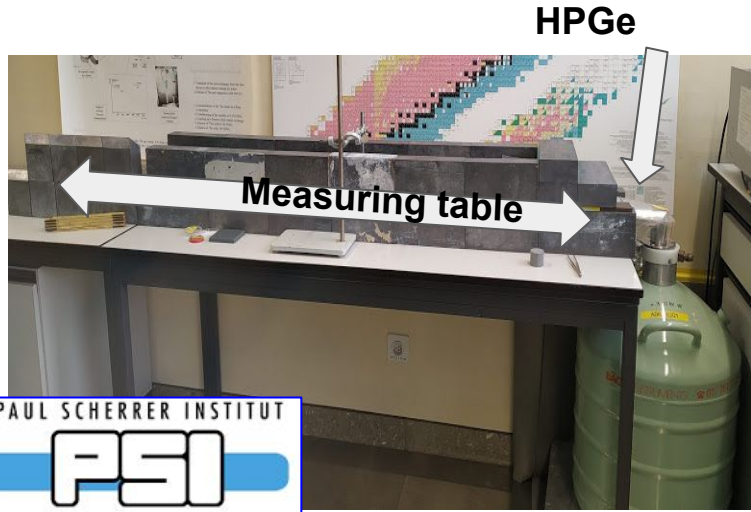


PbSe alloy to avoid low melting point of pure Se



Sample properties

Isotope	Mass (g)	natoms_cm2
Se-78	0.77	4.01E+21
Se-79	0.003	1.53E+19
Pb-208	2.84	5.51E+21
Al-27	1.0244	5.90E+21



PAUL SCHERRER INSTITUT


Gamma activity characterization @ PSI

Isotope	Activity (Bq) (Nov. 2021)	C.Rate C6D6 (Ethr = 250 keV)
Se-75	5.66E+06	2.82E+03
Ag-110m	2.04E+05	4.97E+03
Zn-65	2.33E+05	1.25E+03
Co-60	1.40E+06	2.75E+04
TOTAL	7.50E+06	3.65E+04

$^{79}\text{Se}(n,\gamma)$: Experimental area

- Small mass (3 mg ^{79}Se + 2.84 g Pb + 0.77 g ^{78}Se) + Radioactive sample → **EAR2's physics case**
- Measurement at EAR2: thermal cross-section
- **Measurement at EAR2** seems the best idea to achieve **good statistics in the RRR, thermal and optimize capture/activity.**
- EAR1 has better energy resolution: ideal to disentangle ^{78}Se and ^{79}Se resonances
- $^{78}\text{Se}(n,\gamma)$ at EAR1 → Measure ^{78}Se + ^{79}Se under same experimental conditions
- **Measurement at EAR1 required to keep systematic uncertainties under control in the RRR**

$^{79}\text{Se}(n,\gamma)$: Experimental area

- Small mass (3 mg ^{79}Se + 2.84 g Pb + 0.77 g ^{78}Se) + Radioactive sample → **EAR2's physics case**
- Measurement at EAR2: thermal cross-section
- **Measurement at EAR2** seems the best idea to achieve **good statistics in the RRR, thermal and optimize capture/activity.**
- EAR1 has better energy resolution: ideal to disentangle ^{78}Se and ^{79}Se resonances
- $^{78}\text{Se}(n,\gamma)$ at EAR1 → Measure ^{78}Se + ^{79}Se under same experimental conditions
- **Measurement at EAR1 required to keep systematic uncertainties under control in the RRR**

$^{79}\text{Se}(n,\gamma)$: Detection system

- Challenge: contribution of neutron scattering in Pb, ^{78}Se and ^{79}Se → **Enhanced sensitivity with i-TED**
- i-TED has high energy resolution → extract spectroscopic information of the unknown $^{79}\text{Se}(n,\gamma)$ cascade
- i-TED allows selections in energy deposition → understanding of backgrounds & reduce systematics
- **i-TED** has shown **good performance in EAR1** but probably limited by CR (500 kHz) in EAR2
- **C_6D_6 TEDs are better suited for EAR2**

$^{79}\text{Se}(n,\gamma)$: Experimental area

- Small mass (3 mg ^{79}Se + 2.84 g Pb + 0.77 g ^{78}Se) + Radioactive sample → **EAR2's physics case**
- Measurement at EAR2: thermal cross-section
- **Measurement at EAR2** seems the best idea to achieve **good statistics in the RRR, thermal and optimize capture/activity.**
- EAR1 has better energy resolution: ideal to disentangle ^{78}Se and ^{79}Se resonances
- $^{78}\text{Se}(n,\gamma)$ at EAR1 → Measure ^{78}Se + ^{79}Se under same experimental conditions
- **Measurement at EAR1 required to keep systematic uncertainties under control in the RRR**

$^{79}\text{Se}(n,\gamma)$: Detection system

- Challenge: contribution of neutron scattering in Pb, ^{78}Se and ^{79}Se → **Enhanced sensitivity with i-TED**
- i-TED has high energy resolution → extract spectroscopic information of the unknown $^{79}\text{Se}(n,\gamma)$ cascade
- i-TED allows selections in energy deposition → understanding of backgrounds & reduce systematics
- **i-TED** has shown **good performance in EAR1** but probably limited by CR (500 kHz) in EAR2
- **C_6D_6 TEDs are better suited for EAR2**

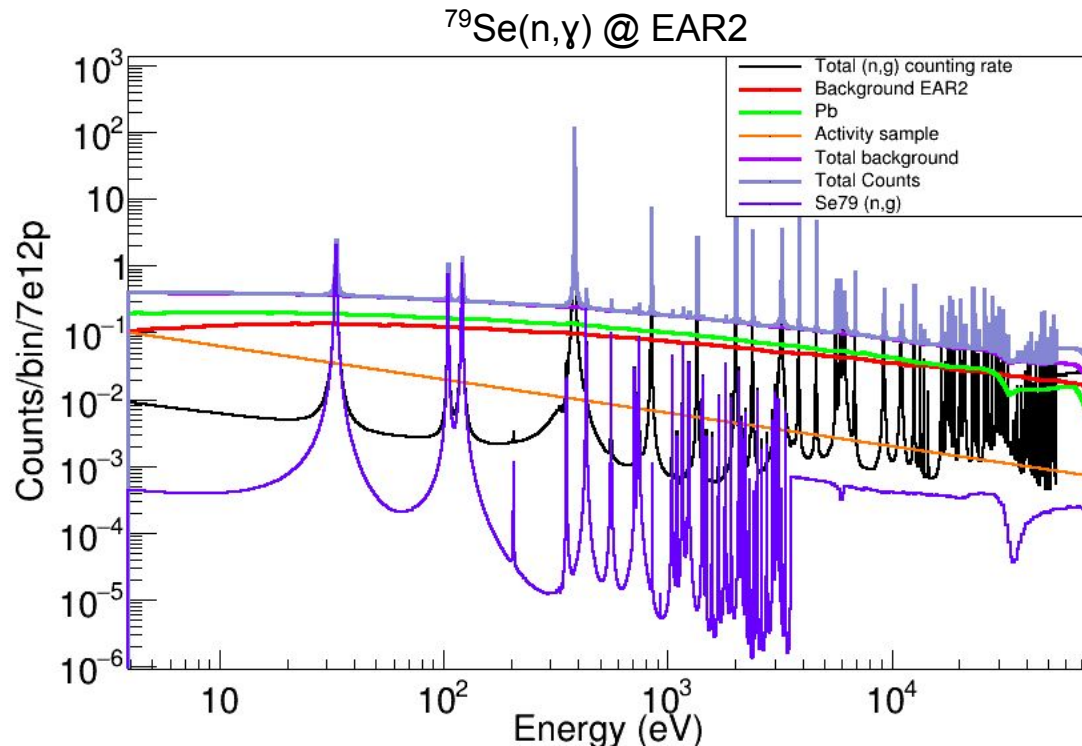
Combined proposal:
i-TED @ EAR1 & C_6D_6 @ EAR2

Similar previous measurements:

- $^{171}\text{Tm}(n,\gamma)$ @ EAR1 and EAR2
- $^{244/246}\text{Cm}(n,\gamma)$ @ EAR1 (TAC) and EAR2(/ C_6D_6)

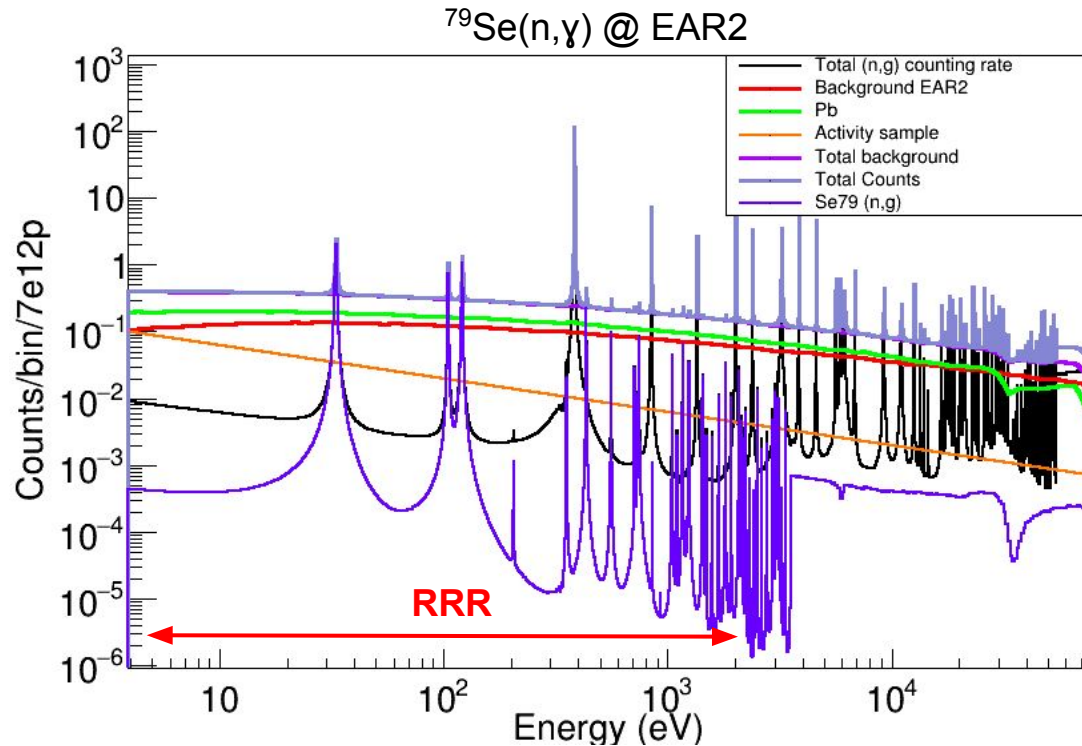
$^{79}\text{Se}(n,\gamma)$: counting rate estimates

- **Sample:** ^{78}Se and $^{79}\text{Se}(n,\gamma)$ cross sections from JEFF-3.3.
- Evaluated neutron Flux EAR1/2, BIF & RF from MC simulations
- (n,γ) efficiency from MC assuming $^{197}\text{Au}(n,\gamma)$ cascade
- **Activity** counting rate calculated with MC simulations of the sample contaminants.
- **Beam background** and **Lead** experimental data with C_6D_6
- **i-TED:** Scaled assuming than $(n,\gamma)/\text{background}$ can improve a factor 5 (*).



$^{79}\text{Se}(n,\gamma)$: counting rate estimates

- **Sample:** ^{78}Se and $^{79}\text{Se}(n,\gamma)$ cross sections from JEFF-3.3.
- Evaluated neutron Flux EAR1/2, BIF & RF from MC simulations
- (n,γ) efficiency from MC assuming $^{197}\text{Au}(n,\gamma)$ cascade
- **Activity** counting rate calculated with MC simulations of the sample contaminants.
- **Beam background** and **Lead** experimental data with C_6D_6
- **i-TED:** Scaled assuming than $(n,\gamma)/\text{background}$ can improve a factor 5 (*).



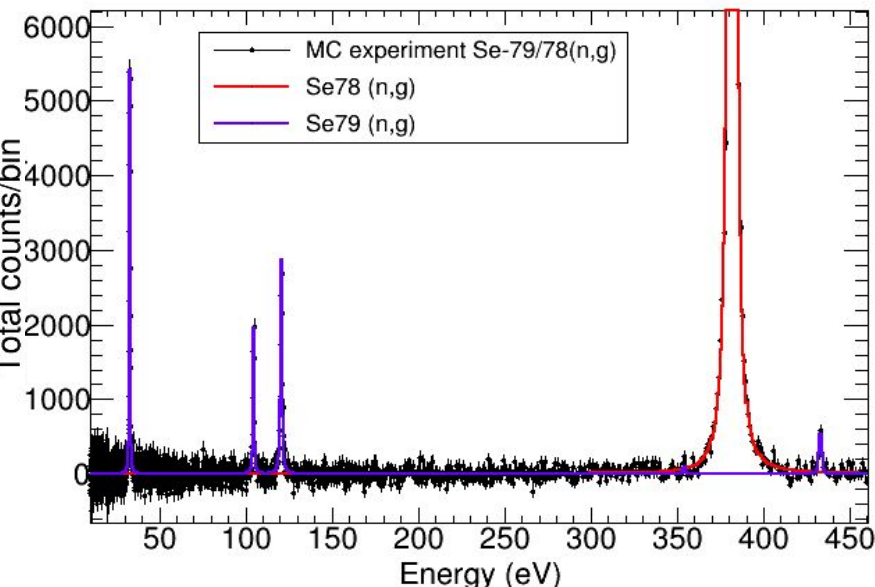
$^{79}\text{Se}(n,\gamma)$ measurement **focused in the RRR** in the 1eV - 2 keV range. Provide a **constraint of the MACS** at the relevant stellar temperatures

$^{79}\text{Se}(n,\gamma)$: feasibility and expected results

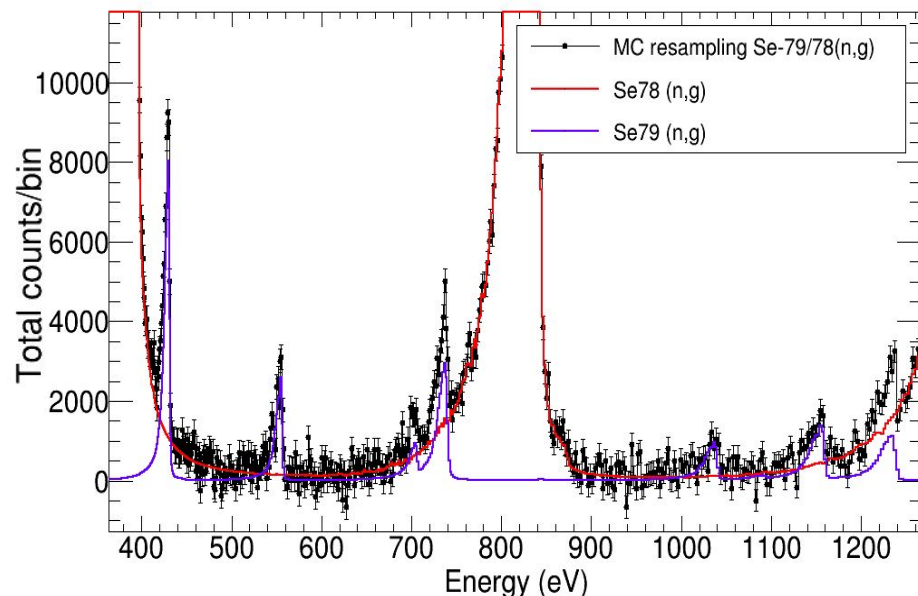
Challenging and relevant
measurement:
Detailed feasibility study

1) Realistic statistical uncertainties: MC resampling method

Assigned No. protons to the sample ($^{79}\text{Se} + ^{78}\text{Se} + ^{208}\text{Pb} + ^{27}\text{Al}$) and the dummy ($^{208}\text{Pb} + ^{27}\text{Al}$) measurements \rightarrow Realistic uncertainties in background subtraction



EAR1: Main $^{79}\text{Se}(n,\gamma)$ resonances with high resolution
 \rightarrow Accurate normalization and ^{78}Se contribution assessment for the measurement at EAR2.



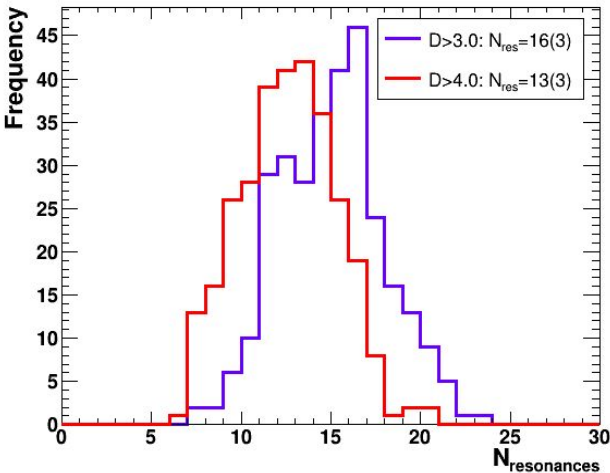
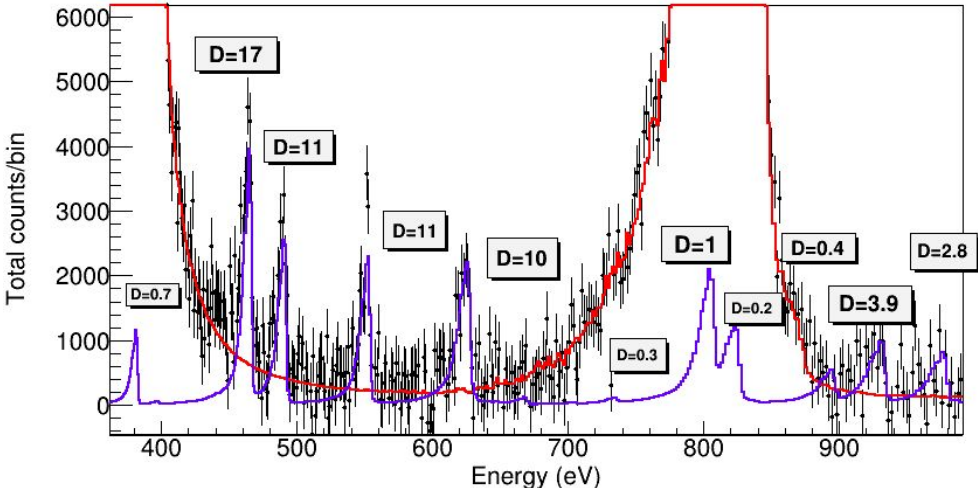
EAR2: Analyze $^{79}\text{Se}(n,\gamma)$ resonances beyond 1 keV.
Results are conservative results since we have used the current RF \rightarrow Improved with Target #3

Challenging and relevant measurement:
Detailed feasibility study

2) Number Observable resonances: Detection limit study

Uncertain resonance energies: 300 sets of ⁷⁹Se(n,g) resonances to study the expected number of observable resonances above a detection threshold for **D**

$$D = (C_{exp} - C_{78Se}) / Unc_{C_{exp}-C_{78Se}}$$



Expected: 9-19 resonances

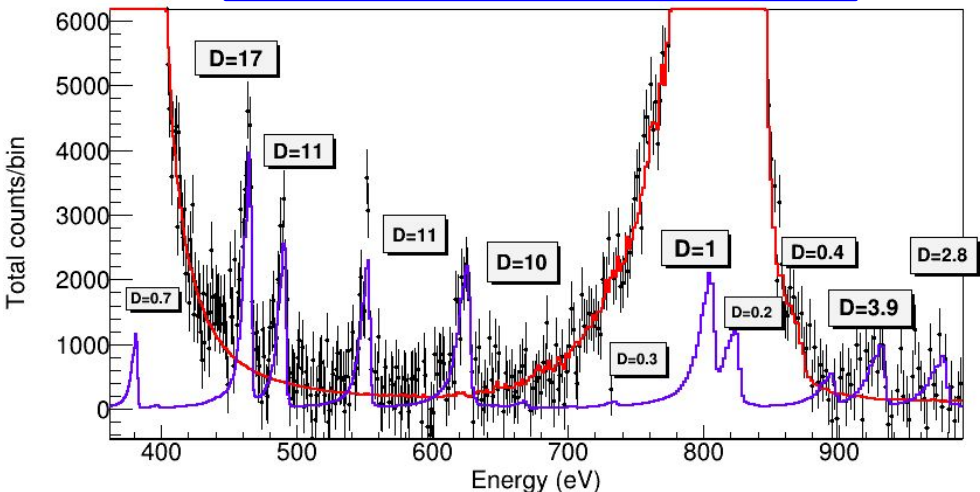
	Distribution Protons (x1e18)	
Threshold	S:1.5 + D: 0.5	S:1.0 + D: 1.0
D>3	15.1(29)	16.0(29)
D>4	12.4(25)	13.3(28)

Challenging and relevant
measurement:
Detailed feasibility study

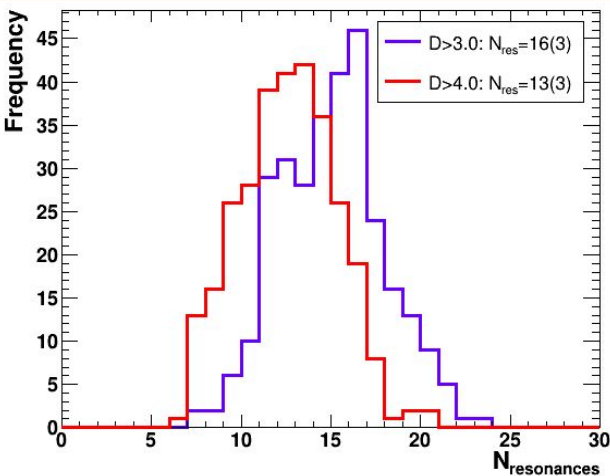
2) **Number Observable resonances:** Detection limit study

Uncertain resonance energies: 300 sets of $^{79}\text{Se}(n,\gamma)$ resonances to study the expected number of observable resonances above a detection threshold for **D**

$$D = (C_{\text{exp}} - C_{78\text{Se}}) / \text{Unc}_{C_{\text{exp}} - C_{78\text{Se}}}$$



Final goal: Experimental constraint to the MACS
Method: Hauser-Feshbach calculation based on
average resonance parameters



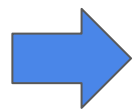
Expected: 9-19 resonances

Min. 10-15 resonances for meaningful
statistical analysis →
Justifies Proton request

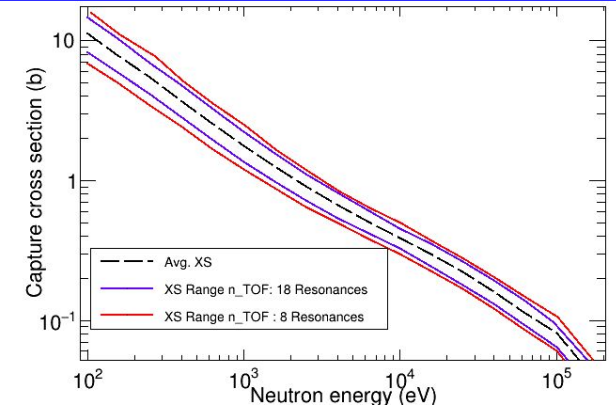
Experimental RRR: (s-wave Avg. Par.)

$\langle D_0 \rangle$	56.8	eV	LVD calculations
$S_0 \times 10^4$	0.93		OMP calculations
Γ_{y0}	78.2 ± 7.8	meV	statistical model calculations
$\langle D_1 \rangle$	30.1	eV	LVD calculations
$S_1 \times 10^4$	1.60		OMP calculations
Γ_{y1}	82.7 ± 8.3	meV	statistical model calculations

Uncertainty
 D_0, S_0
 $\sim \sqrt{N_{\text{res}}}$



SAMMY-FITACS: XS in the URR

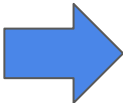


+ P-wave (systematics, ...)

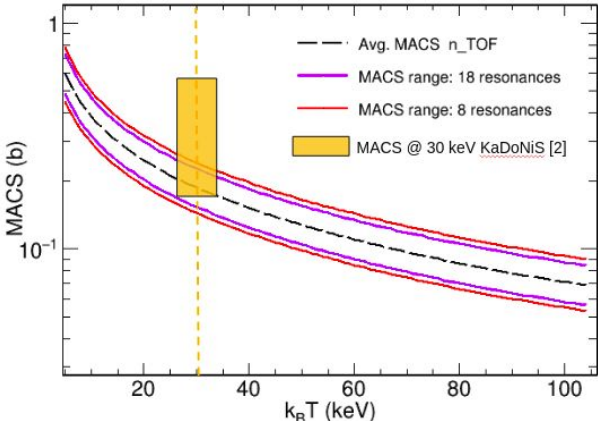
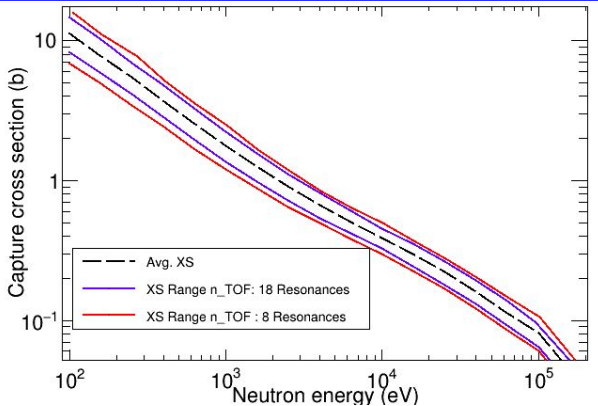
Experimental RRR: (s-wave Avg. Par.)

$\langle D_0 \rangle$	56.8	eV	LVD calculations
$S_0 \times 10^4$	0.93		OMP calculations
$\Gamma_{\gamma 0}$	78.2 ± 7.8	meV	statistical model calculations
$\langle D_1 \rangle$	30.1	eV	LVD calculations
$S_1 \times 10^4$	1.60		OMP calculations
$\Gamma_{\gamma 1}$	82.7 ± 8.3	meV	statistical model calculations

Uncertainty
 D_0, S_0
 $\sim \text{sqrt}(N_{\text{res}})$



SAMMY-FITACS: XS in the URR



+ P-wave (systematics, ...)

- MACS @30 keV: 20-26% unc (from avg. par.)
- Stellar enhancement Factor = 1 at 8, 30 keV
- Direct stringent constraint for the thermal conditions of AGB and MSs

MACS @ different kT:
 Constrain **theor.**
calculations in KaDoNiS
 (@ 30 keV)

Summary and proton request

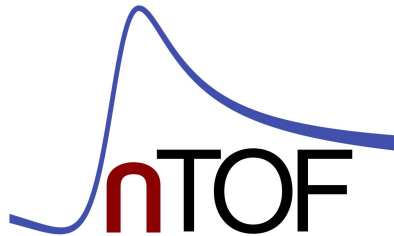
- **First ever** experimental capture data on $^{79}\text{Se}(n,\gamma)$, a key astrophysical s-process branching point.
- Challenging and high-impact experiment: limited mass + high activity \rightarrow **n_TOF unique** case.
- Combination of **EAR1** and **EAR2** to ensure low systematic uncertainties and high statistics.
- **i-TED**: novel detection system with **enhanced sensitivity** developed for this measurement (HYMNS ERC)
- **Relevance** of this measurement has motivated a **detailed and conservative risk-assessment study**.
- **Feasibility** of the proposed experiment and **expected results in the RRR** (9 - 19 resonances).
- Astrophysical impact: FITACS \rightarrow **MACS @ 30 keV (20-26% unc.)** \rightarrow **replace theoretical estimates by first experimental constraints to the MACS**.
- First **empirical constrain to thermal conditions** in AGB and MSs.

SAMPLE	EAR1: i-TED	EAR2: C ₆ D ₆
$^{79}\text{Se}+\text{Se-78}$ (PbSe sample)	$2,5 \cdot 10^{18}$ p	$1,5 \cdot 10^{18}$ p
Dummy (Pb + Al)	$5 \cdot 10^{17}$ p	$5 \cdot 10^{17}$ p
Au, C, Pb, Filters	$\sim 5 \cdot 10^{17}$ p (*)	$\sim 5 \cdot 10^{17}$ p (*)
TOTAL	$3,5 \cdot 10^{18}$ p	$2,5 \cdot 10^{18}$ p

BACK-UP SLIDES

$^{79}\text{Se}(n,\gamma)$ measurement proposal: Appendices

*V. Babiano¹, J. Balibrea-Correa¹, L. Caballero¹, F. Calviño², D. Cano-Ott³, A. Casanovas²,
N. Colonna⁴, S. Cristallo^{5,6}, C. Domingo-Pardo¹, R. Dressler⁷, E. González³, C. Guerrero^{8,9},
S. Heinitz⁷, U. Köster¹⁰, I. Ladarescu¹, C. Lederer-Woods¹¹, J. Lerendegui-Marco¹,
E. A. Mauger⁷, E. Mendoza³, A. Mengoni^{12,13}, T. Rauscher^{14,15}, N. Sosnin¹¹, D. Schumann⁷,
A. Tarifeño-Saldivia², and the n_TOF Collaboration*



n_TOF Collaboration Board Meeting, 11th September 2020



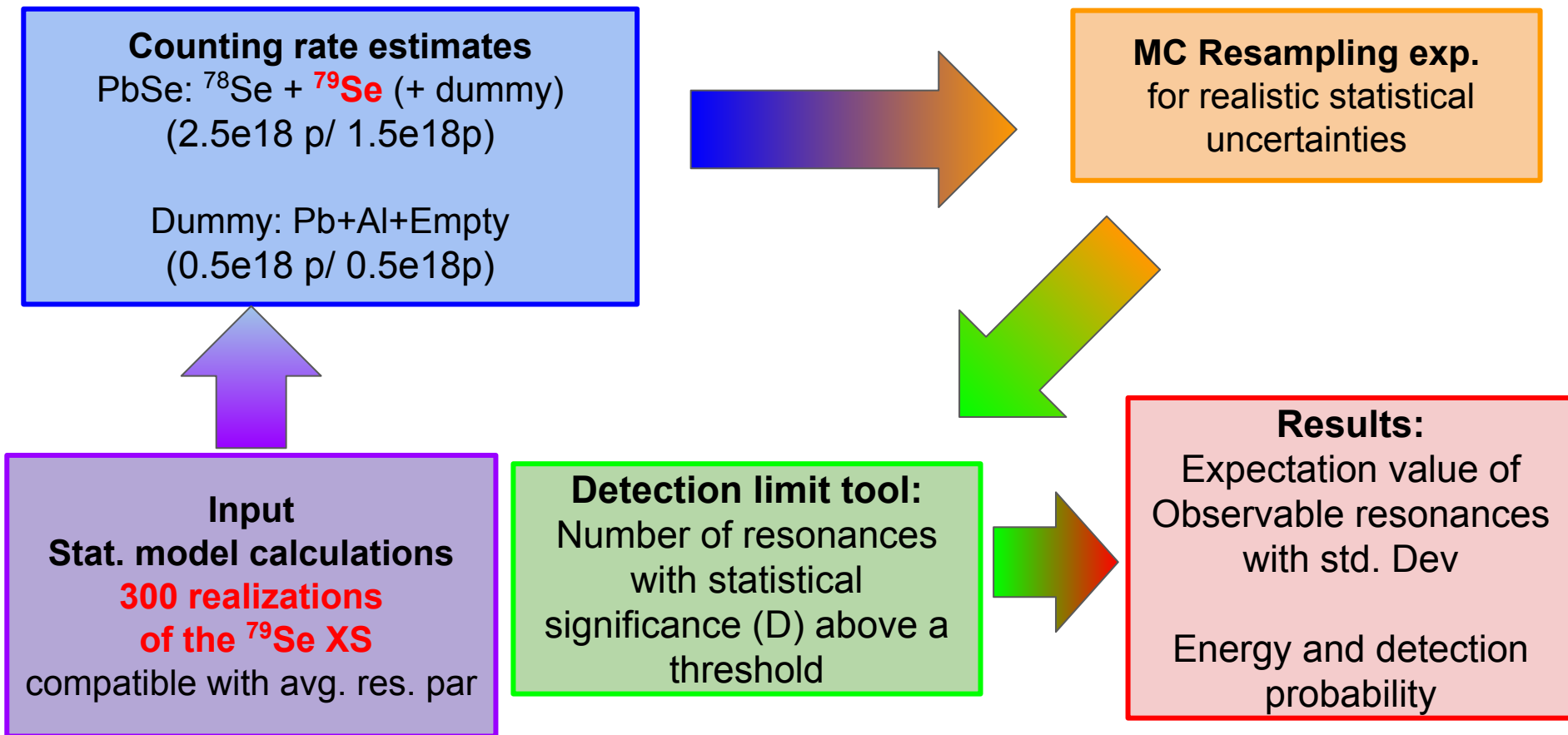
UNIVERSITAT
DE VALÈNCIA



CSIC

CONSEJO SUPERIOR DE INVESTIGACIONES CIENTÍFICAS

App. 1: Detection Limit



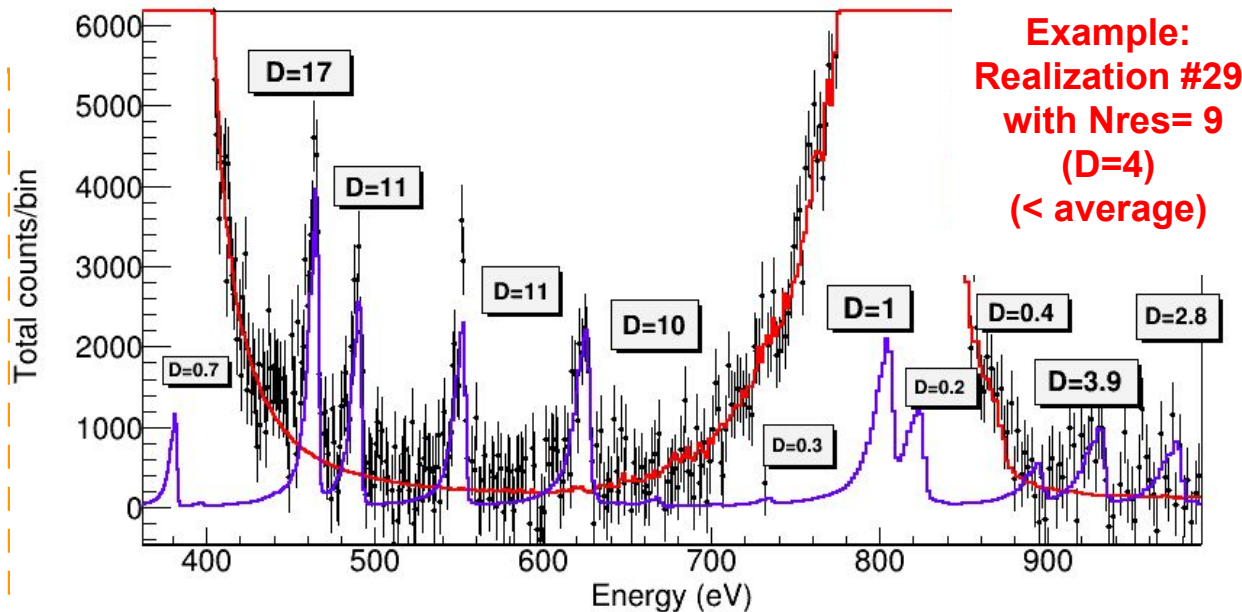
App. 1: Detection Limit

Statistical significance D , calculated for each resonance as $D = (C_{\text{exp}} - C_{78\text{Se}}) / \text{Unc}(C_{\text{exp}} - C_{78\text{Se}})$

Impact of systematics

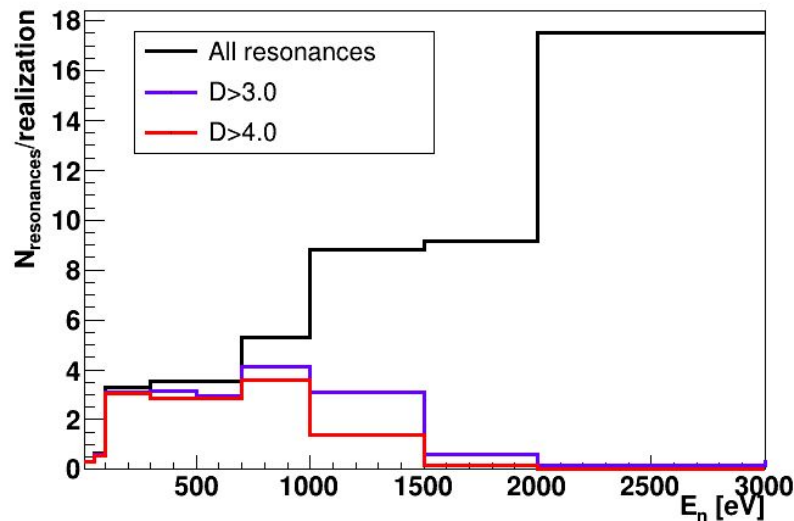
If no systematics are added to the underlying Se-78 contribution, the statistical discrimination does not reject all the overlapping resonances but these are very sensitive to a small (and real) systematic unc. in the level of Se-78 (in the real exp is the unc in the SAMMY Fit)

Adding a conservative 10% rejects all the overlapping while does not affect significantly the others



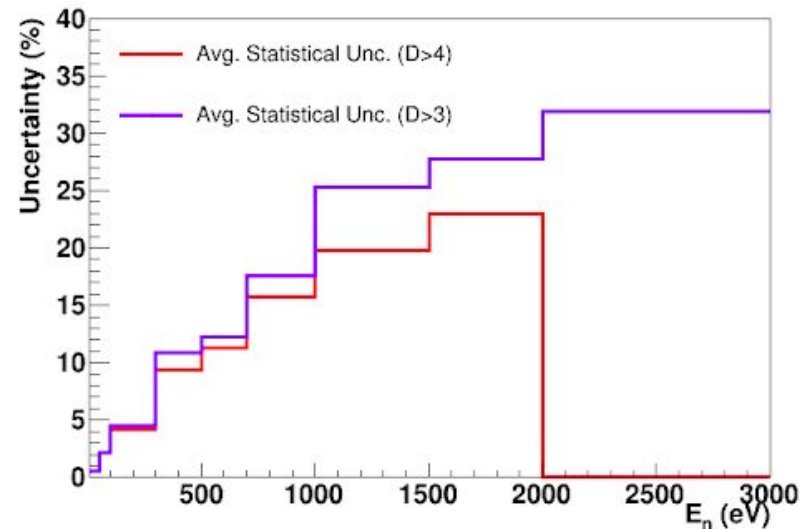
This example validates our choice of threshold:
The resonances with $D > 4$ are clearly detectable + analyzable,
the ones with $D = 3-4$ are detectable

App. 1: Detection Limit



Observed Resonances:

- high probability up to 1 keV.
- >1 keV we expect to observe resonances up to at least 1.5 keV
- with smaller probability up to 2 keV.



Statistical uncertainty:

- <15 % below 1 keV
- Maximum stat. unc: 30 %

App. 2: Constrain Thermal XS

Calculation at thermal

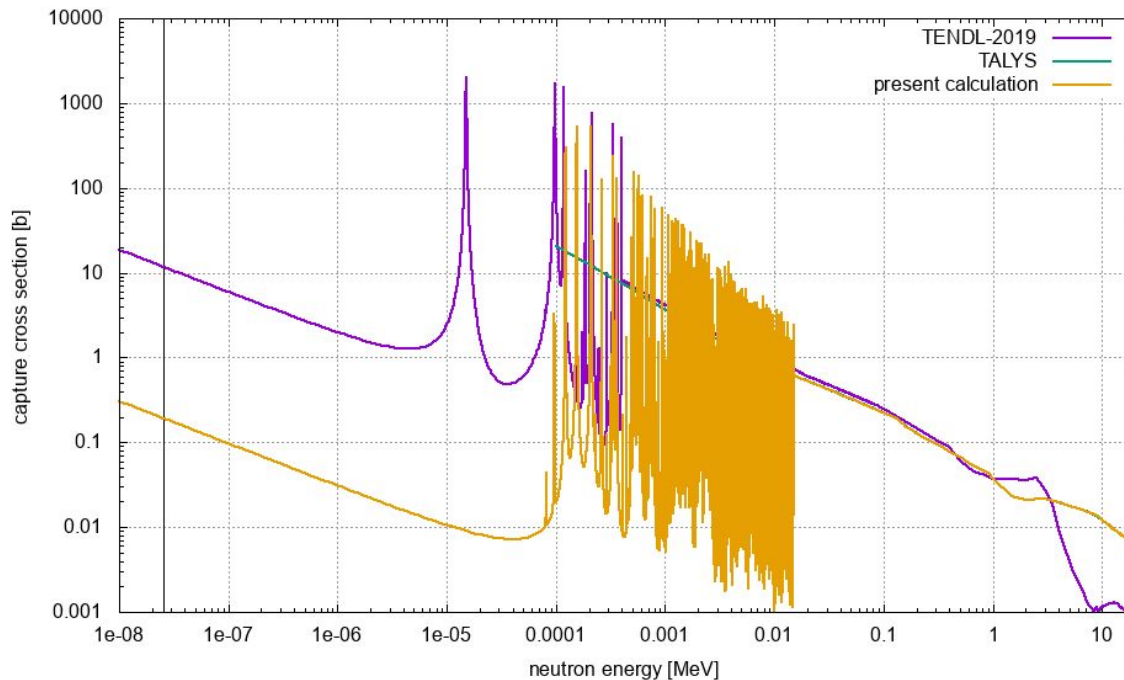
shows remarkable differences
with evaluations

- Calculation: $P(\sigma_{th} < 1b) = 80\%$ + $P(\sigma_{th} < 10b) = 98\%$
- $\sigma_{th} = 50b$ In ENDF/B-VIII.0
 $\sigma_{th} = 11.8b$ in TENDL-2019

Two scenarios:

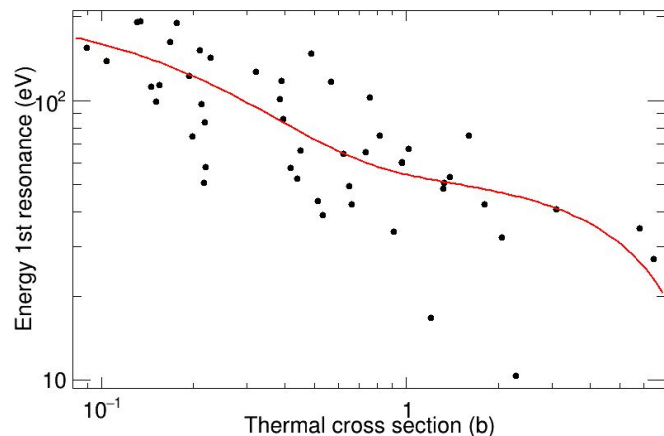
- Thermal XS follows systematics \rightarrow Measurable
- Much smaller \rightarrow Lower limit constrained from RRR

Se-79 neutron capture, simulated resonance set: 1

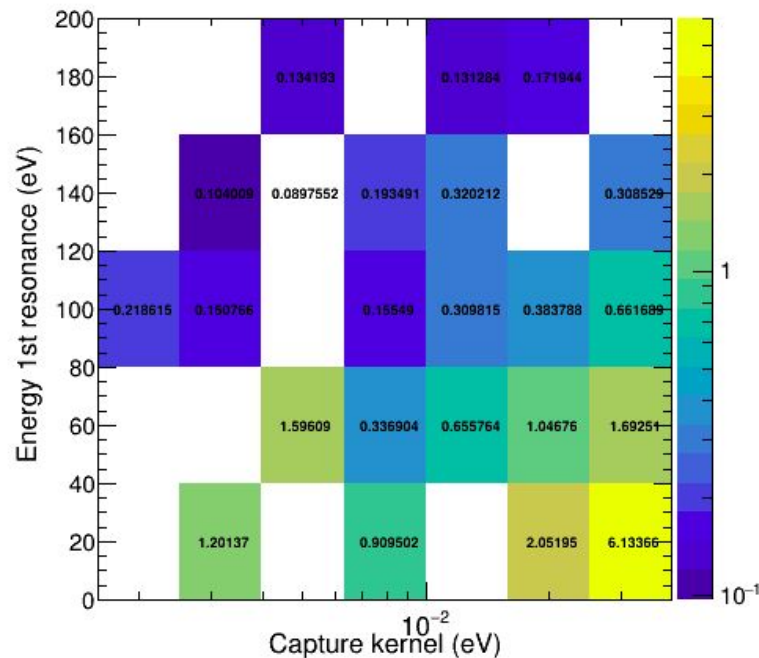


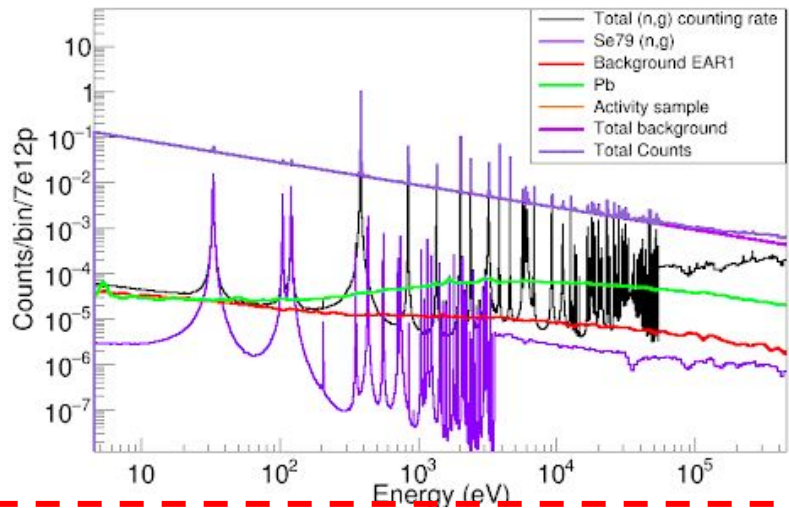
App. 2: Constrain Thermal XS

Much smaller XS \rightarrow Lower limit constrained from RRR \rightarrow First (few) s-wave resonance(s)



Analytical expression to calculate thermal (contrib. Of resonance tails) from s-wave resonance parameters





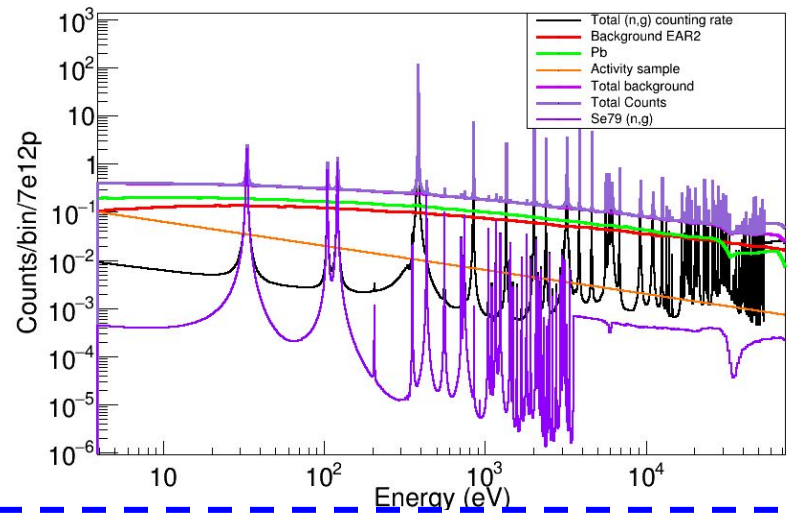
EAR1:

Activity dominates background but fit $1/v$ and subtract.

i-TED expected reduction beam-background up to a factor 5 \rightarrow systematics under control

Empty and **Lead** from experimental C6D6 data.

i-TED: Scaled assuming than $(n,\gamma)/\text{background}$ can improve a factor 5(*).



EAR2:

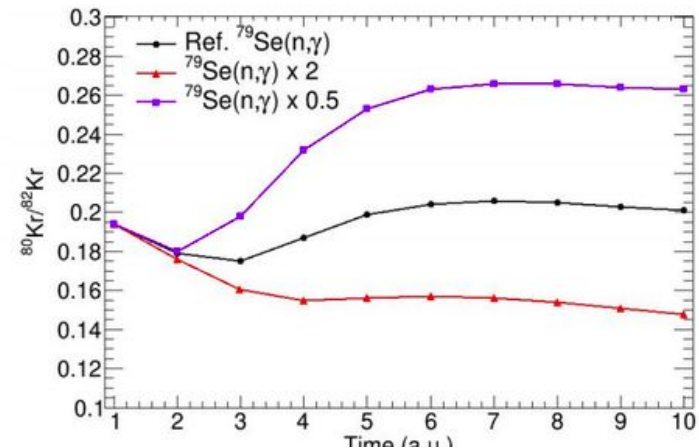
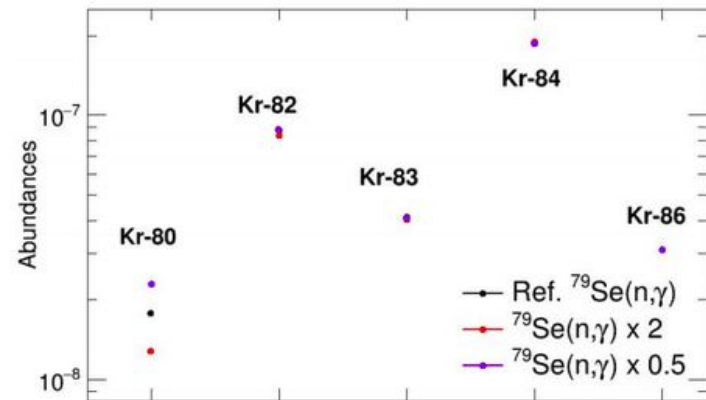
Activity not an issue due to the high instantaneous flux

Capture to background ratio good for **RRR** and thermal. URR very challenging

Activity counting rate via MC simulations of the sample contaminants.

App. 4: Impact of $^{79}\text{Se}(n,g)$ in $^{82}\text{Kr}/^{80}\text{Kr}$

- Sensitivity calculations with the FUNs evolutionary code used in the FRUITY database.
 - These calculations determine the sensitivity of the production of the Kr isotopes induced by variations of the ^{79}Se neutron capture cross section.
 - Reference XS of KaDonis (Bao et al.)
 - Impact of increasing or reducing the cross section in a factor 2 (dispersion in the theoretical MACS).
- Stellar yields of ^{80}Kr vary in $\pm 30\%$ with x2 in $^{79}\text{Se}(n,g)$
 - ^{82}Kr (remaining Kr isotopes) almost insensitive to the branching at ^{79}Se (all the neutron fluence passes through ^{82}Kr)
 - $\pm 30\%$ variation is also found for the $^{80}\text{Kr}/^{82}\text{Kr}$ ratio (the quantity measured in presolar grains)



Feasibility study: a conservative approach

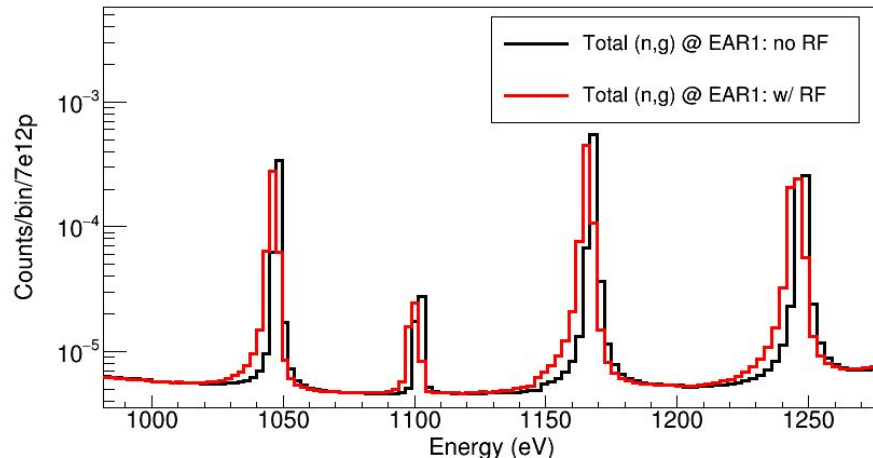
CONSERVATIVE ESTIMATION: EXPECTED IMPROVEMENTS

RF: Impact in EAR2 (resonance broadening) is already big in the ~100 eV range and a clear improvement is expected with the new spallation target.

Capture/background ratio: PHWT Technique (applied for both C6D6 and i-TED) usually enhances the (n,g) detection sensibility with respect to the background.

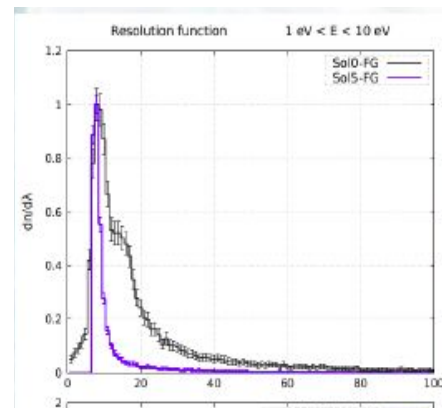
Systematic uncertainty in the ^{78}Se background: A 10% systematic uncertainty in the level of the ^{78}Se contribution has been assumed in the detection limit study. This is conservative, especially since an experimental measurement with the same conditions (EAR1) is available and will allow to disentangle the contribution of the ^{78}Se in the sample with better accuracy.

Resolution Function

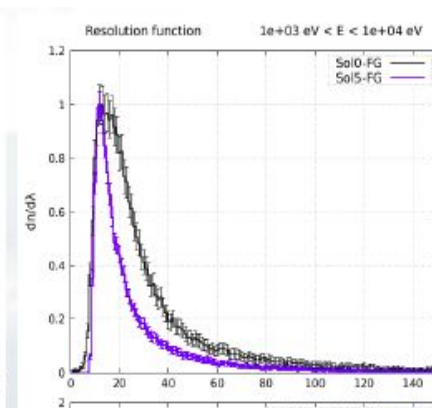


EAR2: Impact of the RF is already big in the ~ 100 eV range and a clear improvement is expected with the new spallation target

EAR1: Impact of the RF is negligible up to few keV and no change is expected with Target #3

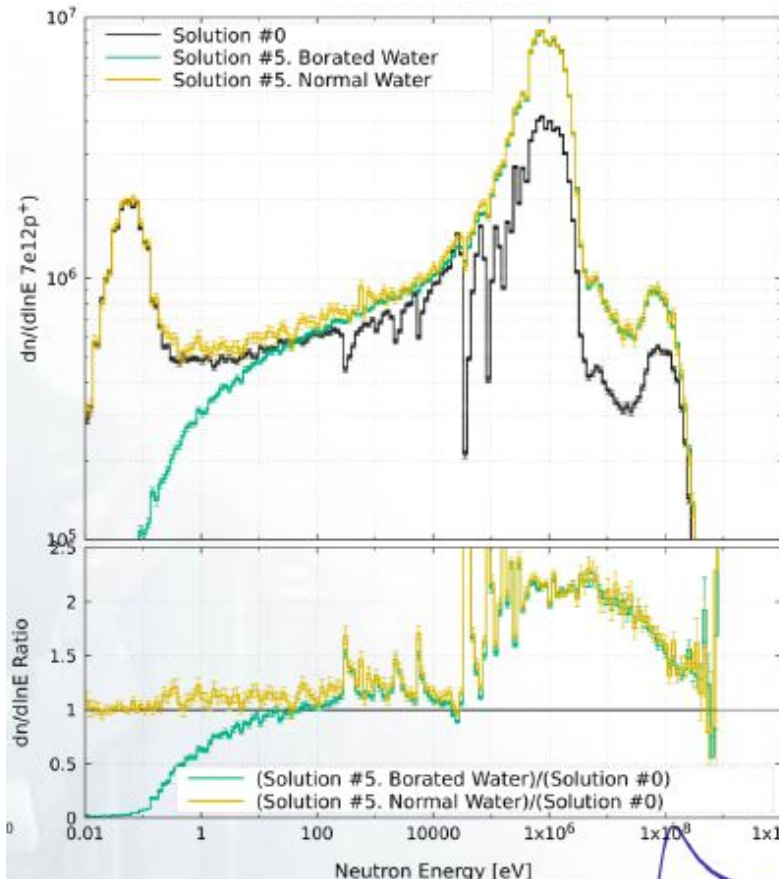


1 to 10 eV



1 to 10 keV

Counting rate limit EAR2

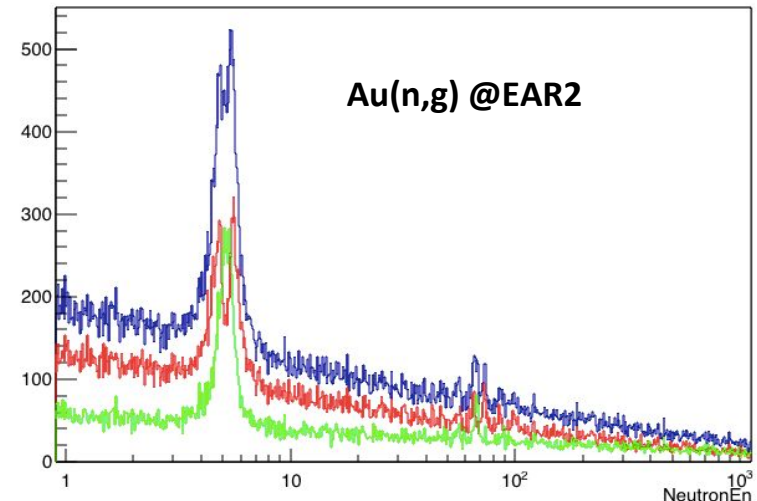


A factor x2 wrt to current situation only above 10 keV

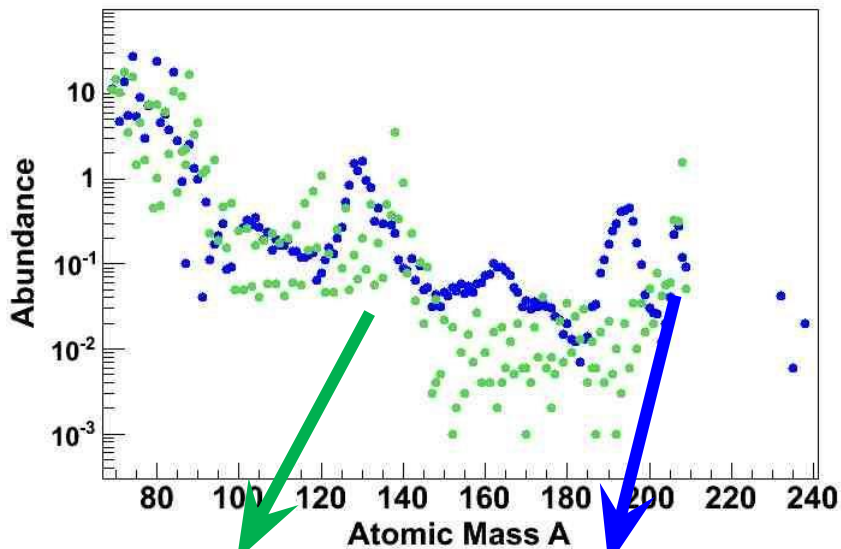
C6D6 have been used
with current CRate values

Tests with and i-TED prototype showed
possible dead time issues → C6D6 better
for CR conditions of EAR2

i-TED [A-detector] En Spectrum



Astrophysical motivation

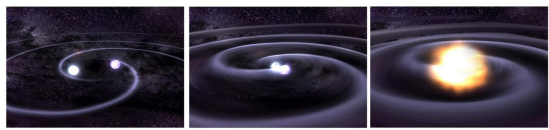
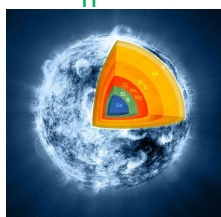


s-process

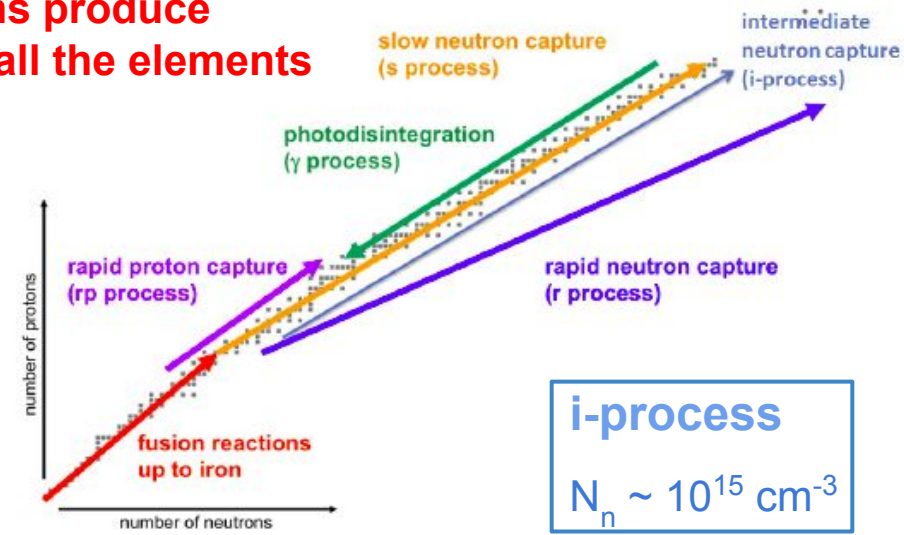
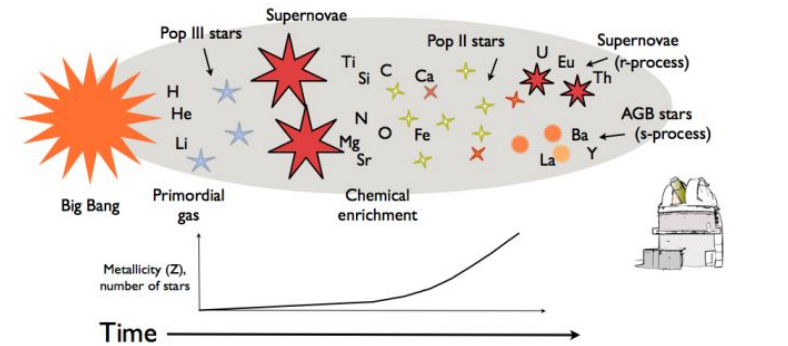
$T = 10^8 - 10^9 \text{ K}$
 $N_n = 10^6 - 10^{12} \text{ cm}^{-3}$

r-process

$T = 10^8 - 10^{10} \text{ K}$
 $N_n = 10^{20} - 10^{27} \text{ cm}^{-3}$

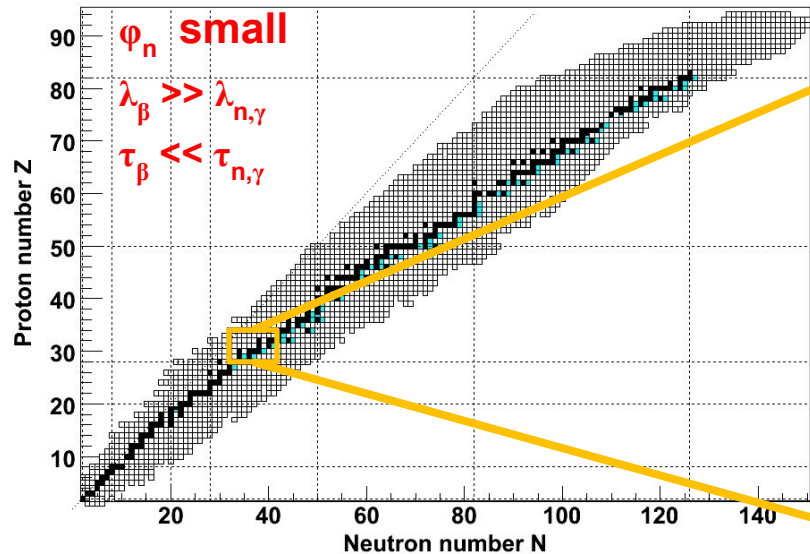


Neutrons produce
75% of all the elements

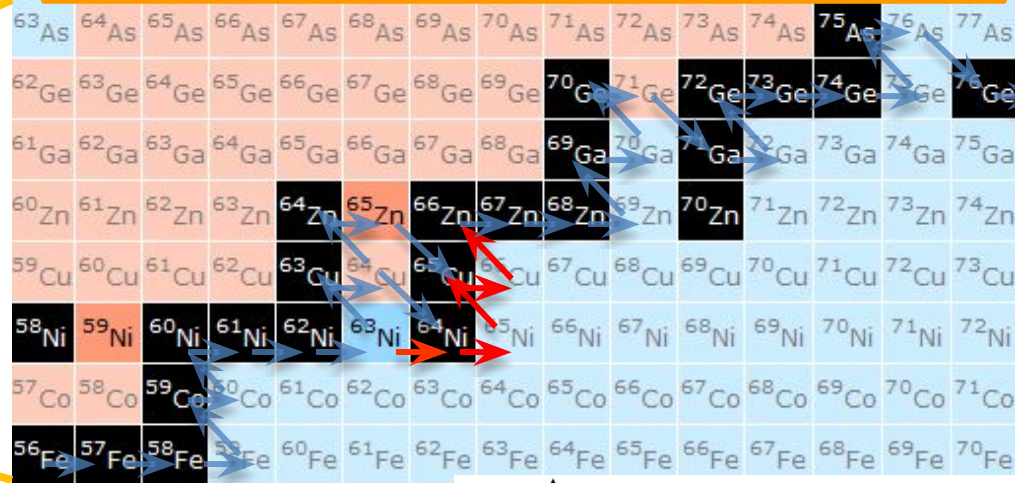


i-process
 $N_n \sim 10^{15} \text{ cm}^{-3}$

Motivation(I): s-process nucleosynthesis



s-process: $\sim 1/2$ of the abundances $A > 56$



s-process: n capture + beta decay along stability valley

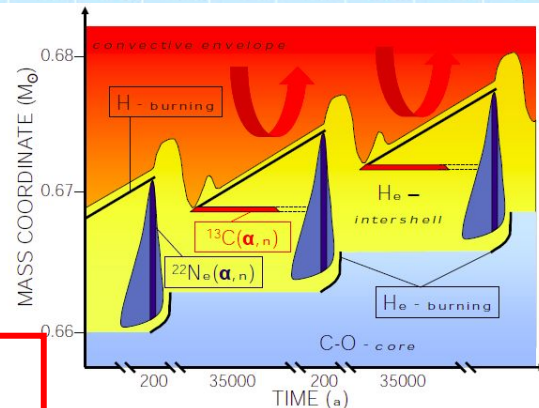
BRANCHING POINTS:

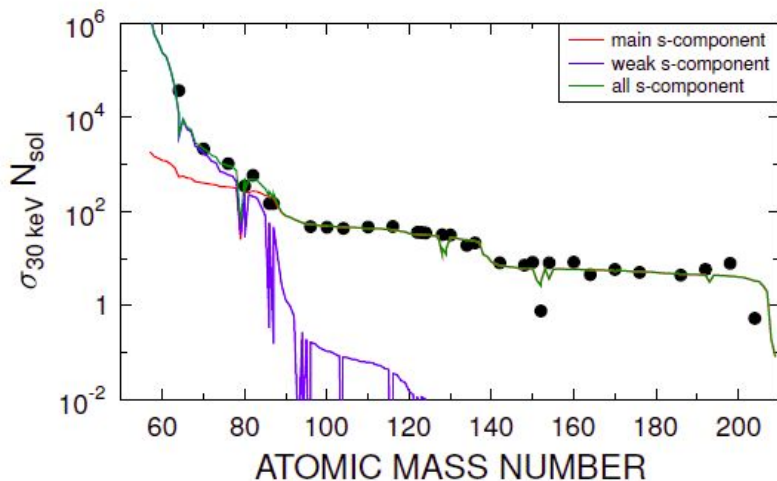
$AZ(n,\gamma) \rightarrow A^{+1}Z$ competes with
 $AZ \rightarrow A(Z+1) + \beta + \nu$

ASTROPHYSICAL SITES

- TP-AGB stars
- Massive stars

(n,γ) cross sections of **branching points** are the **key nuclear input**





⁷⁹Se: One of the few key s-process branchings of the weak component & close to the transition region

S-PROCESS COMPONENTS

MAIN S-PROCESS:

He shell burning phase in AGB STARS

$^{22}\text{Ne}(\alpha, n)$: 10^{12} n/cm^3 , $kT \sim 30 \text{ keV}$

$^{13}\text{C}(\alpha, n)$: 10^7 n/cm^3 , $kT \sim 5 \text{ keV}$

$90 < A < 209$

WEAK S-PROCESS:

Massive stars

$^{22}\text{Ne}(\alpha, n)$

He core burning: 10^6 n/cm^3 , $kT \sim 25 \text{ keV}$

C-shell burning: 10^{12} n/cm^3 , $kT \sim 90 \text{ keV}$

$56 < A < 90$

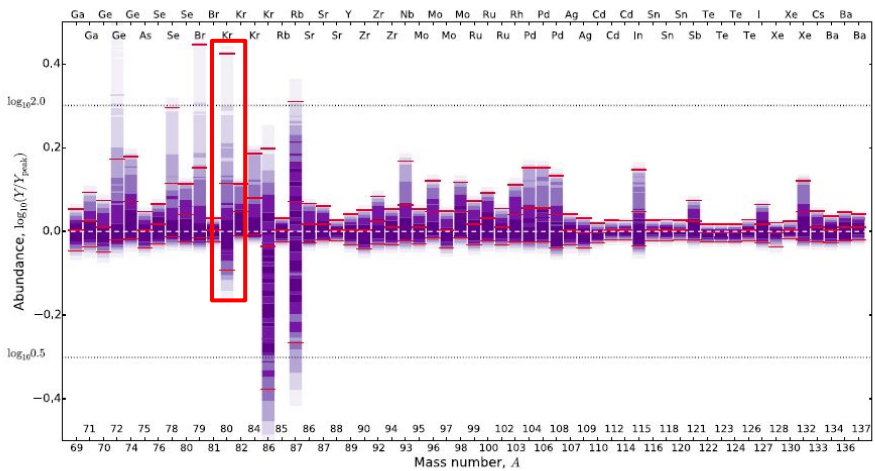
REVIEW OF MODERN PHYSICS, VOLUME 83, JANUARY–MARCH 2011

Sample	Half-life (yr)	Q value (MeV)	Comment
^{63}Ni	100.1	β^- , 0.066	TOF work in progress (Couture, 2009), sample with low enrichment
^{79}Se	2.95×10^5	β^- , 0.159	Important branching, constrains s -process temperature in massive stars
^{84}Kr	2.29×10^5	EC, 0.322	Part of ^{79}Se branching
^{85}Kr	10.73	β^- , 0.687	Important branching, constrains neutron density in massive stars
^{95}Zr	64.02 d	β^- , 1.125	Not feasible in near future, but important for neutron density low-mass AGB stars
^{134}Cs	2.0652	β^- , 2.059	Important branching at $A = 134, 135$, sensitive to s -process temperature in low-mass AGB stars, measurement not feasible in near future
^{135}Cs	2.3×10^6	β^- , 0.269	So far only activation measurement at $kT = 25$ keV by Patronis <i>et al.</i> (2004)
^{147}Nd	10.981 d	β^- , 0.896	Important branching at $A = 147/148$, constrains neutron density in low-mass AGB stars
^{147}Pm	2.6234	β^- , 0.225	Part of branching at $A = 147/148$
^{148}Pm	5.368 d	β^- , 2.464	Not feasible in the near future
^{151}Sm	90	β^- , 0.076	Existing TOF measurements, full set of MACS data available (Abbondanno <i>et al.</i> , 2004a; Wisshak <i>et al.</i> , 2006c)
^{154}Eu	8.593	β^- , 1.978	Complex branching at $A = 154, 155$, sensitive to temperature and neutron density
^{155}Eu	4.753	β^- , 0.246	So far only activation measurement at $kT = 25$ keV by Jaag and Käppeler (1995)
^{153}Gd	0.658	EC, 0.244	Part of branching at $A = 154, 155$
^{160}Tb	0.198	β^- , 1.833	Weak temperature-sensitive branching, very challenging experiment
^{163}Ho	4570	EC, 0.0026	Branching at $A = 163$ sensitive to mass density during s process, so far only activation measurement at $kT = 25$ keV by Jaag and Käppeler (1996b)
^{170}Tm	0.352	β^- , 0.968	Important branching, constrains neutron density in low-mass AGB stars
^{171}Tm	1.921	β^- , 0.098	Part of branching at $A = 170, 171$
^{179}Ta	1.82	EC, 0.115	Crucial for s -process contribution to ^{180}Ta , nature's rarest stable isotope
^{185}W	0.206	β^- , 0.432	Important branching, sensitive to neutron density and s -process temperature in low-mass AGB stars
^{204}Tl	3.78	β^- , 0.763	Determines $^{205}\text{Pb}/^{205}\text{Tl}$ clock for dating of early Solar System

→ One of the **21 key s-nuclei** listed in: Käppeler, *Rev. Mod. Phys.* 83, 157 (2011)

Uncertainties in s-process nucleosynthesis in low-mass stars determined from Monte Carlo variations

G. Cescutti,^{1★†} R. Hirschi,^{2,3†} N. Nishimura,^{4†} J. W. den Hartogh,^{2,5†} T. Rauscher,^{6,7†}
A. St. J. Murphy^{8†} and S. Cristallo^{9,10}



tudy: Cescutti et al., *MNRS* 478 (2018)

Cescutti et al., MNRAS 478 (2018)

Monte Carlo reaction rate variation study concluded that ⁷⁹Se(n,γ) is a key reaction in several investigated s-process nucleosynthesis models with different initial ¹³C abundance

three reactions in Section 3.4.1. There are also a few key weak reactions at branching points, ⁷⁹Se, ⁸⁵Kr, and ¹²⁸I. We will discuss the possibility of reducing the uncertainties of the key reactions linked to the most uncertain final abundances in Section 3.6. For the

1986AAA...167..186W

Astron. Astrophys. 167, 186–199 (1986)

ASTRONOMY AND ASTROPHYSICS

The s-process branching at ^{79}Se

G. Walter¹, H. Beer¹, F. Käppeler¹, G. Reffo², and F. Fabbri²

¹ Institut für Kernphysik III, Kernforschungszentrum Karlsruhe GmbH, P.O.B. 3640, D-7500 Karlsruhe, Federal Republic of Germany

² Laboratorio Dati Nucleari, Ente Nazionale per l'Energie Alternative, Via Mazzini 2, Bologna, Italy

Received March 6, accepted March 27, 1986

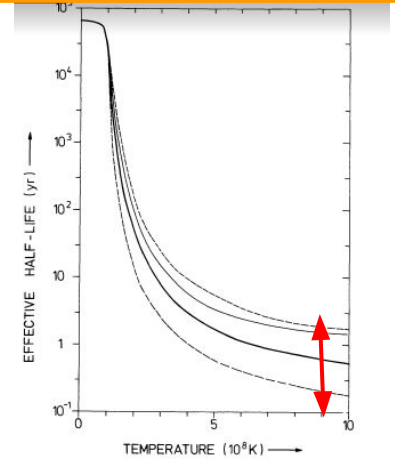
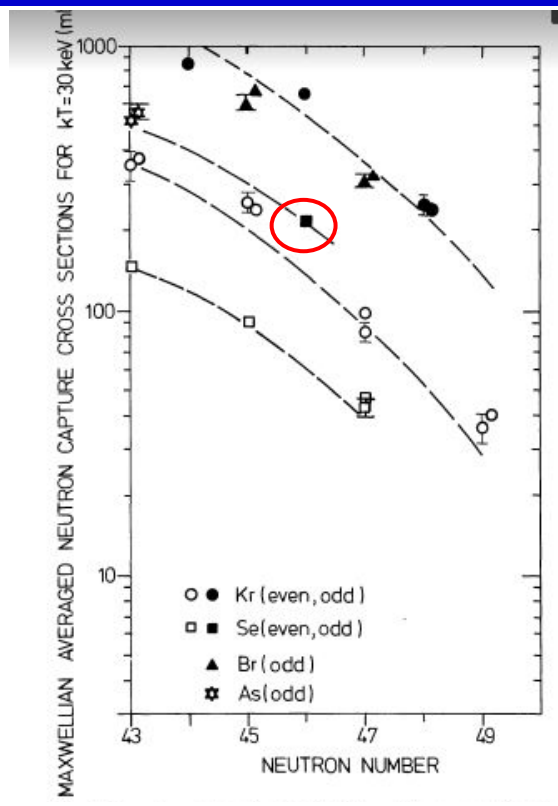
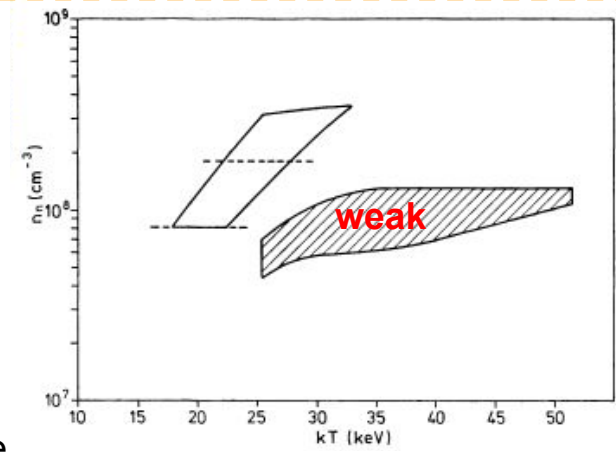


Fig. 10. Effective half-life of ^{79}Se as a function of temperature accor to Conrad (1976). Dashed lines indicate the uncertainty of this calcie tion. The thin solid line represents the result of Newman (1973) Cosner and Truran (1981)

No exp data on ^{79m}Se beta decay → discrepancies in the temp. dependence

Uncertainties (XS and stellar hafl-life) :
Very broad range for thermal range of the weak s-process



Calculated ^{79}Se MACS from
Exp. data of neighbouring nuclei

Temperature and $T_{1/2}$ of ^{79}Se

PHYSICAL REVIEW C

VOLUME 38, NUMBER 1

JULY 1988

β -decay rate of ^{79m}Se and its consequences for the s -process temperature

N. Klay and F. Käppeler

Institut für Kernphysik III, Kernforschungszentrum Karlsruhe, D-7500 Karlsruhe, Federal Republic of Germany

(Received 21 December 1987)

The branching ratio between internal electromagnetic transitions and β^- decays of the isomer ^{79m}Se was determined experimentally. Extremely clean samples of ^{78}Se were activated with thermal neutrons at a high-flux reactor. A mini-orange-Si (Li) detection system was used to measure β^- particles and conversion electrons immediately after neutron irradiation. For the β^- decay we obtain $\log ft = 4.70^{+0.10}_{-0.09}$. Our present result was used to recalculate the temperature dependence of the effective β^- half-life of ^{79}Se in the stellar interior. In combination with the half-life deduced from a quantitative branching analysis, we obtain a possible temperature range between 182 and 295 million degrees for the weak component of the s process.

Nevertheless, the effective stellar half-life at temperatures above 200 million degrees is not changed by the assumed lower limit for the ground state half-life. This leads to the rather strange consequence that, at present, we know the stellar life time of ^{79}Se at a fixed temperature much better than its terrestrial one.

weak s -process component to range between 182 and 295 million degrees. **Need of improved cross sections**

The related uncertainty is mainly due to the uncertainty for the effective stellar half-life deduced from the σ/N systematics which can only be reduced by improved cross section measurements. The present experimental uncer-

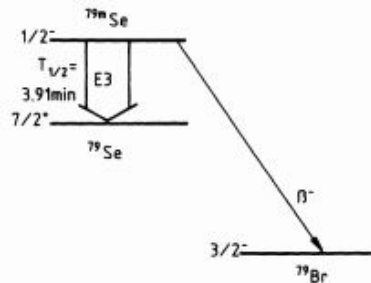
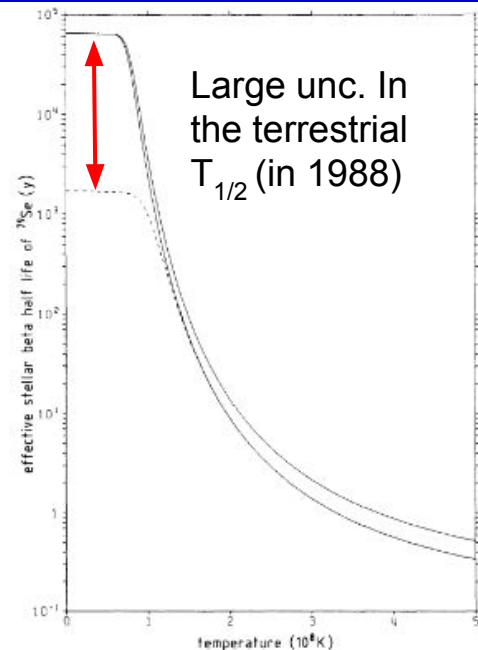
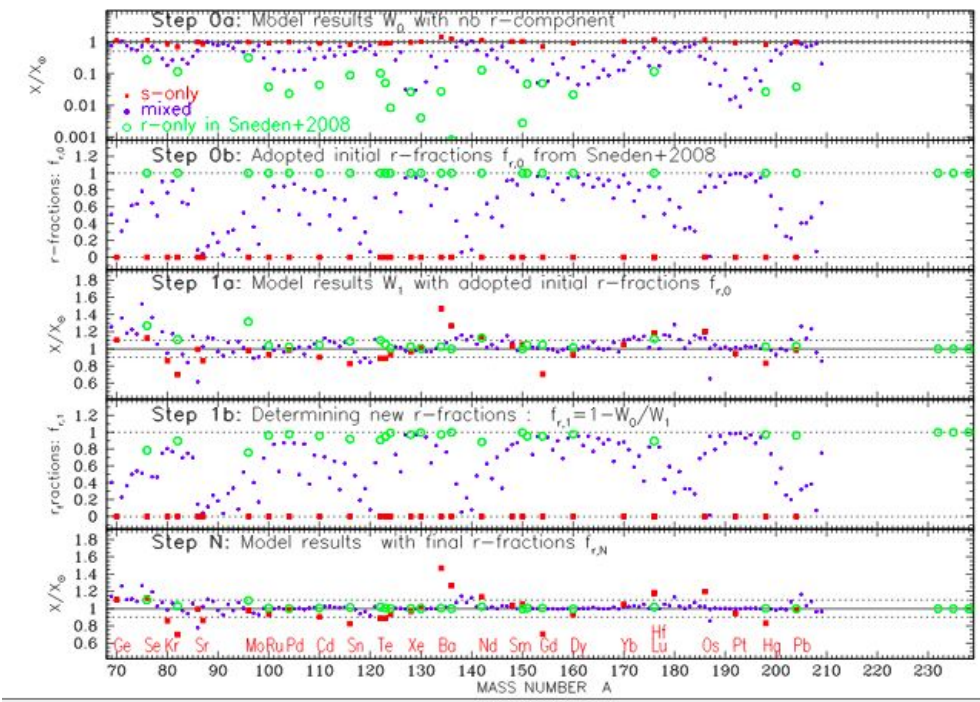
FIG. 1. Decay scheme of ^{79m}Se .

FIG. 7. Stellar half-life of ^{79}Se as a function of temperature. The error band reflects the uncertainty of our measurement. The dashed line refers to $\log ft = 8.5$ for the ground state decay.

Experimental measurement of the $\log ft$ of the beta decay of the ^{79m}Se state at 96 keV, thermally populated at stellar temperatures

Chemical evolution with rotating massive star yields II. A new assessment of the solar s- and r-process components



Massive Stars

Prantzos et al., MNRAS 491 (2020)

Underproduction of ^{80}Kr in their Galactic Chemical Evolution model, compared to the abundances observed in the Sun. The reason for such a discrepancy is probably related to the limited accuracy of the nuclear inputs.

Among the s-only nuclei (red dots), most are reproduced within a factor of 20 per cent solar abundances (see also [Paper I](#)⁵), except Kr, Ba, and Gd which differ from their solar values by 20–40 per cent. Taking into account the uncertainties in nuclear, stellar, and galactic physics involved in the calculation, which lead to a larger dispersion for the lighter nuclei (up to 100 per cent, factor of ~ 2 , see fig. 11 in [Paper I](#)), we think that this agreement is quite satisfactory.

Published: 22 November 1990

Meteoritic silicon carbide: pristine material from carbon stars

Roy S. Lewis, Sachiko Amari & Edward Anders

AGB Stars

All five noble gases in interstellar silicon carbide grains have grossly non-solar isotopic and elemental abundances that vary with grain size but are strikingly similar to calculated values for the helium-burning shell of low-mass carbon stars. Apparently these grains formed in carbon-star envelopes, and were impregnated with noble gas ions from a stellar wind. Meteoritic SiC provides a detailed record of nuclear and chemical processes in carbon stars.

The Kr isotopic ratios have been measured in bulk SiC acid residues providing details on AGB stars evolved prior to the formation of the Solar System.

Presolar grain measurements give the **most precise data** currently available on s-process nucleosynthesis (at least one order of magnitude better than spectroscopic observations)



Geochimica et Cosmochimica Acta

Volume 58, Issue 1, January 1994, Pages 471-494



Interstellar grains in meteorites: II. SiC and its noble gases

Roy S. Lewis, Sachiko Amari^{*}, Edward Anders[†]

interstellar SiC, isolated from the Murchison C2 chondrite. All are mixtures of a highly anomalous component bearing the isotopic signature of the astrophysical s-process and a more normal component, generally solar-like but with anomalies of up to 30% in the heavy isotopes. As these two components strikingly resemble predictions for the He-burning shells and envelopes of red giant carbon stars, it appears that the SiC grains are pristine circumstellar condensates from such stars. A number of elemental and isotopic ratios (such as $\text{K}^{80}\text{K}^{82}$ and $\text{K}^{86}\text{Kr}^{82}$) vary with grain size, suggesting that the SiC comes from carbon stars representing a range of masses, metallicities, temperatures, and neutron densities.

Published: 22 November 1990

Meteoritic silicon carbide: pristine material from carbon stars

Roy S. Lewis, Sachiko Amari & Edward Anders

AGB Stars

release temperature of the gas on heating or combustion^{7,8}. The variations of ⁸⁰Kr and ⁸⁶Kr reflect branching of the s-process at their radioactive progenitors, ⁷⁹Se and ⁸⁵Kr (ref. 7). These branchings depend sensitively on neutron density and temperature in the s-process region^{7,12}, and thus can provide clues about the stars in which the Kr was formed. What we would

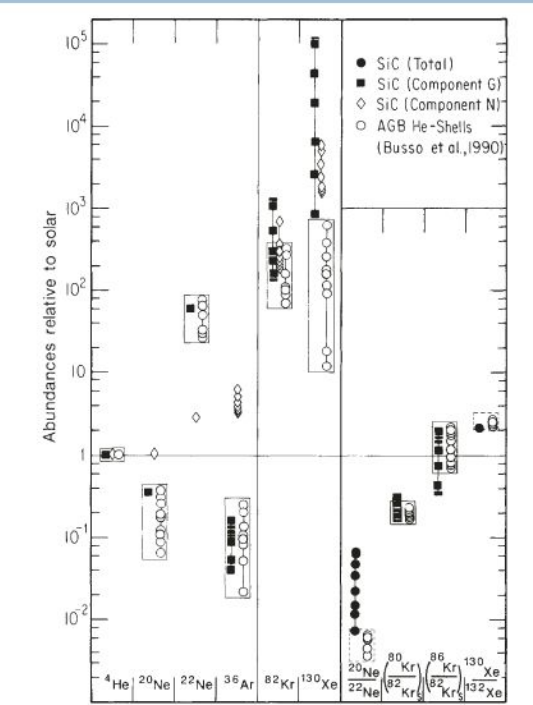


FIG. 3 Right, isotope ratios of SiC and AGB-star He shells, normalized to

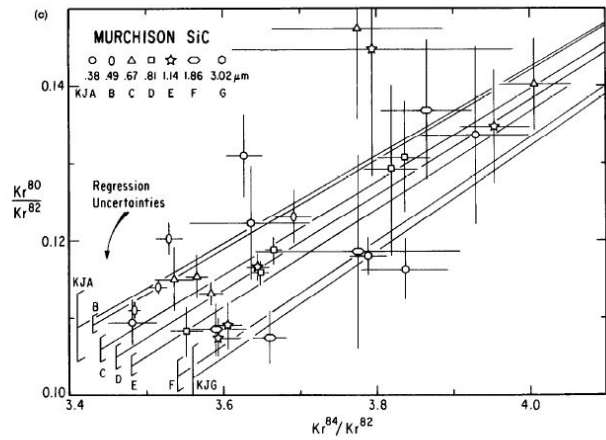
TABLE 1 Noble gases in SiC size fractions from Murchison chondrite

Sample	Size (μm)	³ He ⁴ He	²⁰ Ne	³⁸ Ar	⁸⁴ Kr	¹³⁰ Xe	^(80Kr) _s	^(86Kr) _s
		×10 ⁻⁴	²² Ne	³⁶ Ar	⁸² Kr	¹³² Xe		
KJA	0.05–0.1	1.32 (18)	0.9075 (10)	0.1927 (5)	3.702 (24)	0.3532 (10)	0.0597 (67)	0.621 (44)
KJB	0.1–0.2	2.00 (10)	0.8933 (3)	0.1919 (1)	3.603 (6)	0.3602 (4)	0.0586 (16)	0.695 (24)
KJC	0.2–0.3	1.48 (7)	0.6345 (3)	0.1907 (2)	3.693 (10)	0.3604 (6)	0.0526 (27)	1.145 (19)
KJD	0.3–0.5	1.16 (6)	0.4582 (5)	0.1935 (1)	3.769 (8)	0.3558 (5)	0.0490 (25)	1.733 (23)
KJE	0.5–0.8	0.81 (4)	0.2977 (5)	0.2051 (2)	3.756 (11)	0.3465 (10)	0.0451 (21)	2.363 (34)
KJF	0.8–1.5	0.56 (3)	0.2001 (2)	0.2210 (5)	3.776 (21)	0.3291 (22)	0.0365 (37)	2.710 (71)
KJG	1.5–3	0.53 (5)	0.1556 (2)	0.2313 (6)	3.915 (21)	0.2716 (28)	0.0336 (72)	2.872 (62)
KJH	3–5		0.0979 (19)	0.2090 (23)	4.500 (87)	0.1606 (52)	0.055 (58)	
Solar ²¹		1.42	13.7	0.188	4.988	0.1643		
He-Shell, Range*			0.05–0.084	0.57–1.25	2.2–2.6	0.39–0.44		
He-Shell, Typical		0	0.0808	0.74	2.55	0.485†		

Very accurate 80Kr/82Kr abundances ratios

The low values of $(80/82)_s$ —first noted by OTT et al. (1988)—decisively favor the $\text{C}^{13}(\alpha,n)\text{O}^{16}$ neutron source over the $\text{Ne}^{22}(\alpha,n)\text{Mg}^{25}$ neutron source (GALLINO et al., 1988; BUSO et al., 1990). The superior fit for $(84/82)_s = 2.40$

overlap factors closer to 0.6 than to 0.8. For Xe and Kr, the SiC data are accurate enough to suggest errors in the neutron capture cross sections, and for Kr, isotopes 80 and 86 provide information on neutron density and temperature. Elemental



AGB Stars

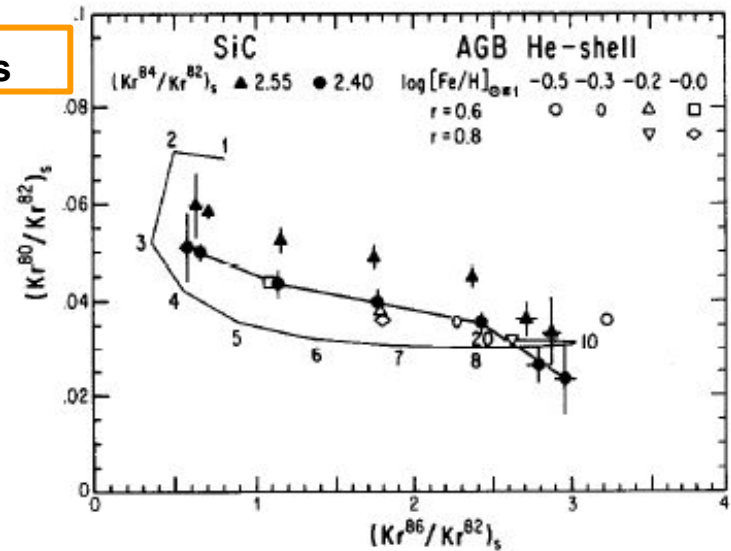



FIG. 3. The isotopic ratios of s-process Kr from SiC agree strikingly well with theoretical compositions for AGB stars of 1.5–3 M_{\odot} , metallicity $1/3$ to $1\times$ solar, and overlap factor $r = 0.6$ – 0.8 . The choice of $(\text{Kr}^{84}/\text{Kr}^{82})_s = 2.40$ yields the better match between theory and data. (Adapted from GALLINO et al., 1990.)



Geochimica et Cosmochimica Acta

Volume 58, Issue 1, January 1994, Pages 471–494

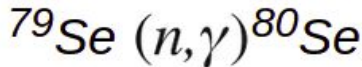
Interstellar grains in meteorites: II. SiC and its noble gases

Roy S Lewis, Sachiko Amari ^{*}, Edward Anders [†]

Knowledge of the ^{79}Se cross section

Not an uncertainty
(no exp. constant)
but a spread of calculations

Recommended MACS30 (Maxwellian Averaged Cross Section @ 30keV)



Total MACS at 30keV: $263 \pm 46^*$ mb

Cross sections do not include stellar enhancement factors!
* only theoretical data available

History

Version	Total MACS [mb]	Partial to gs [mb]	Partial to isomer [mb]
0.0	$263 \pm 46^*$	-	-

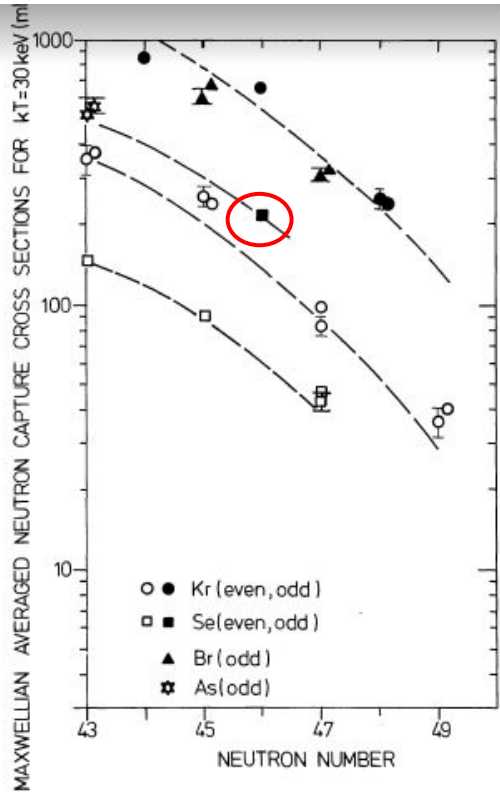
(Version 0.0 corresponds to Bao et al.)

Comment

Last review: 1999

List of all available values

original	renorm.	year	type	Comment	Ref
233		2000	t		RaT99
218 ± 50		1982	t		Ref82
514		1981	t		Har81
260		1978	t		WFH78
572		2002	t	MOST 2002	Gor02
415		2005	t	MOST 2005	Gor05



Walter et al.,
Astron. Astrophys.
167, 186 (1986).

Photodisintegration of ⁸⁰Se: Implications for the *s*-process branching at ⁷⁹Se

A. Makinaga, H. Utsunomiya, S. Goriely, T. Kaihori, S. Goko, H. Akimune, T. Yamagata, H. Toyokawa, T. Matsumoto, H. Harano, H. Harada, F. Kitatani, Y. K. Hara, S. Hohara, and Y.-W. Lui
 Phys. Rev. C **79**, 025801 – Published 5 February 2009

Indirect methods_

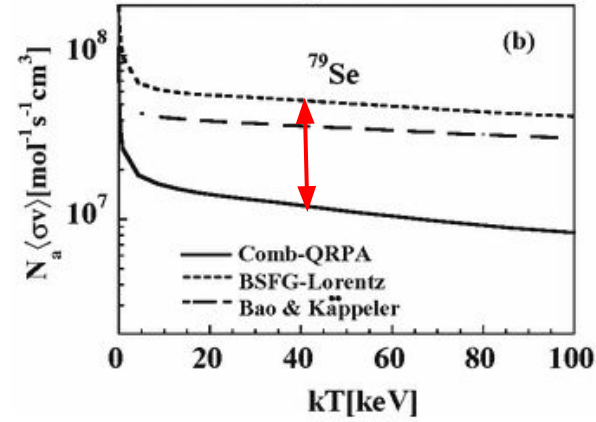
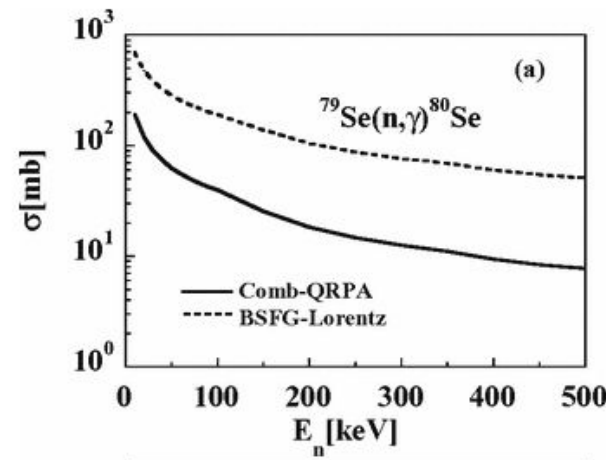
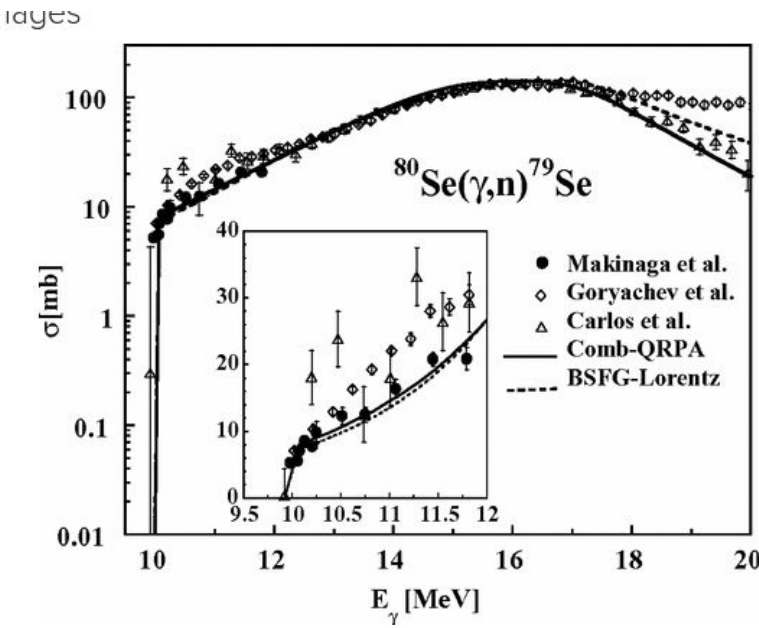
80Se(g,n) →

Large deviation

In the

calculations for

(n,g)

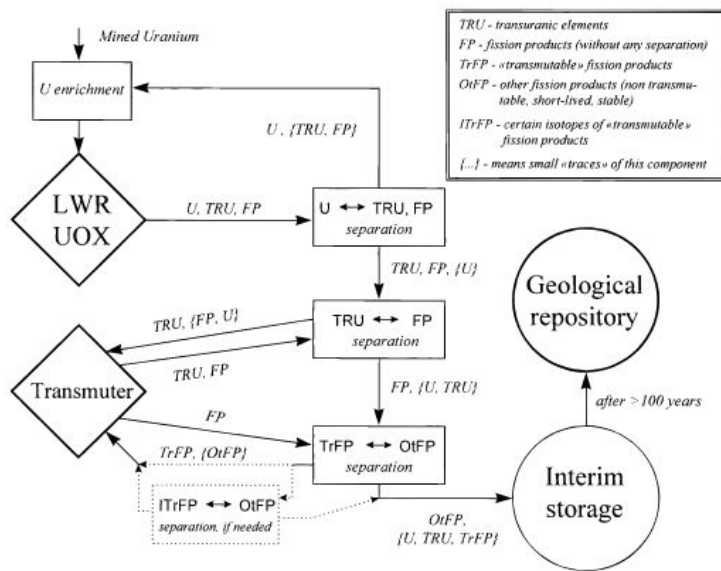


Motivation: Transmutation of long-lived fission products (LLFPs)

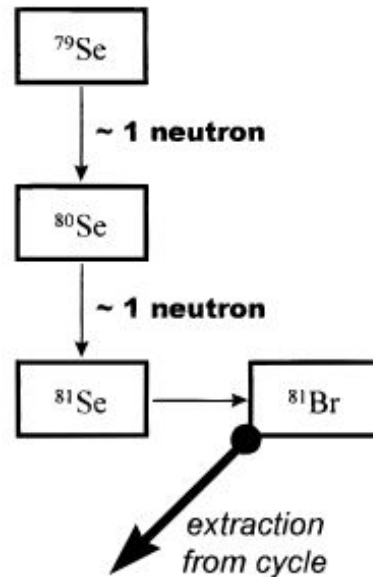
$^{79}\text{Se}(\text{n},\text{g})$: Transmutation of LLFP

The Transmutation of Long-Lived Fission Products by Neutron Irradiation

M. Salvatores,* I. Slessarev, and A. Tchistiakov



^{79}Se is one of the main contributors among the fission products to the long-term radiotoxicity of spent fuel due to its long half-life



The Transmutation of Long-Lived Fission Products by Neutron Irradiation

M. Salvatores,* I. Slessarev, and A. Tchistiakov

TABLE I

Parameters of Long-Lived Nuclei to be Eventually Transmuted in Fast [E_n (Neutron Energy) = 0.2 MeV, JEF-2.2] and Thermal (E_n = 1 eV, JEF-2.2) Spectra with Standard Flux Levels*

Isotopes, J	$\sigma_{n,\gamma}^J$ (b)		$T_{1/2}$ (yr)	T_f^{transm} (yr)		Radiotoxicity, at $t = T_f^{transm}$ (Sv/g)	Recommendation to Transmutation
	Fast Spectrum	Thermal Spectrum		Fast Spectrum	Thermal Spectrum		
⁷⁹ Se	0.03	0.1	6.5×10^4	7.3×10^2	2.2×10^3	6.0	Questionable
⁹³ Sr	0.01	0.14	29	2.2×10^2	1.6×10^2	---	Nontransmutable
⁹³ Zr	0.03	0.28	1.5×10^6	730	790	0.04	Transmutable
⁹⁴ Nb	0.04	2.2	2.0×10^4	5.5×10^2	1×10^2	9.0	Questionable or transmutable
⁹⁹ Tc	0.2	4.3	2.1×10^5	110	51	0.2	Transmutable
¹⁰⁷ Pd	0.5	0.3	6.5×10^6	44	730	0.0007	Transmutable
¹²⁶ Sn	0.005	0.05	1×10^5	4.4×10^3	4.4×10^3	4.0	Questionable
¹²⁹ I	0.14	4.3	1.6×10^7	160	51	0.5	Transmutable
¹³⁵ Cs	0.07	1.3	2.3×10^6	310	170	0.08	Transmutable
¹³⁷ Cs	0.01	0.02	30	2.2×10^3	1.1×10^4	---	Nontransmutable
¹⁵¹ Sm	0.7	700	89	31	0.3	---	Nontransmutable or questionable

* $\Phi = 10^{15}$ (n/cm²·s), $\Phi = 10^{14}$ (n/cm²·s), respectively.

M. Salvatores et al., Nucl. Sci. and Eng., 130,309-319 (1998).

⁷⁹Se: Non-transmutable or questionable
 Very different Se79(n,g) assumed →
 Reflects the impact of the cross section

Unknown ⁷⁹Se(n,g) cross section makes
 the feasibility of its transmutation very
 uncertain→ Different conclusions in
 different publications

Long-Lived Fission Product Transmutation Studies

W. S. Yang,* Y. Kim,† R. N. Hill, T. A. Taiwo, and H. S. Khalil

TABLE II

Generic Transmutability of LLFPs in Fast and Thermal Neutron Fields

Isotope	Capture Cross Section ^a		Half-Life (yr)	Transmutation Half-Life ^b		Pure Isotope Transmutability
	Fast Neutron	Thermal Neutron		Fast Neutron	Thermal Neutron	
⁷⁹ Se	0.002	0.33	$6.5\text{E}+4^c$	$1.1\text{E}+4$	666	Nontransmutable
⁹³ Sr	0.01	0.08	29	$2.2\text{E}+3$	$2.7\text{E}+3$	Nontransmutable
⁹³ Zr	0.09	1.03	$1.5\text{E}+5$	244	213	Questionable
⁹⁴ Nb	0.22	4.22	$2.0\text{E}+4$	100	52	Transmutable
⁹⁹ Tc	0.45	9.32	$2.1\text{E}+5$	49	24	Transmutable
¹⁰⁷ Pd	0.53	2.79	$6.5\text{E}+6$	42	79	Transmutable
¹²⁶ Sn	0.007	0.03	$1.0\text{E}+5$	$3.1\text{E}+3$	$7.3\text{E}+3$	Nontransmutable
¹²⁹ I	0.35	3.12	$1.6\text{E}+7$	63	70	Transmutable
¹³⁵ Cs	0.07	2.48	$2.3\text{E}+6$	314	89	Transmutable
¹³⁷ Cs	0.01	0.03	30	$2.2\text{E}+3$	$7.3\text{E}+3$	Nontransmutable
¹⁵¹ Sm	2.09	660	89	11	0.33	Transmutable

^aORIGEN2 library (fast: oxide fuel liquid-metal fast breeder reactor; thermal: standard PWR).

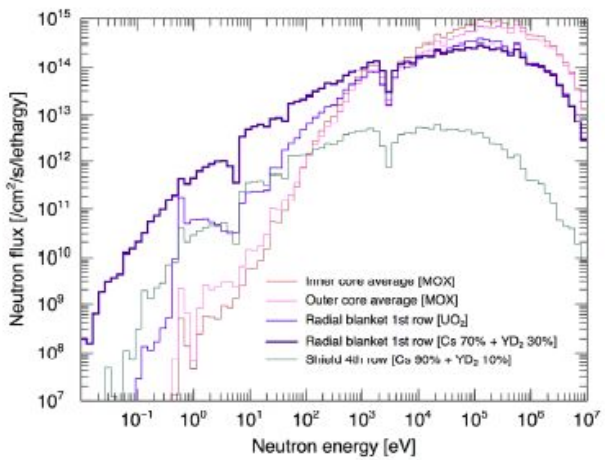
^bThermal flux = 1.0×10^{14} , fast flux = 1.0×10^{15} (n/cm²·s).

^cORIGEN2 library

W. S. Yang, Y. Kim, R. N. Hill, T. A. Taiwo and H. S. Khalil,
 Nucl. Sci. and Eng., 146 :3, 291-318 (2004).

Method to Reduce Long-lived Fission Products by Nuclear Transmutations with Fast Spectrum Reactors

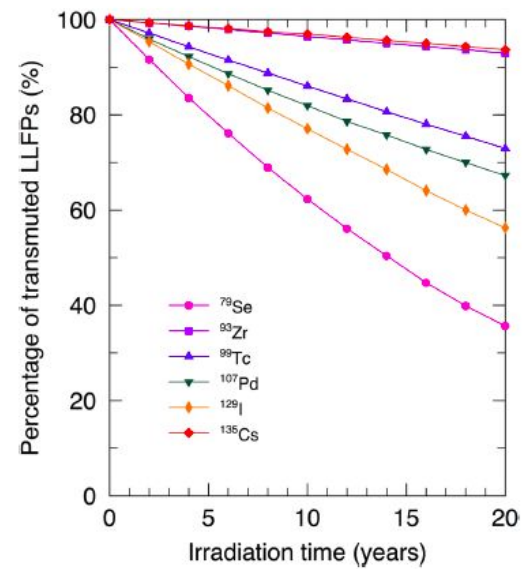
Satoshi Chiba¹, Toshio Wakabayashi², Yoshiaki Tachi³, Naoyuki Takaki⁴, Atsunori Terashima⁴, Shin Okumura¹ & Tadashi Yoshida¹



Element	Isotope	Initial composition (%)	Final composition (%)
Se	^{76}Se	0.027	0.016
	^{77}Se	2.786	1.12
	^{78}Se	5.587	6.49
	^{79}Se	13.32	4.75
	^{80}Se	22.75	31.00
	^{82}Se	55.52	54.89

^{79}Se reduced to <40% after 20 years of irradiation

Unknown $^{79}\text{Se}(\text{n},\text{g})$ cross section makes the feasibility of its transmutation very uncertain→ Different conclusions in different publications



^{79}Se : Fastest transmutation among LLFP in fast reactors (JENDL 4.0 XS)

i-TED: concept, experimental validation & expected performance

i-TED: Motivation & concept



Contents lists available at ScienceDirect

Nuclear Instruments and Methods in
Physics Research A

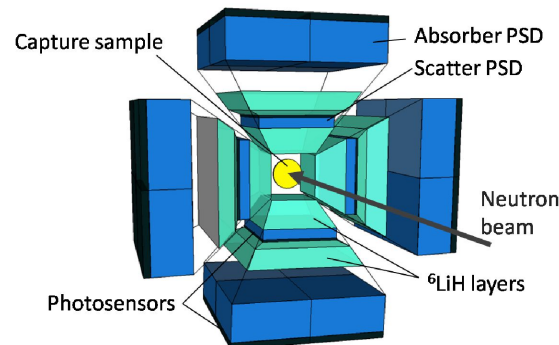
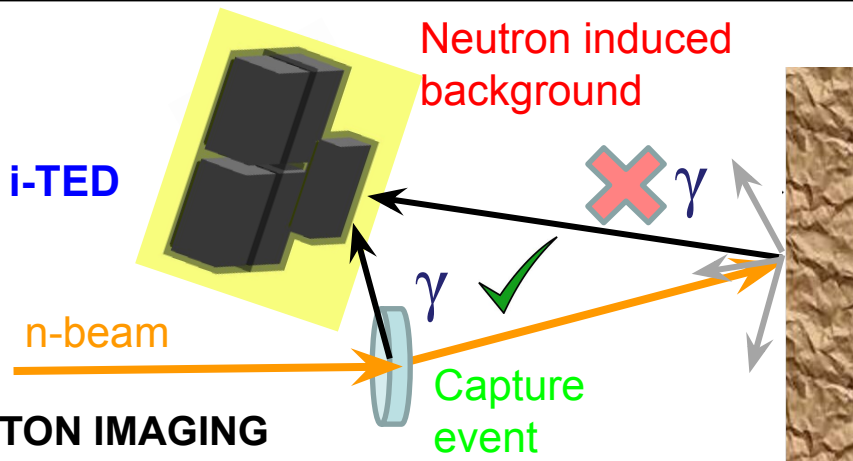
journal homepage: www.elsevier.com/locate/nima



i-TED: A novel concept for high-sensitivity (n, γ) cross-section measurements

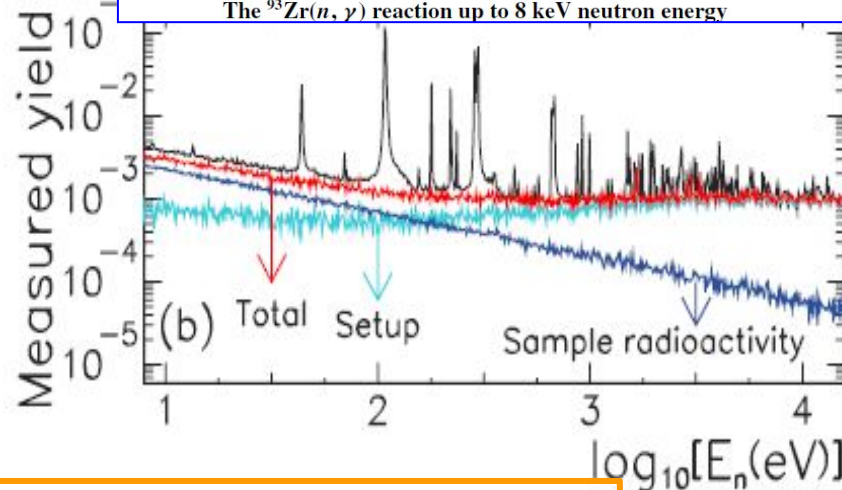
C. Domingo-Pardo

Instituto de Física Corpuscular, CSIC-University of Valencia, Spain



PHYSICAL REVIEW C 87, 014622 (2013)

The $^{93}\text{Zr}(n, \gamma)$ reaction up to 8 keV neutron energy

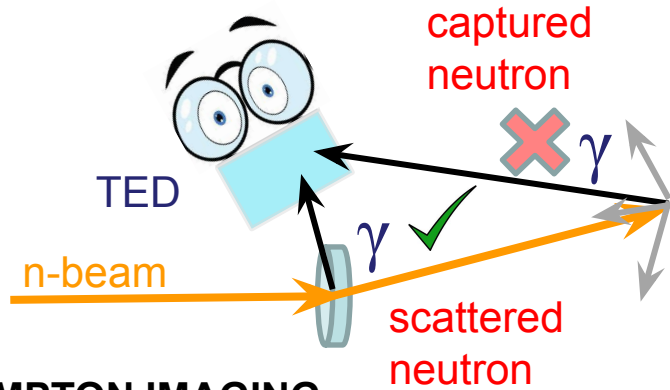


**COMPTON IMAGING
TECHNIQUE**

GOAL: Enhance detection sensitivity by reducing the extrinsic neutron background

Background suppression i-TED

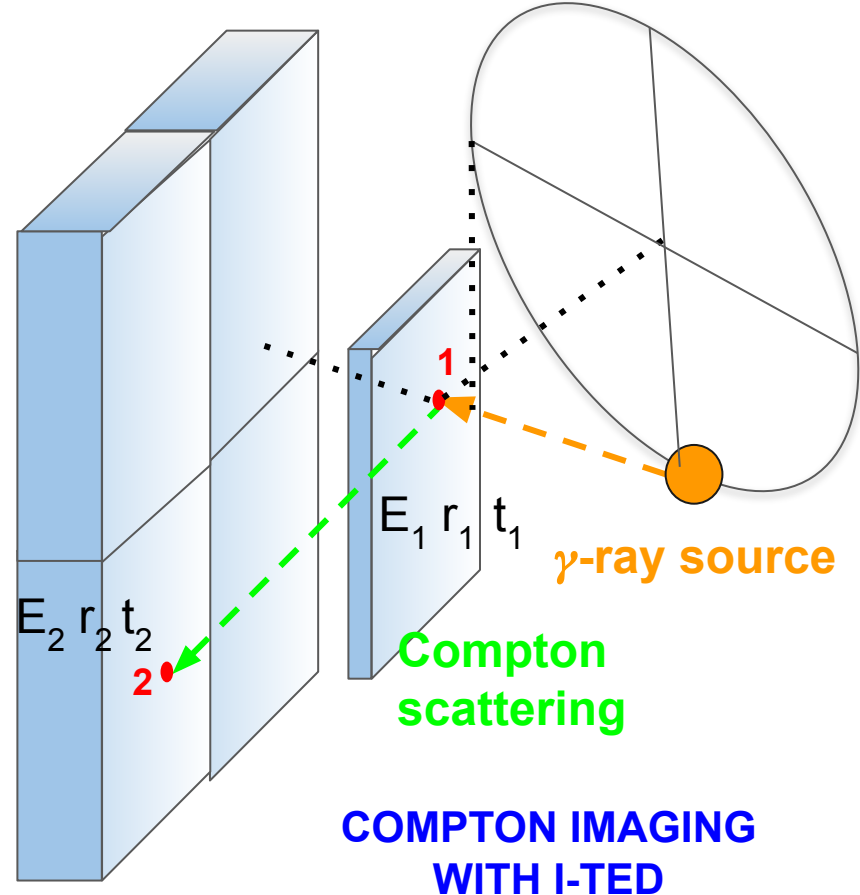
i-TED CONCEPT



COMPTON IMAGING TECHNIQUE

$$\theta = \arccos \left[1 - m_e c^2 \left(\frac{1}{E_2} - \frac{1}{E_1 + E_2} \right) \right]$$

$$\Delta \theta = \frac{E_1 + E_2}{\sin \theta} \left[\frac{1}{E_1^2} \left(\frac{\Delta E_1}{E_1} \right)^2 + 2 \sin^2 \theta \left(\frac{\Delta r}{r} \right)^2 \right]^{1/2}$$

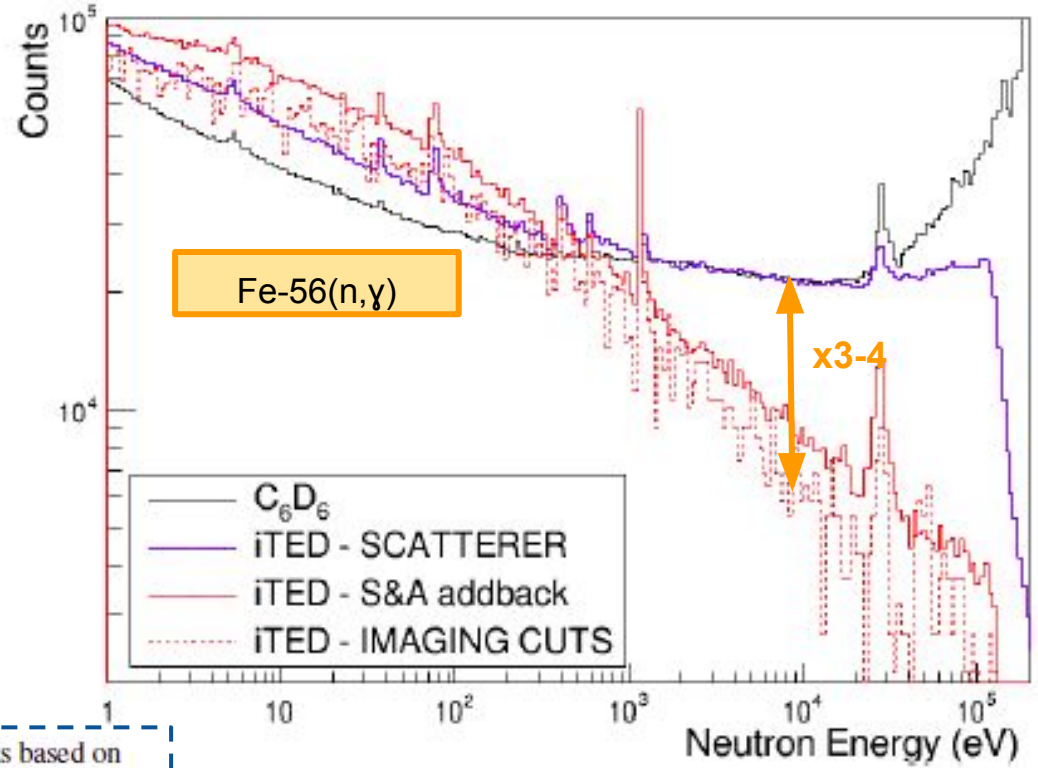


(n, γ)/background gain vs C6D6: first experimental proof-of-concept

Scatterer alone very similar counting rate that **C6D6** but:

- + Higher resolution
- + Spectroscopic

ii-TED improves (n, γ)/background ratio in the keV range after **coincidences** between absorber-scatterer + **Compton imaging**



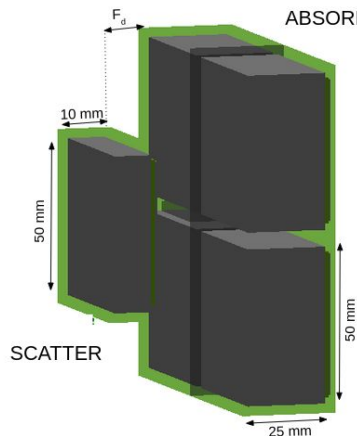
i-TED: prototype & full detector array

Prototype (i-TED 5.3) vs final detector (4 x i-TED 5)



Prototype (i-TED 5.3):

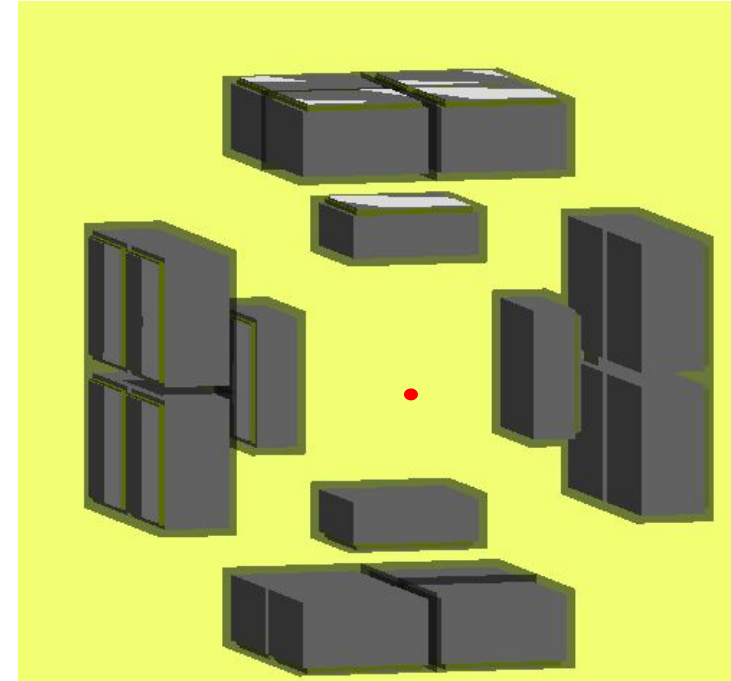
Limited background rejection,
only 2 absorber crystals



i-TED 5:

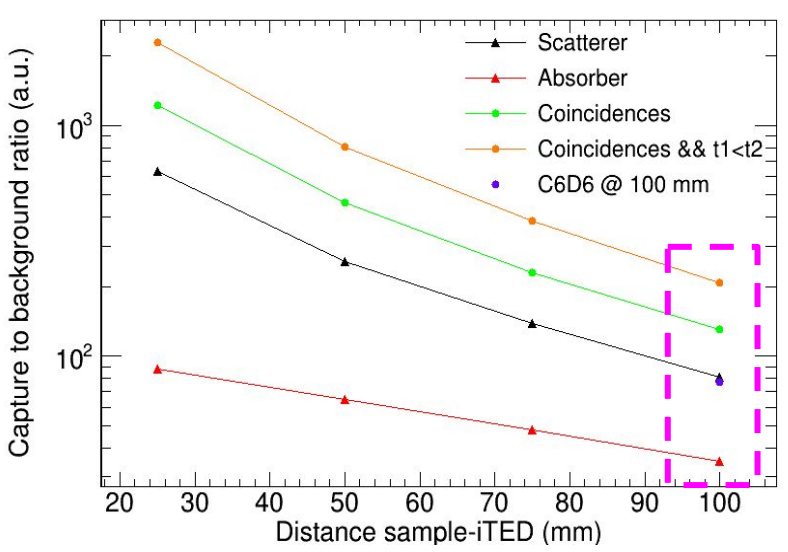
- Each of the modules of the final detector
- Improve S/B & efficiency
- Further improvement with ML techniques under study

4pi i-TED: 4x i-TED 5

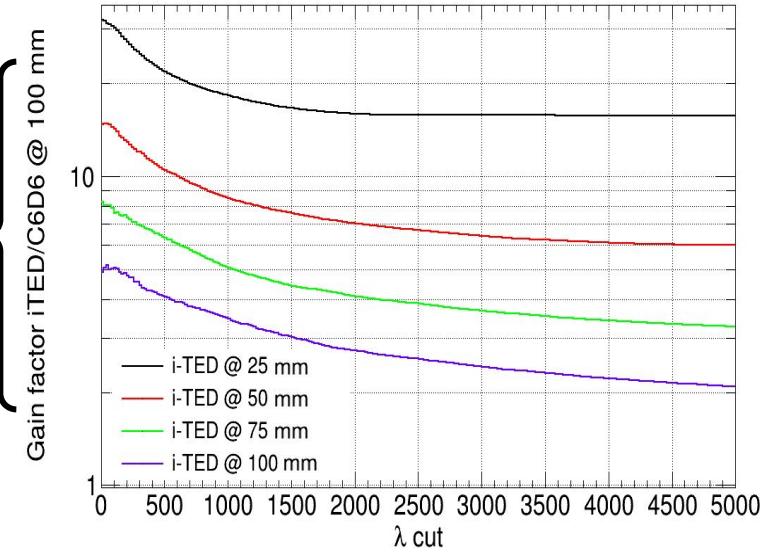


i-TED: First experimental proof-of-concept and future prospects based on
Machine-Learning techniques [\(link to draft\)](#)

MC :C6D6 & i-TED to capture & background



Best gain factors (n, γ)/bckg ratio wrt to C6D6

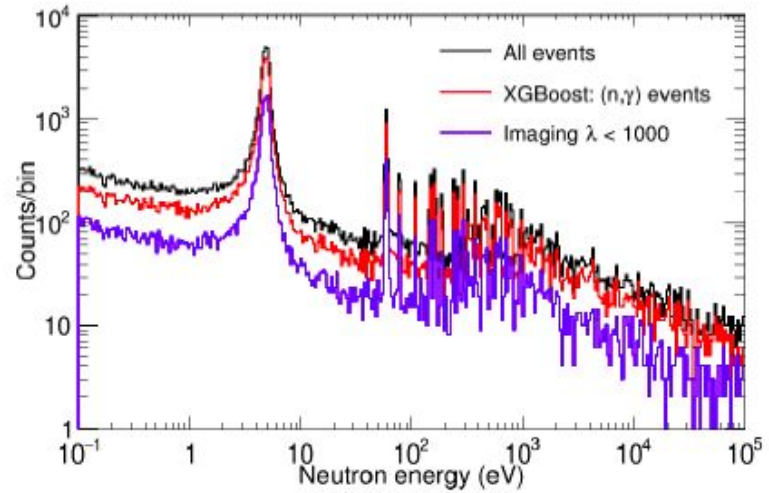
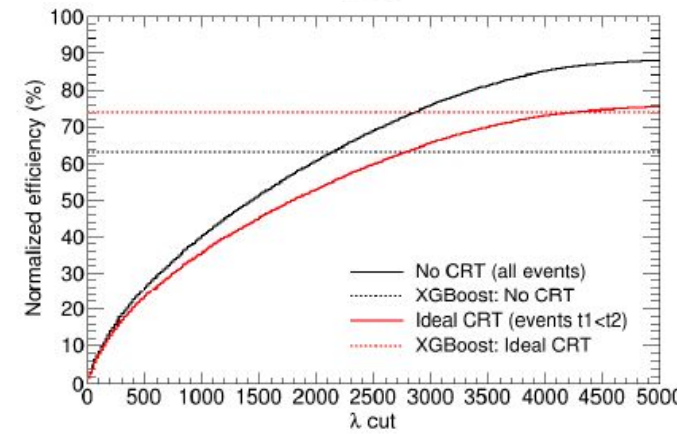
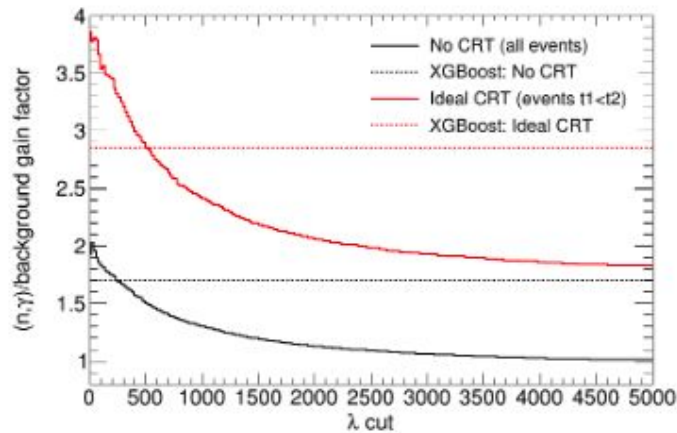


Values with no imaging cut

Coincidences and time resolution make a factor 2-3 in (n,γ)/background gain

Feasible (n,γ)/background gain:
Factor 5-10 depending of the sample-i-TED distance

i-TED 5: Promising results of ML techniques



ML- based background rejection:
Similar background rejection & (n,g) Efficiency x3 wrt
imaging

i-TED: First experimental proof-of-concept and future prospects based on
Machine-Learning techniques

V. Babiano-Suárez, J. Lerendegui-Marco¹, J. Balibrea, L. Caballero, D. Calvo, I. Ladarescu, C. Domingo-Pardo

^{79}Se vs Previous challenging capture measurements at n_TOF

79Se & Nb-94 vs others (n,g) @ n_TOF

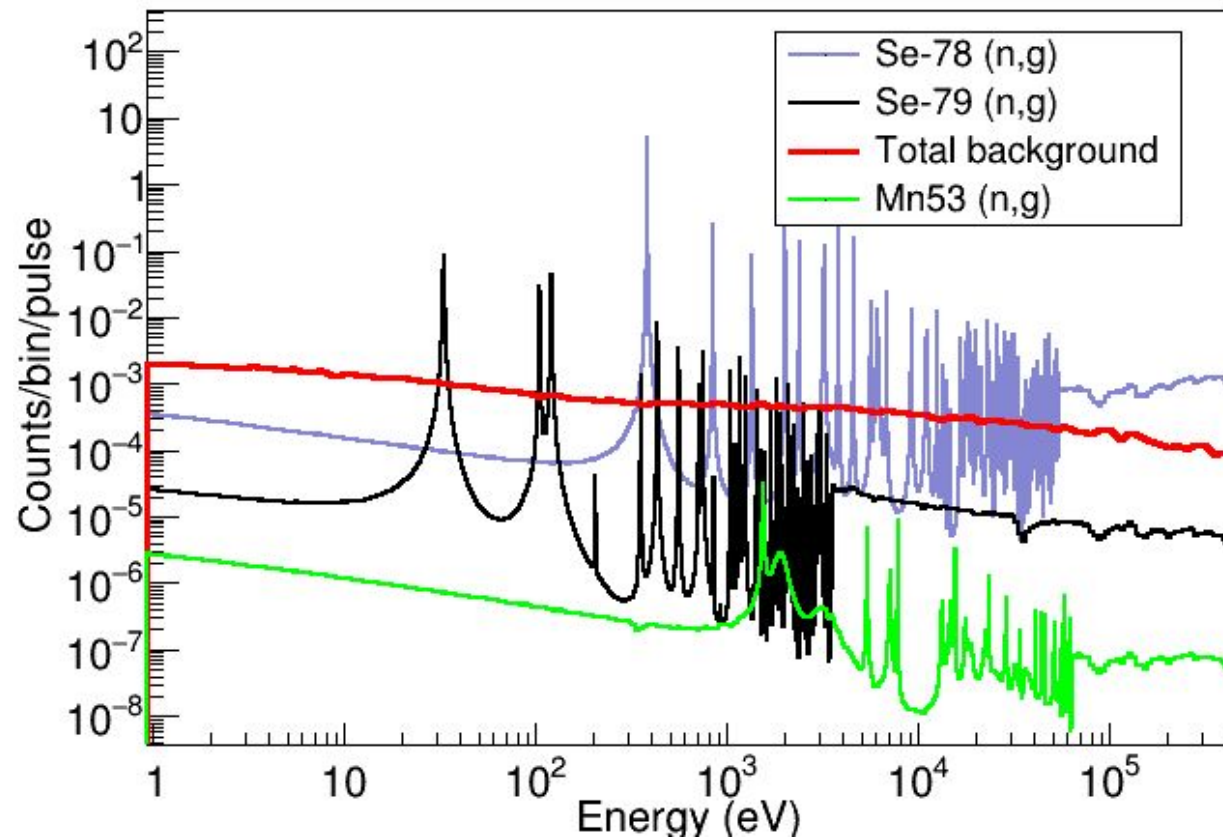
SAMPLE	Radius (cm)	Mass(mg)	Natoms	Natoms/barn	EAR	BIF
Mn-53	1	4.40E-02	5.00E+017	1.59E-007	2	0.45
TI-203	0.25	210	6.23E+020	3.17E-003	1	0.1
TI-204	0.25	9	2.66E+019	1.35E-004	1	0.1
Tm-171	1.1	3.03	1.07E+019	2.81E-006	1	0.65
Se-79	0.7	3	2.29E+019	1.49E-005	1 / 2	0.4 / 0.25
Se-78	0.7	1064	8.22E+021	5.34E-003	1 / 2	0.4 / 0.25
Nb-93	Different shapes	247.09	1.60E+21	5.94E-04	2	~0.25
Nb-94	Different shapes	1.43	9.24E+18	3.05E-06	2	~0.25

Sample properties 79Se and Nb-94 vs recent measurements:

- Number of atoms very similar to:
 - TI-204 (+TI-203): Feasible, analysis finished, writing Thesis → Very similar measurement (dominant amount of the A-1 isotope used as a seed in the irradiation)
 - Tm-171: Feasible and accepted for publication
- **Number of atoms/barn 10-20 times larger** than Mn-53: After measurement → Conclusion: Not feasible

Mn-53(n,g) vs 79Se(n,g)

SAMPLE	Radius (cm)	Mass(mg)	Natoms	Natoms/barn	EAR	BIF
Mn-53	1	4.40E-02	5.00E+017	1.59E-007	2	0.45

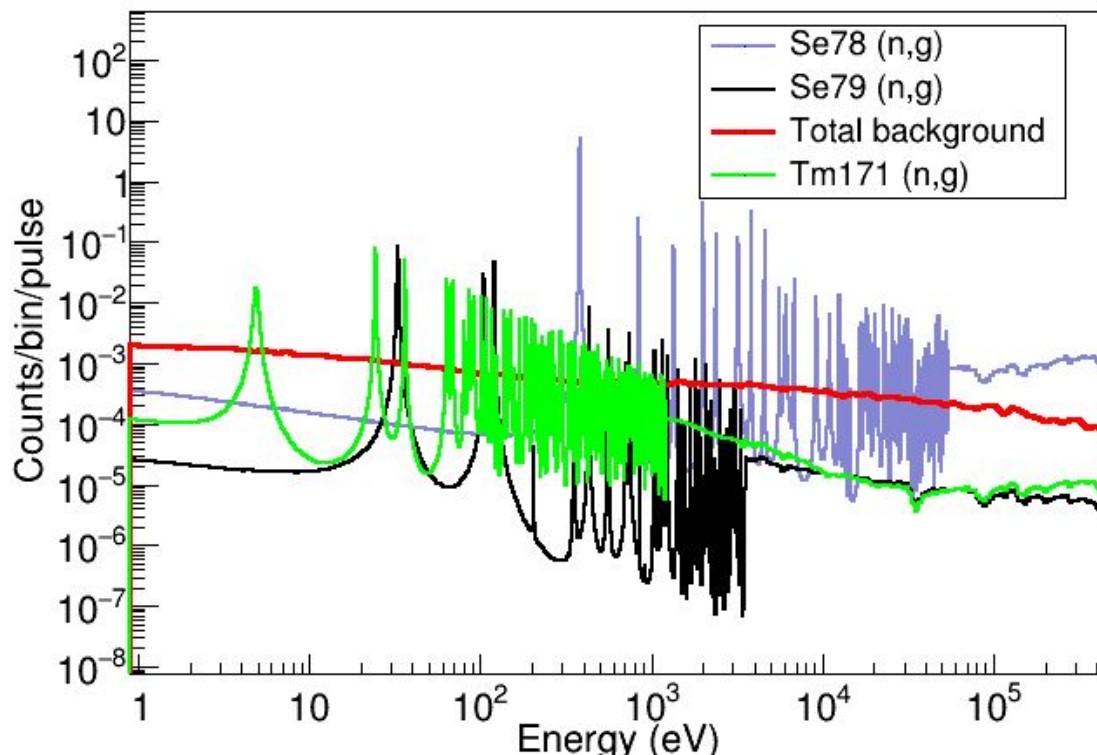


79Se has nothing to do with the case of the UNFEASIBLE Mn-53:

- Mn-53: Resonances were 2 orders of magnitude below background
- RESULT: Data useless
- 79Se: ≥ 10 resonances above background or at the level of background

Tm-171(n,g) vs 79Se(n,g)

SAMPLE	Radius (cm)	Mass(mg)	Natoms	Natoms/barn	EAR	BIF
Tm-171	1.1	3.03	1.07E+019	2.81E-006	1	0.65

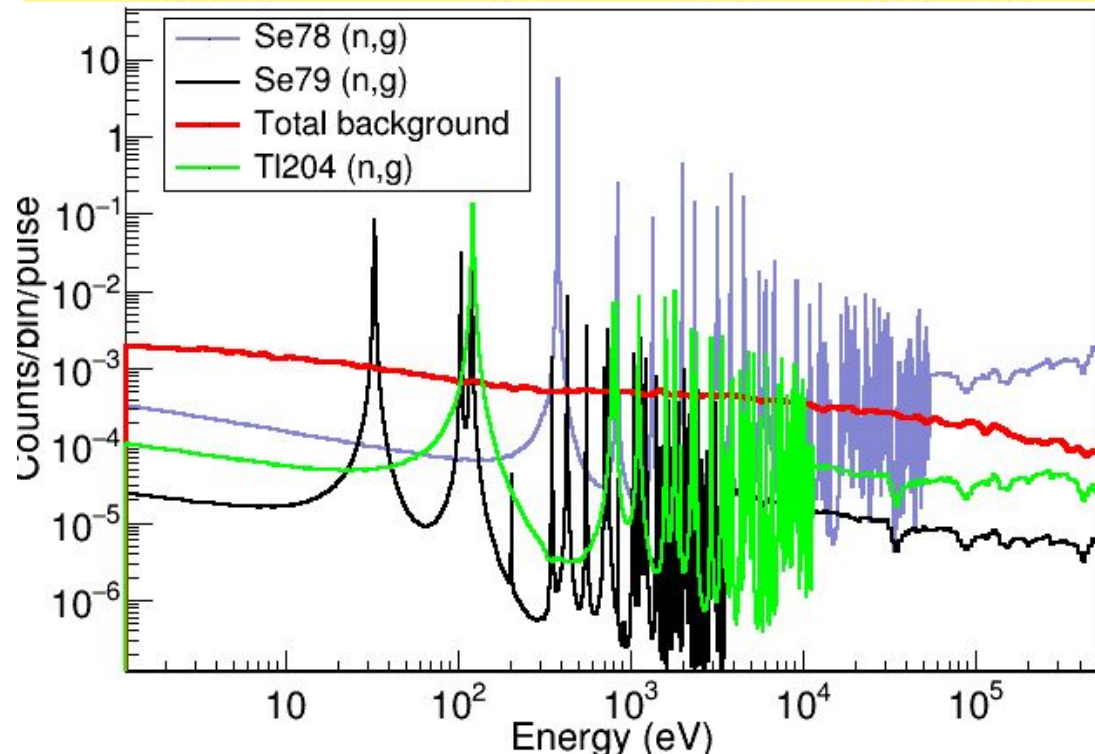


Feasibility of 79Se vs the SUCCESSFUL Tm-171(n,g):

- Tm-171: Level density found to be 40% of the expected value + smaller strength (MACS 40% of the value with JEFF-3.3) →
- RESULT: 28 resonances found up to 700 eV
- 79Se: Similar or higher resonance strength but less level density expected → Realistic: ≥ 10 resonances

Tl-204(n,g) vs 79Se(n,g)

SAMPLE	Radius (cm)	Mass(mg)	Natoms	Natoms/barn	EAR	BIF
TI-203	0.25	210	6.23E+020	3.17E-003	1	0.1
TI-204	0.25	9	2.66E+019	1.35E-004	1	0.1

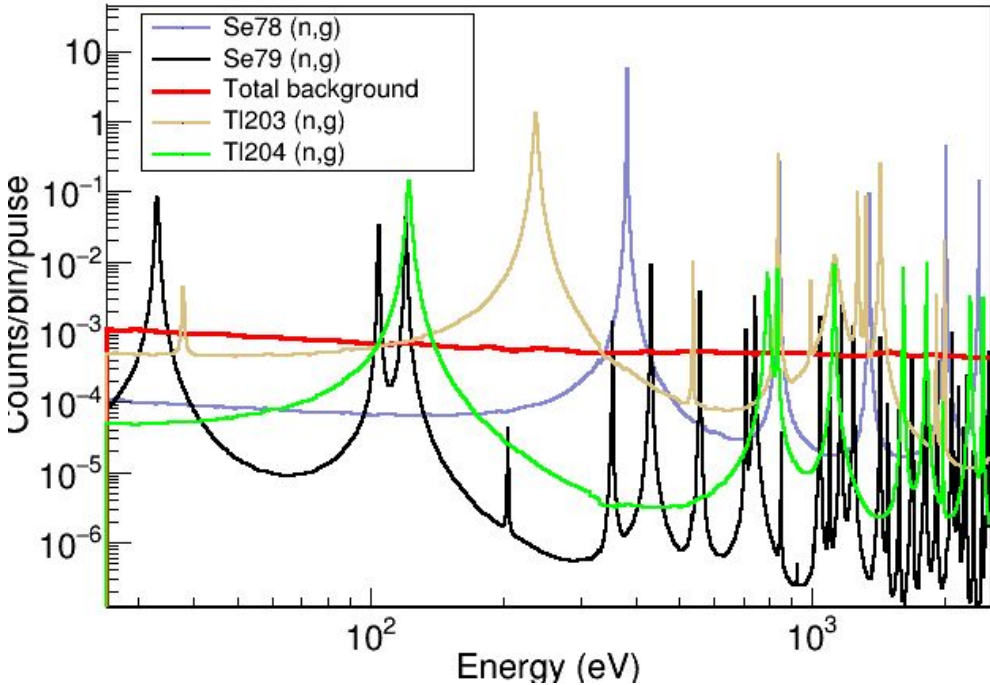


Feasibility of 79Se vs the SUCCESFUL TI-204(n,g):

- TI-204: Resonances could be analyzed. Lower level density than 79Se → less resonances.
- RESULT: 5 resonances found (+ several candidates) below 2 keV.
- 79Se: Similar resonance strength expected, higher level density than TI-204 and resonances at lower energies

Shape of TI-204/203 strange → Assumed 5 mm diam (BIF ~ 0.1)

SAMPLE	Radius (cm)	Mass(mg)	Natoms	Natoms/barn	EAR	BIF
TI-203	0.25	210	6.23E+020	3.17E-003	1	0.1
TI-204	0.25	9	2.66E+019	1.35E-004	1	0.1



Impact of the dominant isotope:

- TI-204: TI-203 matrix has higher level density than Se-78 →Some Overlaps.
- RESULT: 5 resonances found (+ several candidates) below 2 keV.
- 79Se: Similar resonance strength expected + advantages:
 - Larger level spacing of Se-78 than TI-203
 - Smaller level spacing of 79Se than TI204
 - Resonances at lower energies → More to be observed

Zoom in the RRR to compare Se-78/79 and TI-203/204

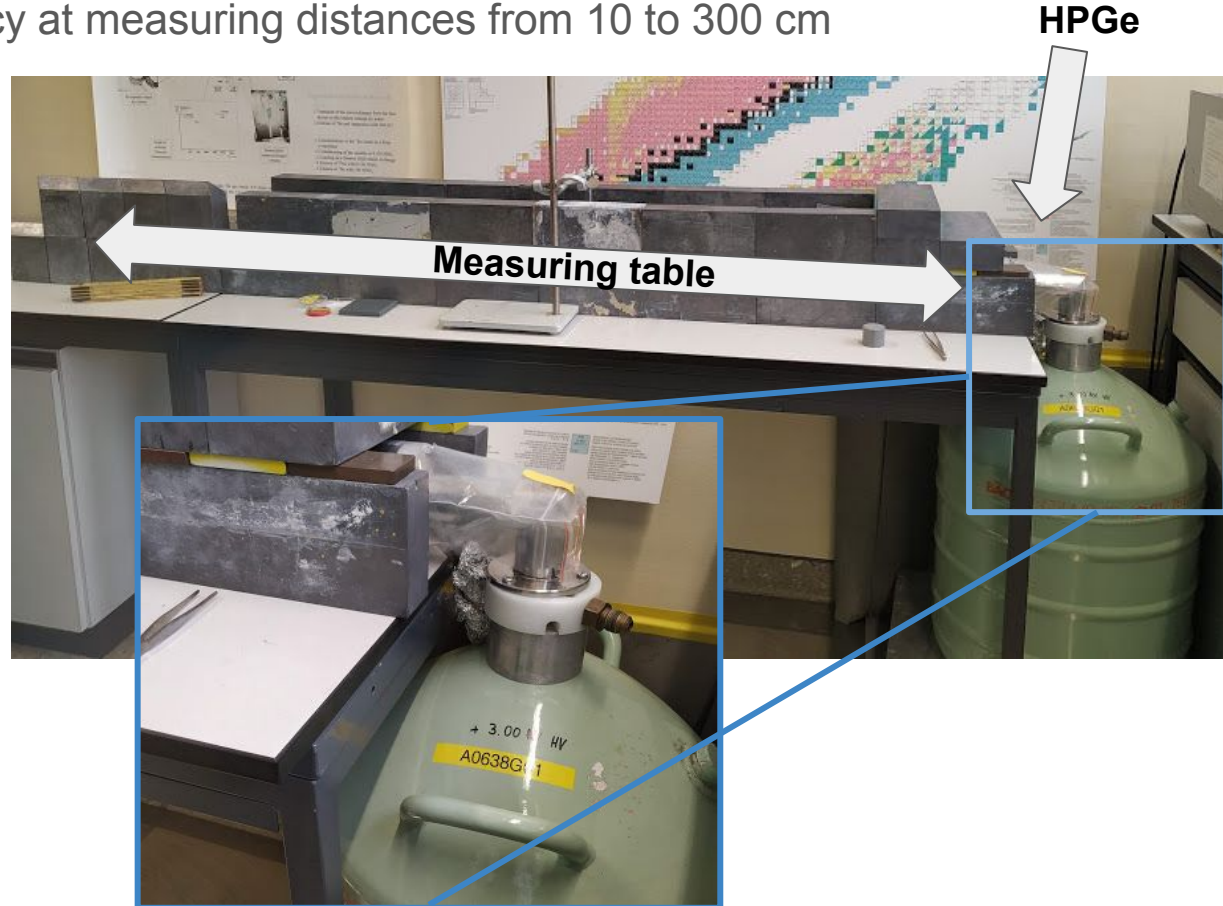
Sample characterization @ PSI

Experimental setup

- HPGe calibrated efficiency at measuring distances from 10 to 300 cm



NIM Rack: HV setup, Amplifier, ADC



Experimental setup

- Positioning at reference distances in the table and beyond



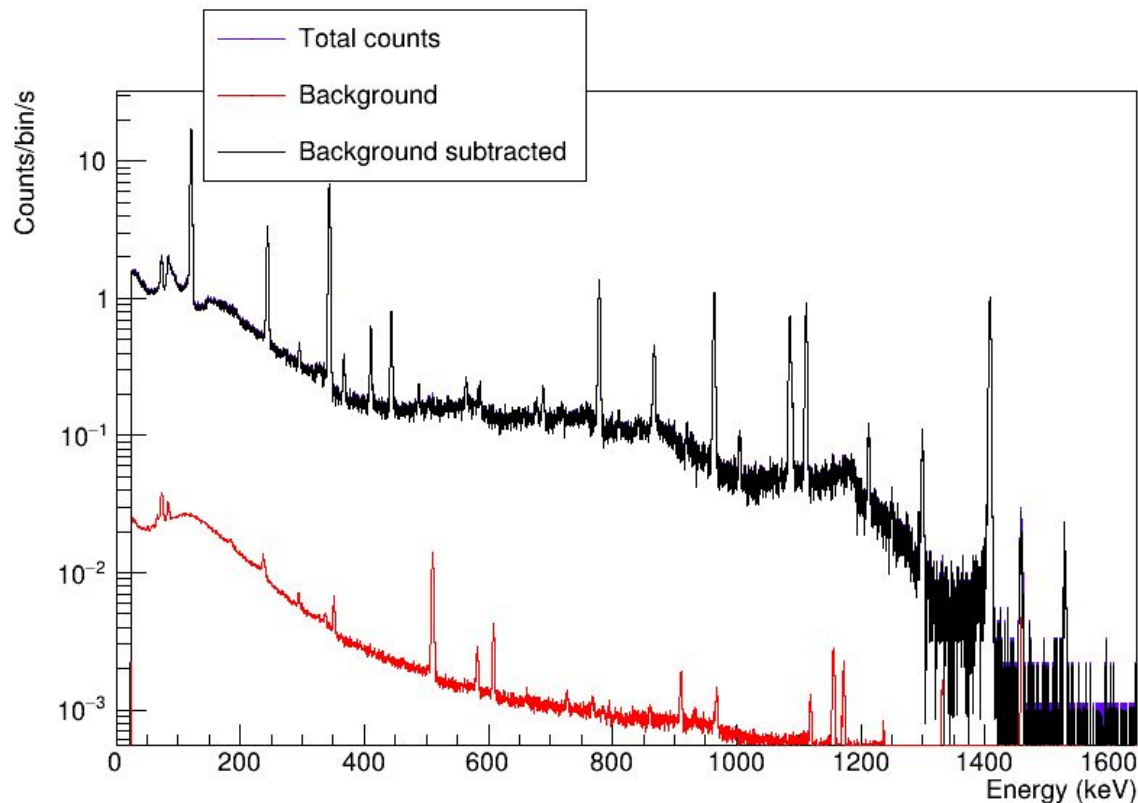
Nb samples @
150cm



Background subtraction

- All spectra Normalized to time → Subtract background with/without lead

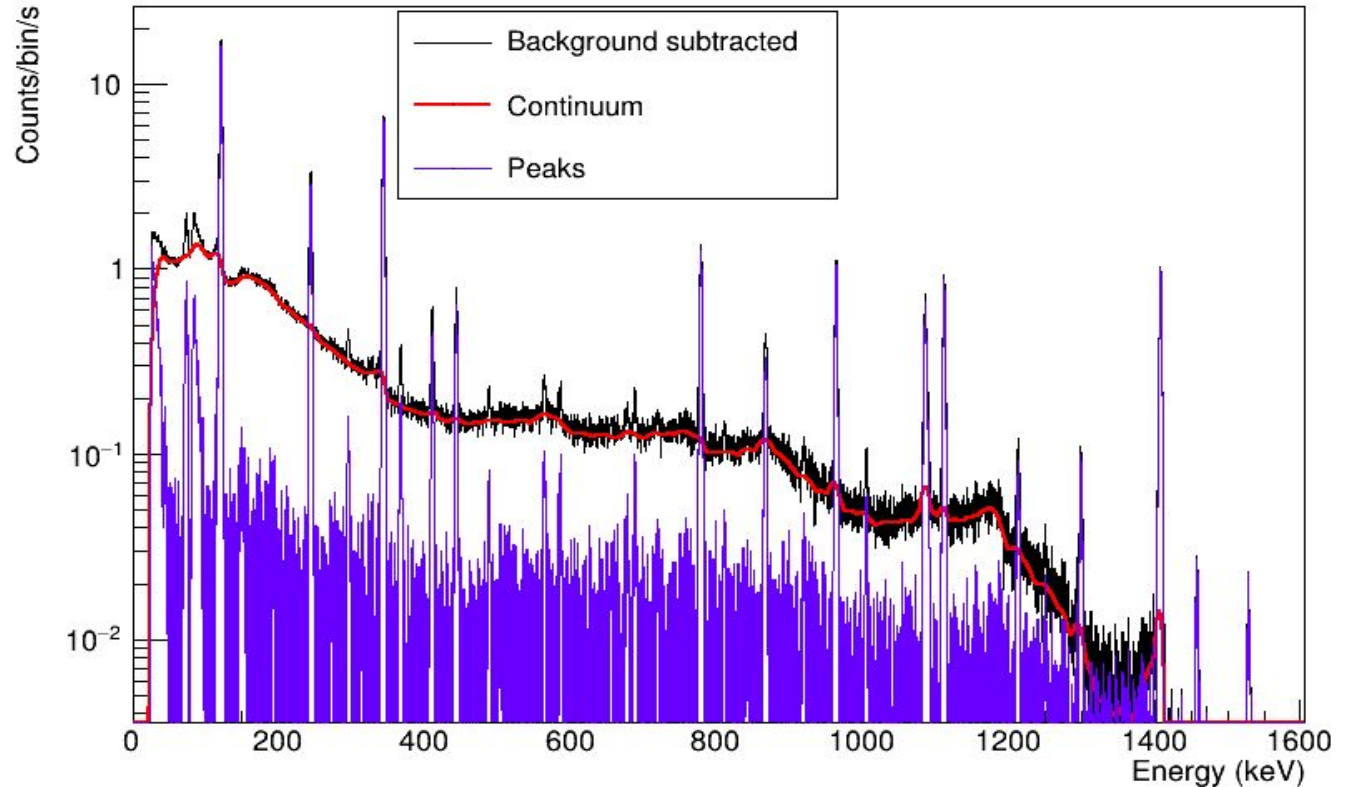
Example:
Eu-152
@ 10 cm



Continuum fitting

- TSpectrum: Background()

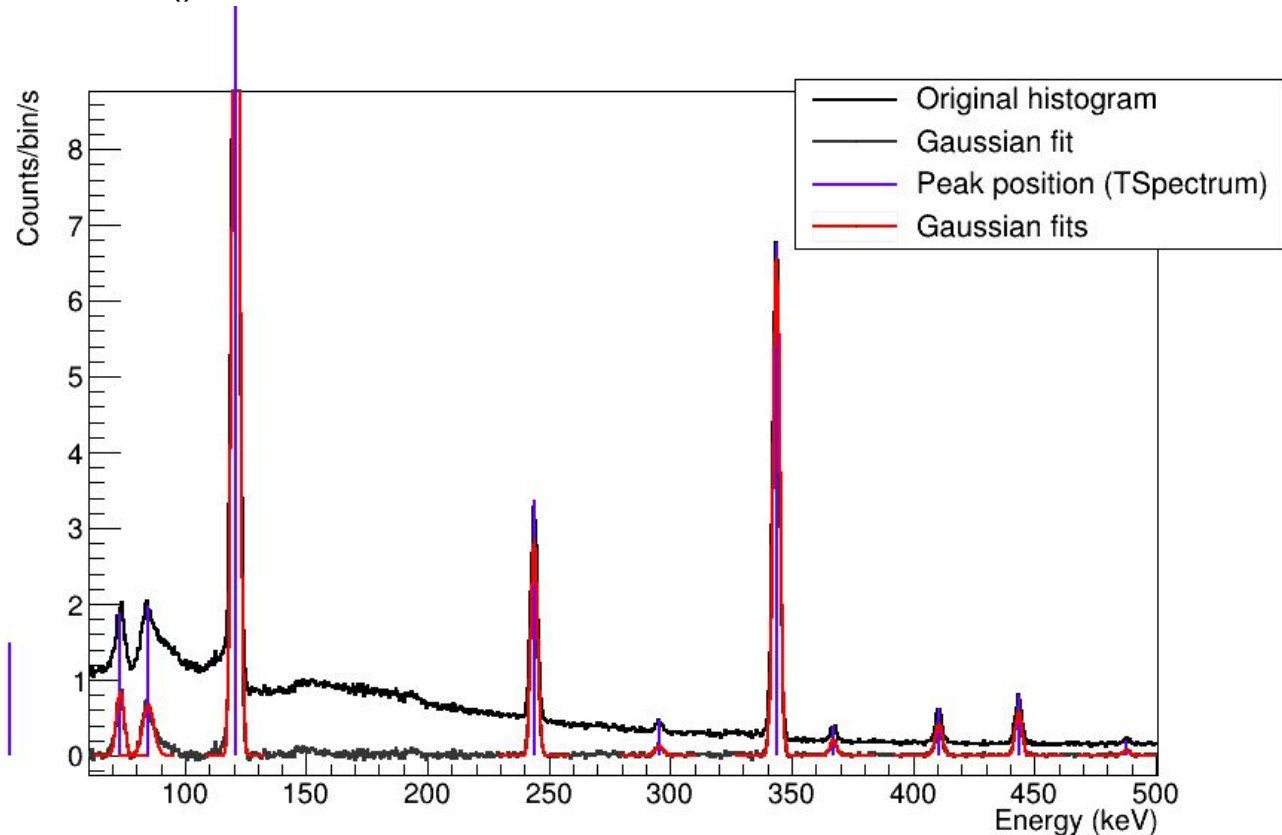
Example:
Eu-152
@ 10 cm



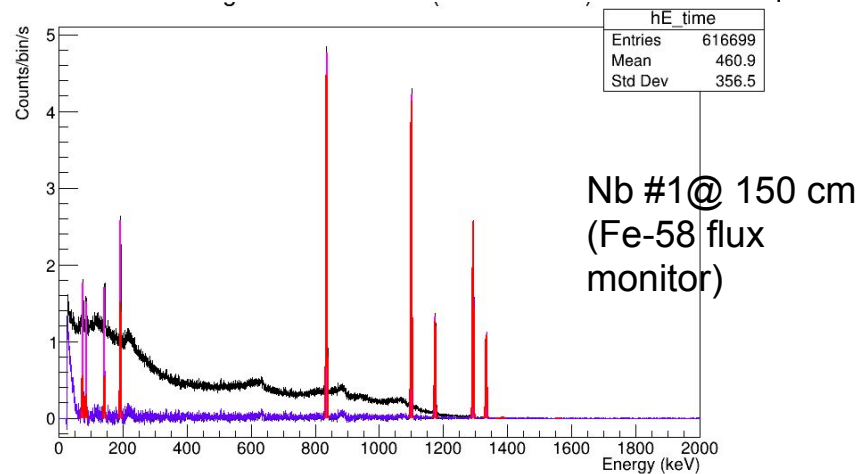
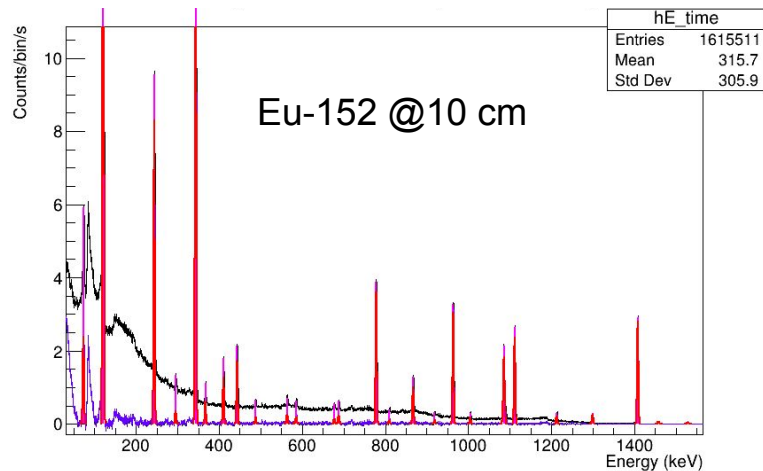
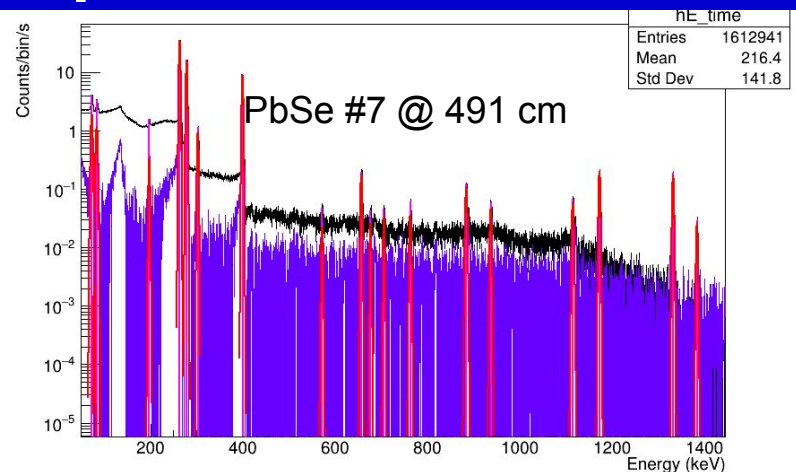
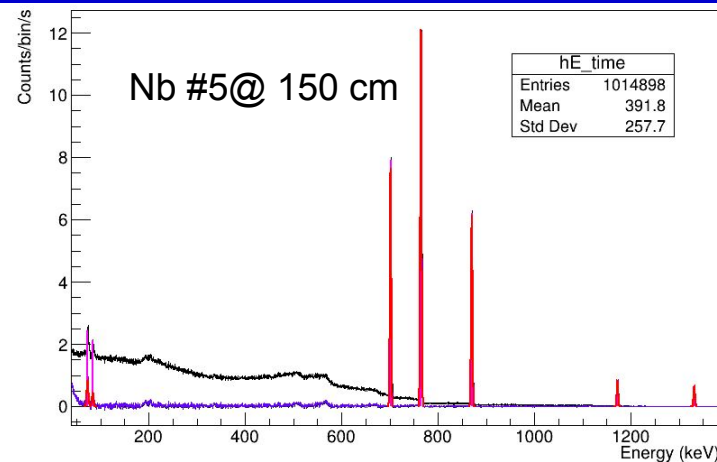
Peak search and fitting

- TSpectrum: Search()

Example:
Eu-152
@ 10 cm



Example of peak fits



Validation efficiency calibration

- Activity from average of lines found:

	Exp. Eu-152 Activity (kBq)					
	10 cm		50 cm		150 cm	
Ref. Efficiency curves	137.5	0.8	123.1	1.1	124.5	1.7
Corrected Efficiency	118.9	1.6	118	2	117.5	2.5
Corrected Efficiency (I>10%)	118	2.3	117.2	2.4	116	2.8
Real Activity	116.1	1.6	1.38%			

Deviation (wrt W. Avg)	10 cm	50 cm	150 cm
Ref. Efficiency curves	14.98%	4.18%	6.36%
Corrected Efficiency	2.35%	1.61%	1.19%
Corrected Efficiency (I>10%)	1.61%	0.94%	-0.09%

Deviations are ~2% or below:
Assume 2% uncertainty in the efficiency

Final results: validation lead correction

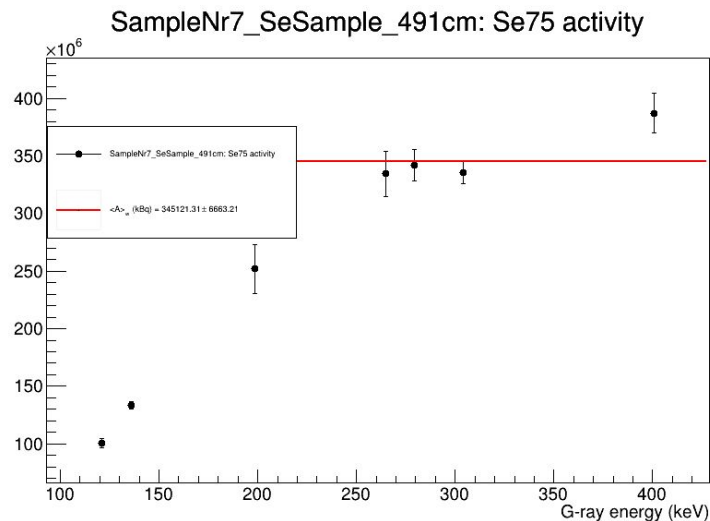
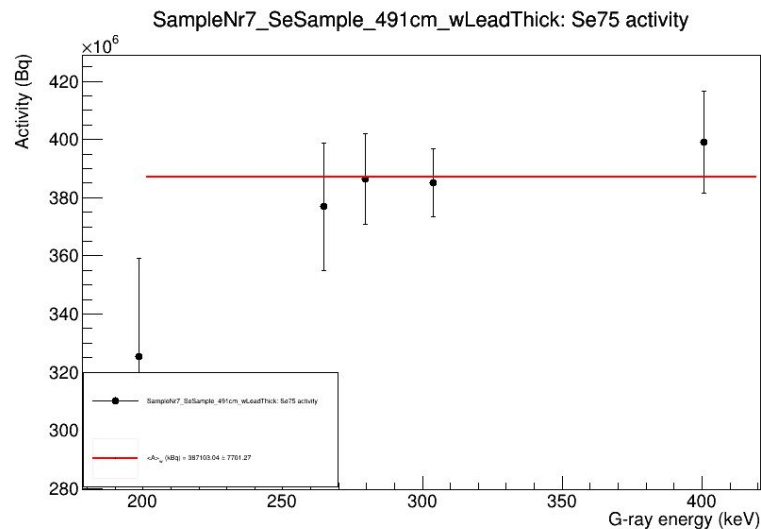
- After corrections for attenuation: Activity of Eu-152 from measurements with and without lead

	Exp. Eu-152 Activity (Bq)					
	10 cm		50 cm		150 cm	
No Lead	118.9	1.6	118	2	117.5	2.5
2 mm Lead shielding	118.8	1.7	119	3	118.0	2.4
Real Activity	116.1	1.6	1.38%			

- Compatible values for the Eu-152 activity** are extracted from the measurements **with and without lead**.
- This applies for the **measurements at 3 different distances**
- All **compatible with the certified activity within 1-2%**

Final results: PbSe sample

- Summary of the g-ray emitters in the measured PbSe sample



PbSe with Lead →

Se- 75 Line at 197 keV deviates significantly

Reason: **90% correction for lead shielding, attenuation air?)** .

PbSe Without Lead →

Se-75: Activity extracted from lowE Peaks is underestimated.

Reason: Significant **dead time (10%) (BStrahlung at low E), attenuation air ?**

Final results: PbSe sample

- Summary of the g-ray emitters in the measured PbSe sample

PbSe + Lead (491 cm)		PbSe (No lead) (491 cm)	
Isotope	Activity (Mbq)(*)	Isotope	Activity (Mbq)(*)
Se-75	387(7)	Se-75	345(6)
Ag-110m	1.55(4)	Ag-110m	1.48(4)
Zn-65	1.85(19)	Zn-65	1.98(19)
Co-60	2.82(8)	Co-60	2.86(8)

Differences in Se-75 between lead and no lead

Compatible for all other isotopes

Possible Reason: Se-75 has low energy gammas

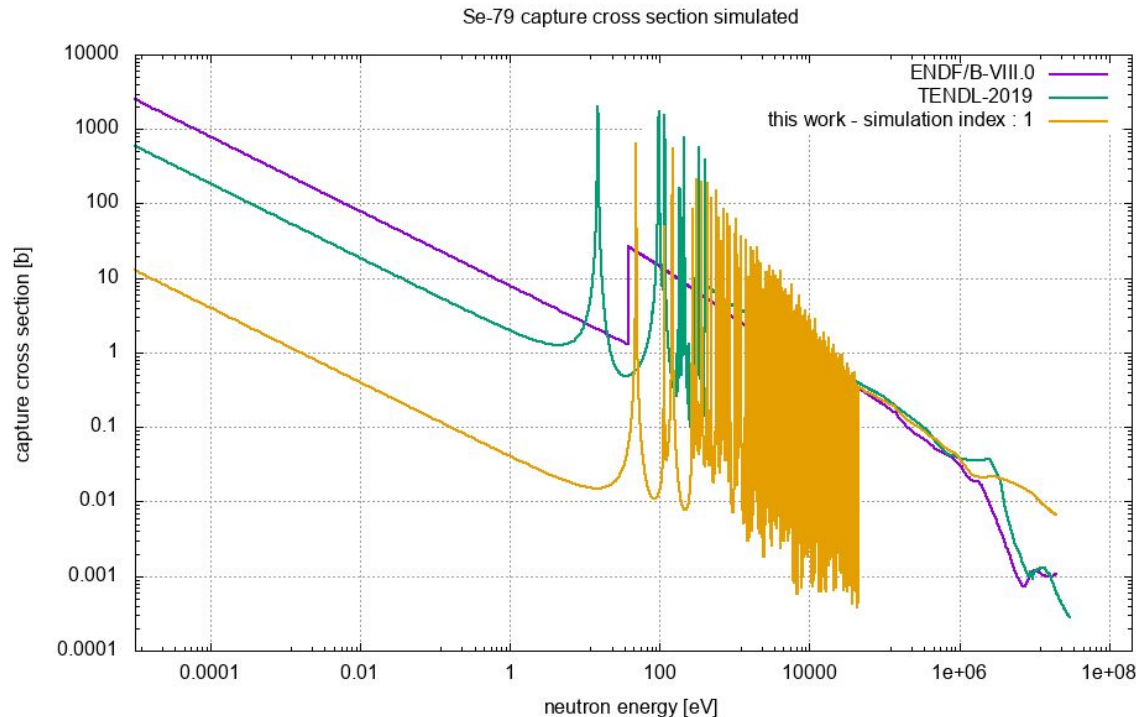
Details on the counting rate estimates and feasibility study

A. Mengoni's calculations:

300 sets of resonance using
average parameters in
TALYS:

- $\langle D0 \rangle = 56.8 \text{ eV}$
- $S0 = 0.98 \times 10^{-4}$
- $\langle \Gamma_{g(0)} \rangle = 0.078$
(+10%)

JEFF-3.3 (TENDL 2019)
uses $\langle \Gamma_{g(0)} \rangle =$
0.100 meV

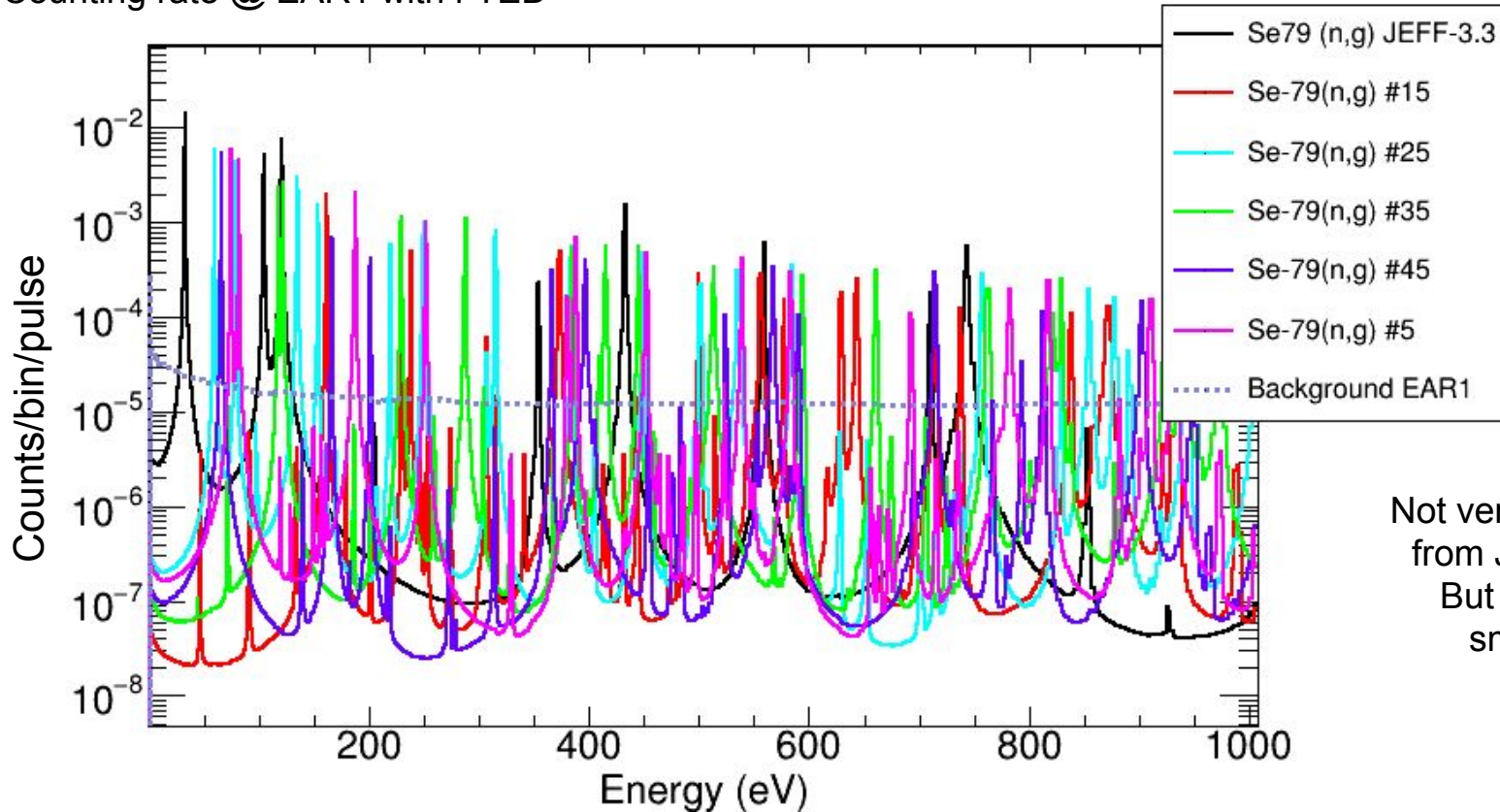


Calculation RRR: some realizations are compatible to JEFF-3.3 (used for the estimates).
In some cases the strength of resonances is smaller

Calculation URR: Above 55 keV, TALYS Statistical model

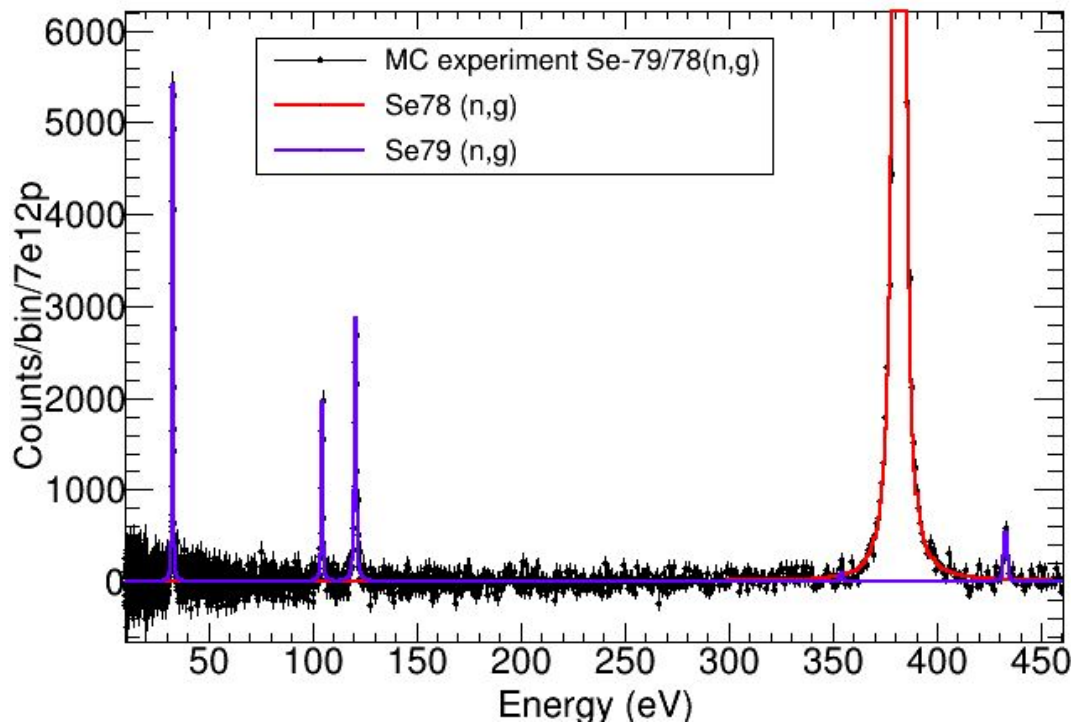
Input: ^{79}Se C. Rate

Counting rate @ EAR1 with i-TED



Not very different
from JEFF-3.3
But slightly
smaller

MC experiment: Se-78 + 79Se



i-TED @ EAR1

2.5e18 protons PbSe sample

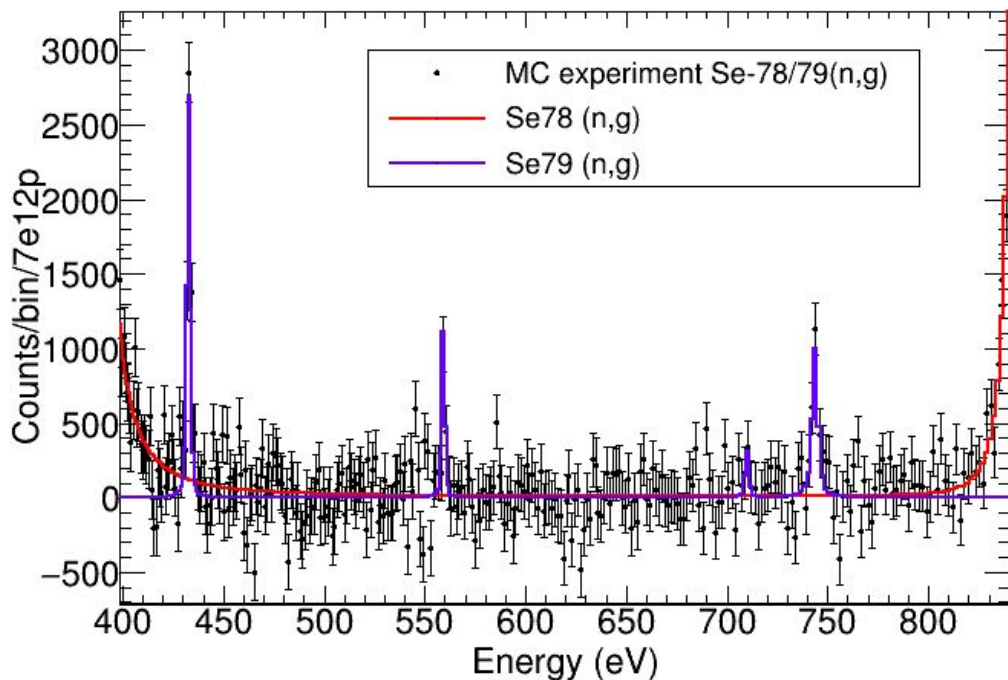
0.5 protons dummy (Pb + Al + empty)

Detection Limit
For a given resonance (ROI)

$$D = (\text{Exp. Counts} - \text{Se-78}) / \text{unc_Counts}$$

Based on JEFF-3.3
XS (TENDL)

MC experiment: Se-78 + 79Se



Detection Limit
For a given resonance (ROI)

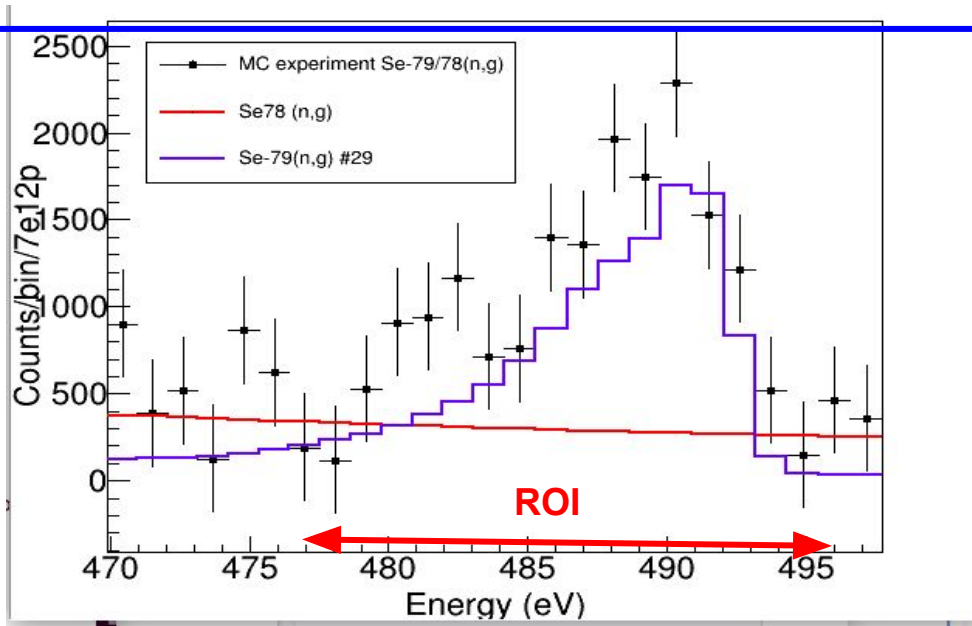
$$D = (\text{Exp. Counts} - \text{Se-78}) / \text{unc_Counts}$$

Based on JEFF-3.3
XS (TENDL)

C6D6 or i-TED Scatterer @ EAR1
2.5e18 protons PbSe sample
0.5 protons dummy (Pb + Al + empty)

Detection limit study: Validation

Statistical significance D, calculated for each resonance as $D = (C_{\text{exp}} - C_{78\text{Se}}) / \text{Unc}(C_{\text{exp}} - C_{78\text{Se}})$



ROI adjusted to consider the RF broadening of the resonances in EAR2

Example: Realization #29

Integration window (ROI) adjusted:

- Resonance maximum found in the theoretical counting rate of ^{79}Se (blue)
- Integration windows: +4,-4 eV @ EAR1 (RF negligible), -8,+3 eV @ EAR2

Details on the HF calculation in the URR & the calculation of the MACS

^{79}Se : Avg. Parameters from RRR

energy range	0 - 15	keV	restricted to include p-waves
$\langle D_0 \rangle$	56.8	eV	LVD calculations
$S_0 \times 10^4$	0.93		OMP calculations
$\Gamma_{\gamma 0}$	78.2 ± 7.8	meV	statistical model calculations
$\langle D_1 \rangle$	30.1	eV	LVD calculations
$S_1 \times 10^4$	1.60		OMP calculations
$\Gamma_{\gamma 1}$	82.7 ± 8.3	meV	statistical model calculations

Observable resonances

S: $1.5\text{e}18$ + B: $5\text{e}17$: 15(4) - 11(3)

S: $1.\text{e}18$ + B: $1\text{e}18$: 15(3) - 14(3)

Uncertainty in S_0 and D_0 (only statistical properties)

Best: 18 resonances: $\text{unc_D0} = 12\%$, $\text{unc_S0} = 36\%$

Worst: 8 resonances: $\text{unc_D0} = 18\%$, $\text{unc_S0} = 53\%$

79Se: Avg. Parameters from RRR

Th. Avg. parameters	S0 (e-4)	Gg0 (eV)	D0 (eV)	S1 (e-4)	Gg1
Mean XS	0.930	0.078	56.8	1.6	0.0827

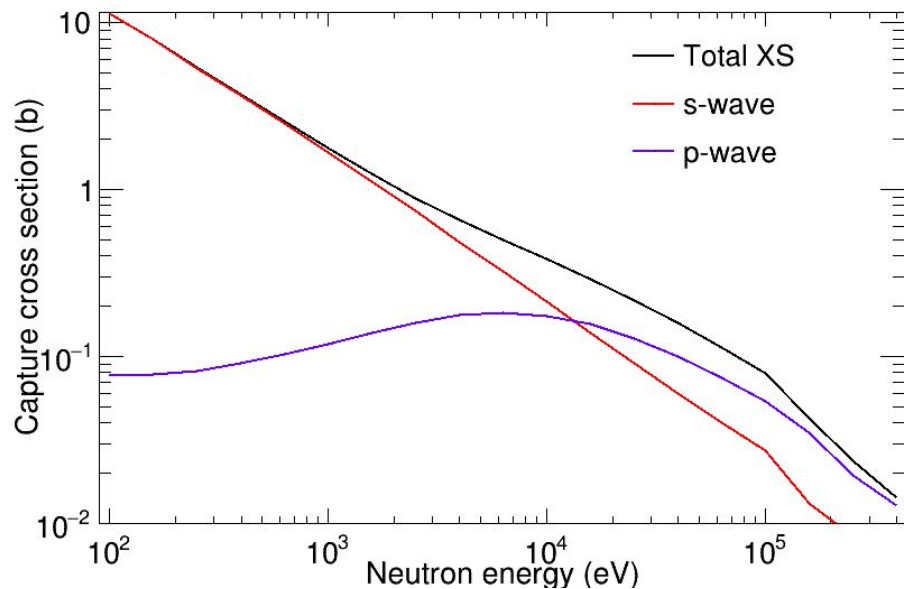
Observed 8 resonances	S0 (e-4)	Gg0 (eV)	D0 (eV)	S1 (e-4)	Gg1
Minimum XS	0.434	0.0702	67.2973	1.6	0.0744
Maximum XS	1.426	0.0858	46.3027	1.6	0.091

Observed 18 resonances	S0 (e-4)	Gg0 (eV)	D0 (eV)	S1 (e-4)	Gg1
Minimum XS	0.600	0.0702	63.7982	1.6	0.0744
Maximum XS	1.261	0.0858	49.8018	1.6	0.091

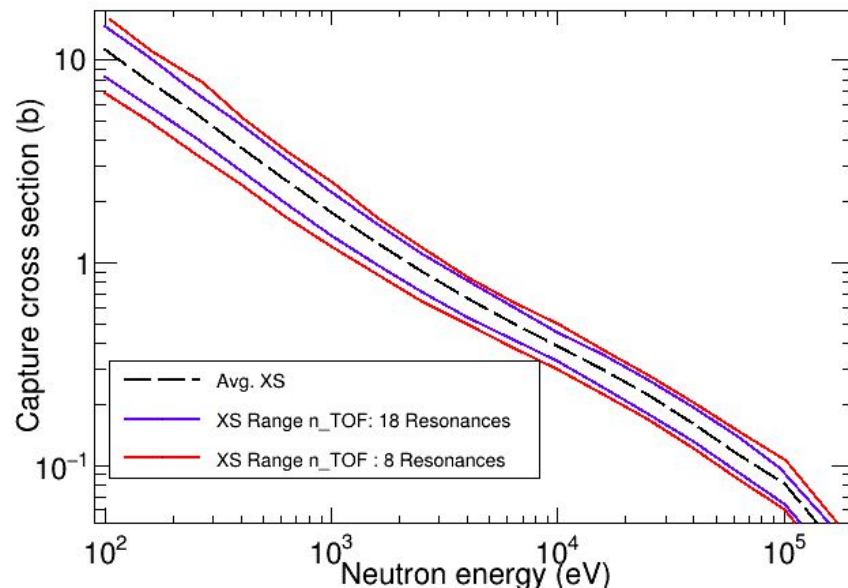
INPUT FOR SAMMY FITACS TO EVALUATE:

- Impact of the s-wave XS in the MACS @ 30 keV
- Max and min Uncertainty in the extracted MACS vs nr. Observed resonances

$^{79}\text{Se}(n,g)$: FITACS calculation URR

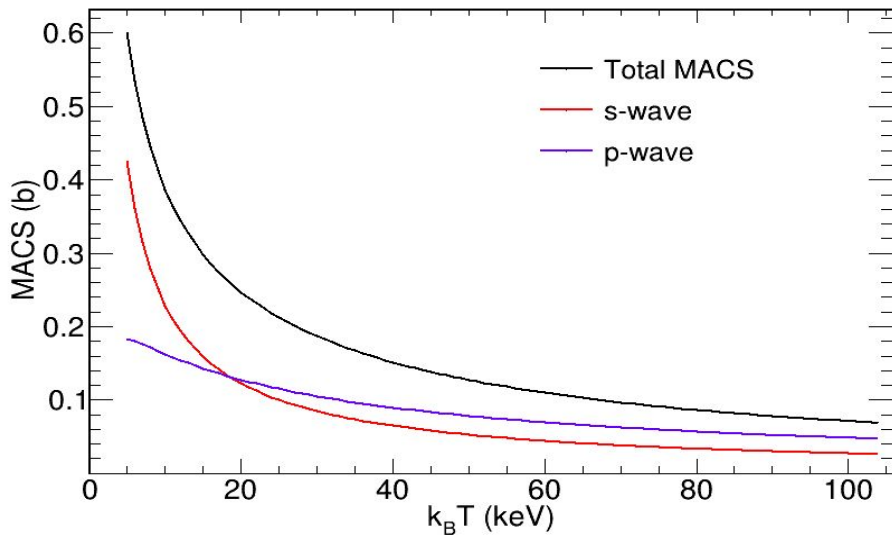


Contribution of s-wave and p-wave



Impact of the uncertainty in the Avg. Parameters extracted vs Nr resonances

$^{79}\text{Se}(n,g)$: Impact RRR in the MACS

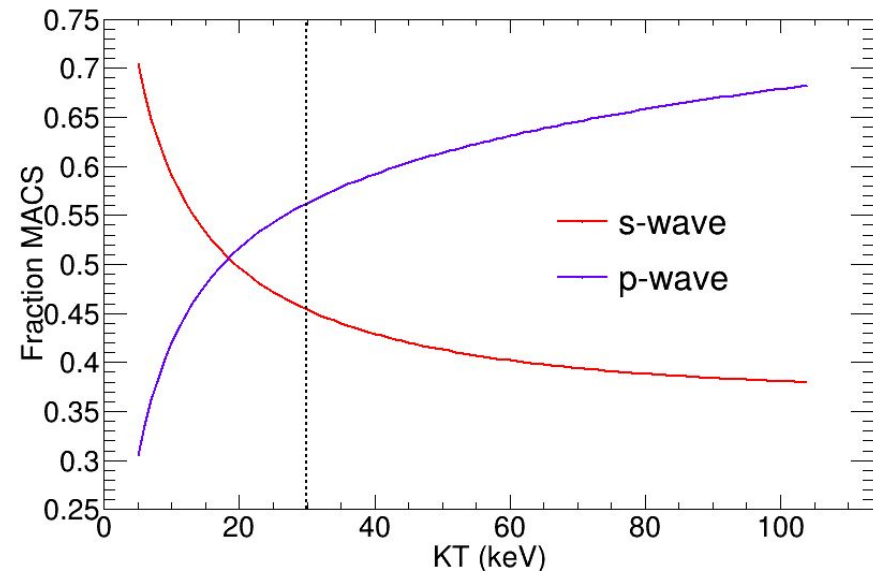


Contribution of s-wave and p-wave

Final A. Mengoni's parameters

MACS @ 30 keV (b)

TOTAL	0.187
S-wave	0.085
P-wave	0.102

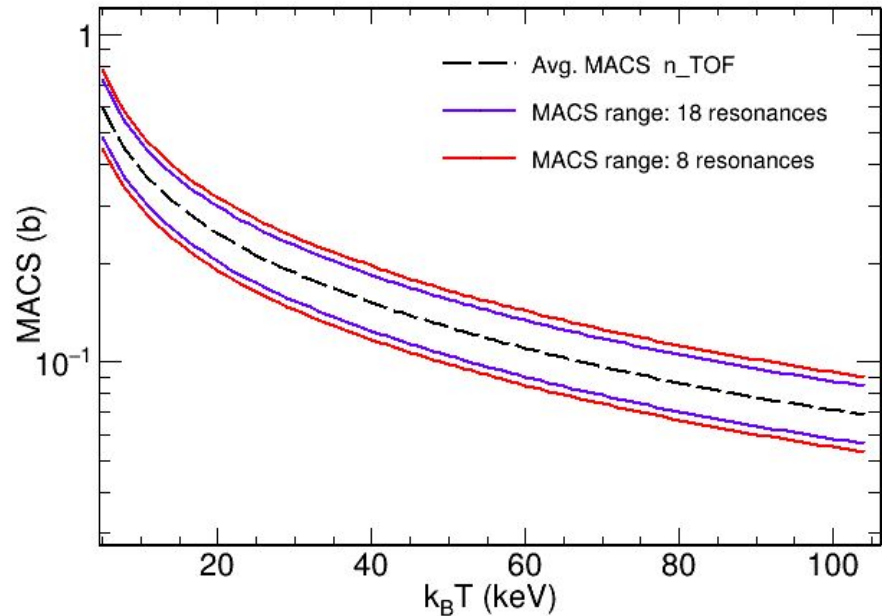


Fraction of s- and p-wave: Impact of the RRR in the MACS

Measurement of the RRR (s-wave only observed)
constraints 45% of the MACS value

$^{79}\text{Se}(n,g)$: Constraining the MACS

Impact of the uncertainties
in the final MACS @ 30 keV



Se-79 MACS @ 30 keV: s-wave (RRR) + p-wave (syst.)				
Nr. resonances	Mean XS (b)	Upper Limit (b)	Lower limit (b)	Avg. Uncertainty (%)
8	0.187	0.241	0.144	26%
18	0.187	0.226	0.153	20%

Previous s-process branching points @ n_TOF: The example of ^{171}Tm

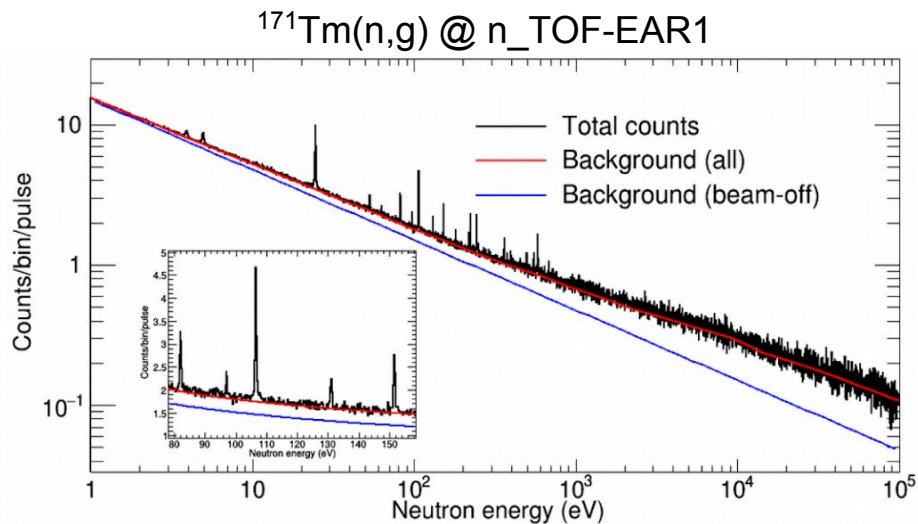
s-process branching points at n_TOF

REVIEW OF MODERN PHYSICS, VOLUME 83, JANUARY–MARCH 2011

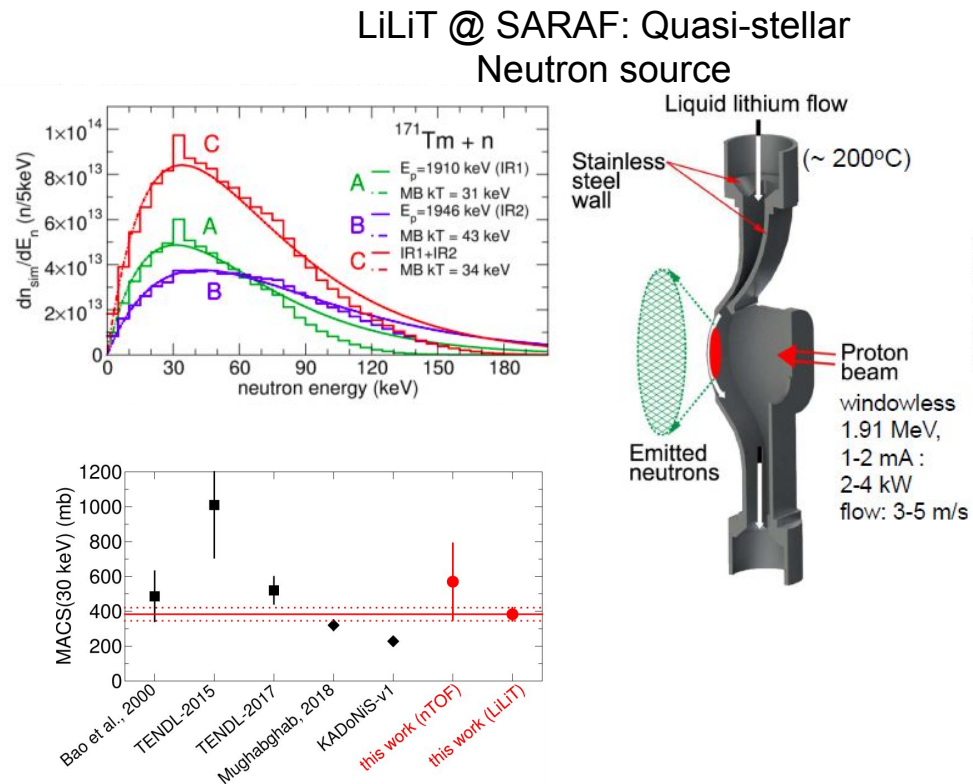
Sample	Half-life (yr)	Q value (MeV)	Comment
^{63}Ni	100.1	β^- , 0.066	TOF work in progress (Couture, 2009), sample with low enrichment
^{79}Se	2.95×10^3	β^- , 0.159	Important branching, constrains s -process temperature in massive stars
^{81}Kr	2.29×10^5	EC, 0.322	Part of ^{79}Se branching
^{85}Kr	10.73	β^- , 0.687	Important branching, constrains neutron density in massive stars
^{95}Zr	64.02 d	β^- , 1.125	Not feasible in near future, but important for neutron density low-mass AGB stars
^{134}Cs	2.0652	β^- , 2.059	Important branching at $A = 134, 135$, sensitive to s -process temperature in low-mass AGB stars, measurement not feasible in near future
^{135}Cs	2.3×10^6	β^- , 0.269	So far only activation measurement at $kT = 25$ keV by Patronis <i>et al.</i> (2004)
^{147}Nd	10.981 d	β^- , 0.896	Important branching at $A = 147/148$, constrains neutron density in low-mass AGB stars
^{147}Pm	2.6234	β^- , 0.225	Part of branching at $A = 147/148$
^{148}Pm	5.368 d	β^- , 2.464	Not feasible in the near future
^{151}Sm	90	β^- , 0.076	Existing TOF measurements, full set of MACS data available (Abbondanno <i>et al.</i> , 2004a; Wisshak <i>et al.</i> , 2006c)
^{154}Eu	8.593	β^- , 1.978	Complex branching at $A = 154, 155$, sensitive to temperature and neutron density
^{155}Eu	4.753	β^- , 0.246	So far only activation measurement at $kT = 25$ keV by Jaag and Käppeler (1995)
^{153}Gd	0.658	EC, 0.244	Part of branching at $A = 154, 155$
^{160}Tb	0.198	β^- , 1.833	Weak temperature-sensitive branching, very challenging experiment
^{163}Ho	4570	EC, 0.0026	Branching at $A = 163$ sensitive to mass density during s process, so far only activation measurement at $kT = 25$ keV by Jaag and Käppeler (1996b)
^{170}Tm	0.352	β^- , 0.968	Important branching, constrains neutron density in low-mass AGB stars
^{171}Tm	1.921	β^- , 0.098	Part of branching at $A = 170, 171$
^{179}Ta	1.82	EC, 0.115	Crucial for s -process contribution to ^{180}Ta , nature's rarest stable isotope
^{185}W	0.206	β^- , 0.432	Important branching, sensitive to neutron density and s -process temperature in low-mass AGB stars
^{204}Tl	3.78	β^- , 0.763	Determines $^{205}\text{Pb}/^{205}\text{Tl}$ clock for dating of early Solar System

Recent (2015-2017): +3 measured at CERN n_TOF (Suiza) and SARAF-LiLIT (Israel)

Previous s-process branchings at n_TOF: ^{171}Tm

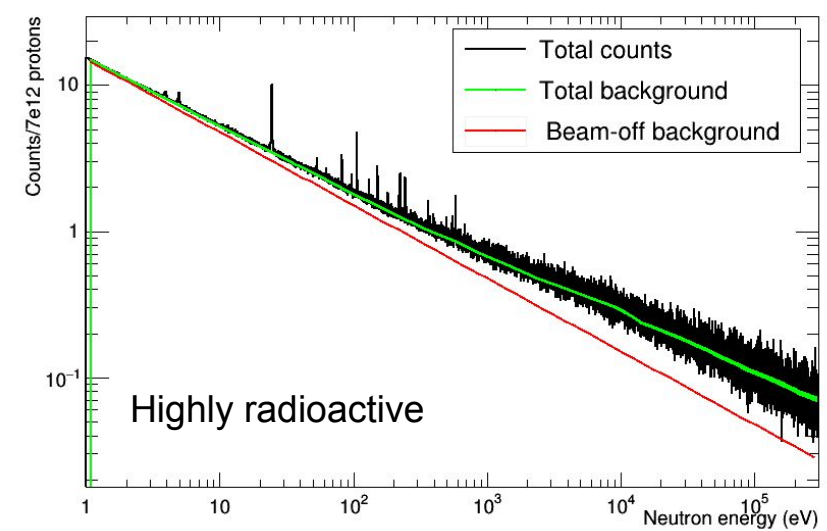


Constraining the MACS from the TOF measurement of the resonance region:
Same method proposed for ^{79}Se



Compatible MACS: LiLiT & n_TOF

- C. Guerrero, J. Lerendegui-Marco et al., **Phys. Rev. Letters** **125**, 142701 (2020).

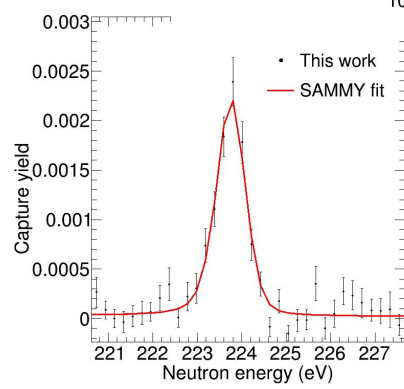
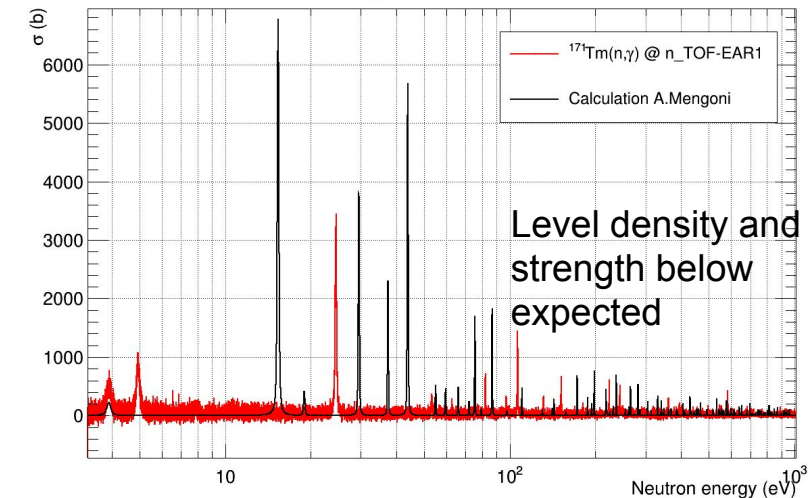


R-Matrix analysis RRR:
28 resonances

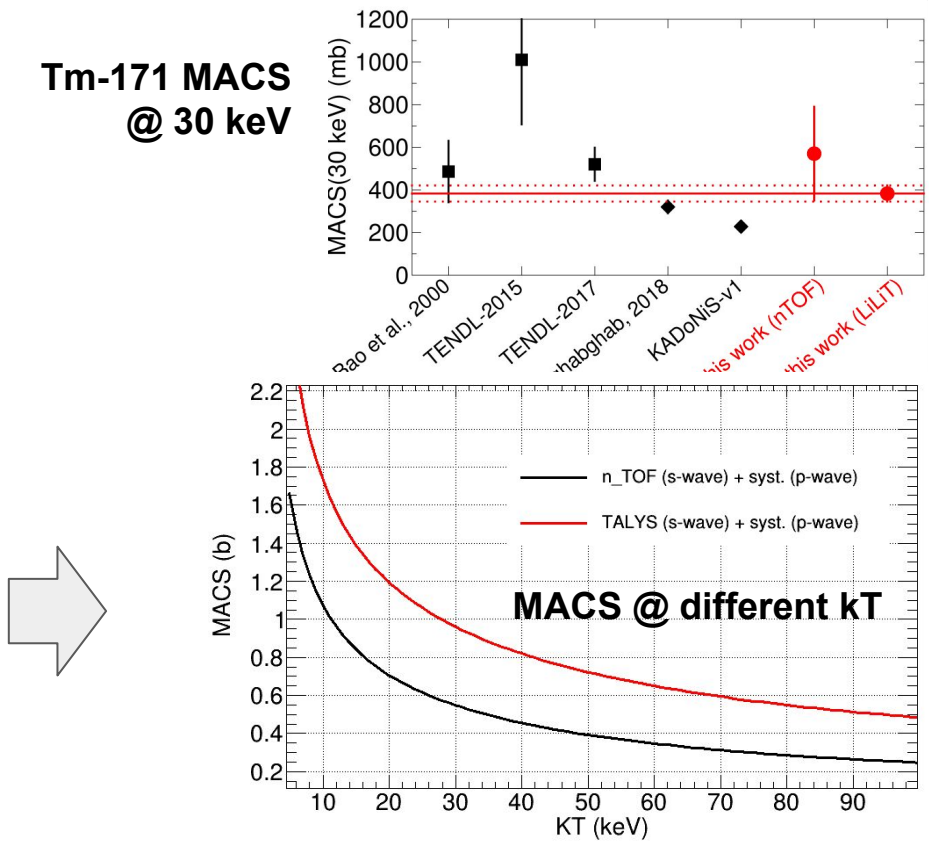
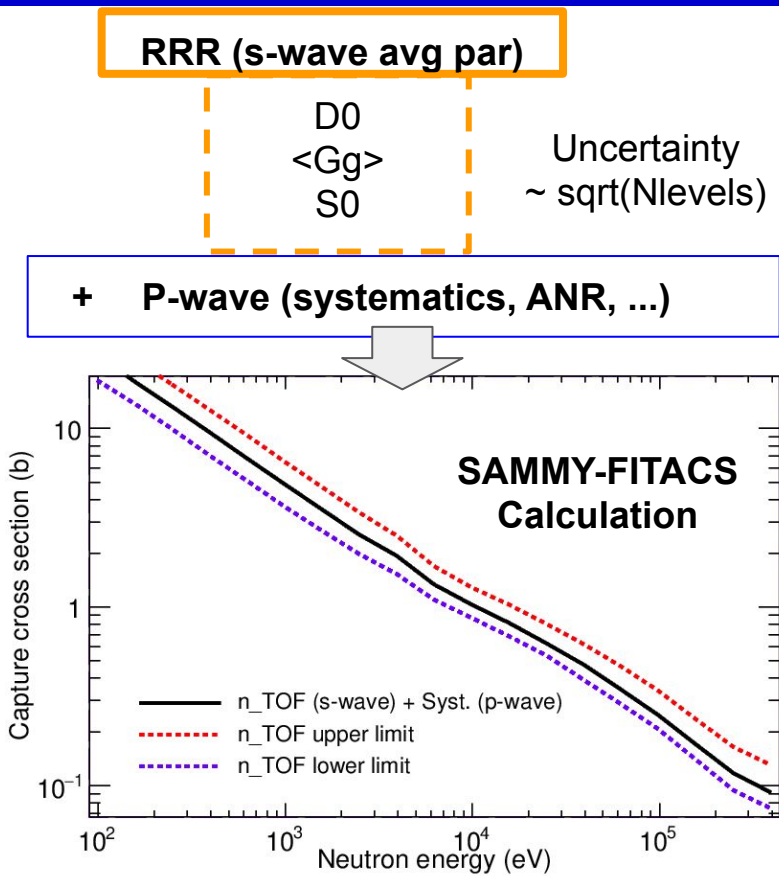
D0

<Gg>

S0



- C. Guerrero, J. Lerendegui-Marco et al., Phys. Rev. Letters **125**, 142701 (2020).



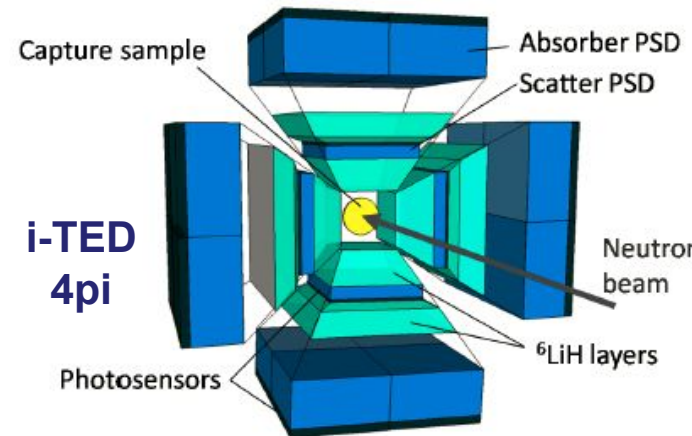
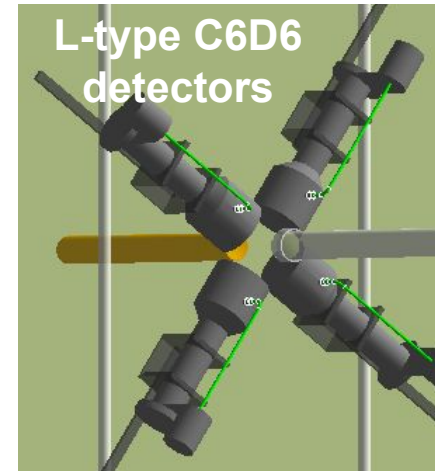
- C. Guerrero, J. Lerendegui-Marco et al., Phys. Rev. Letters **125**, 142701 (2020).

$^{79}\text{Se}(n,\gamma)$ @ EAR1: i-TED vs C6D6

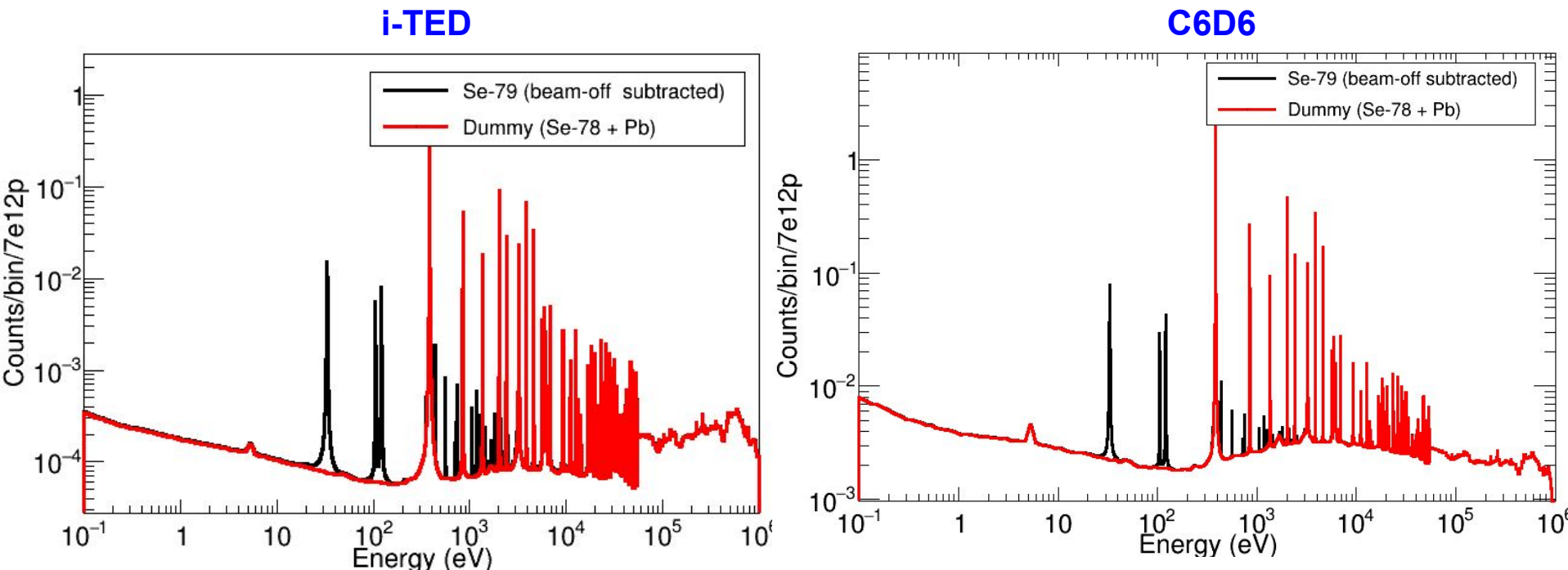
Detectors and EARs: summary

DETECTOR EAR		
	EAR1	EAR2
C6D6	Higher efficiency, Worse background rejection (large neutron scattering)	Better Performance @ high CR More statistics Activity not an issue
I-TED	~ 5-10 x Better (n, γ)/background in the keV range. C. Rate is not an issue.	Performance in EAR2 is still uncertain, probably too high CR

**Combined proposal:
i-TED (+ C6D6?) @ EAR1 & C6D6 @ EAR2**

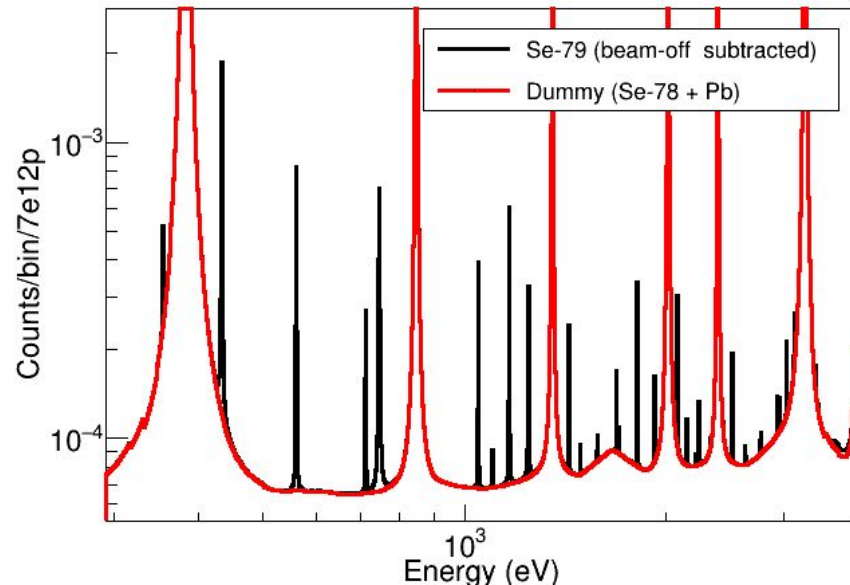


$^{79}\text{Se}(n,\gamma)$ @ EAR1: i-TED vs C6D6

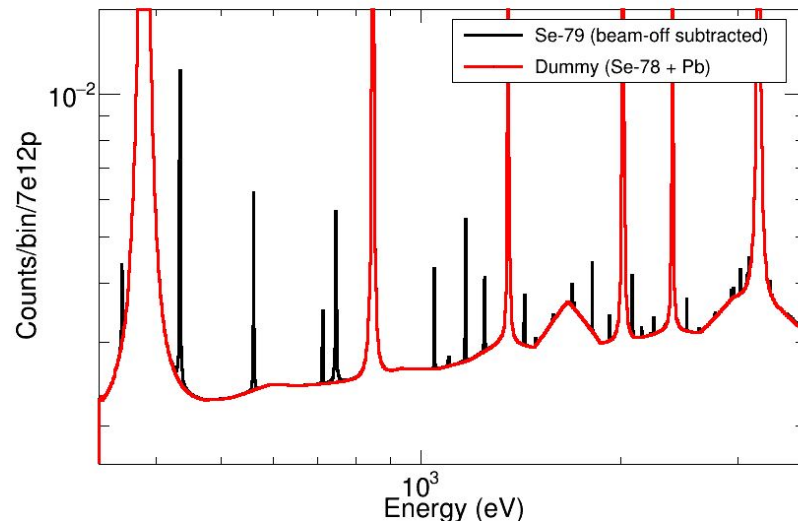


Theoretical estimation: After $1/v$ activity subtracted \rightarrow Total counts vs “dummy” sample
 i-TED: improved $^{79}\text{Se}(n,\gamma)$ /background above 100 eV
 Background due to $^{78}\text{Se}(n,n)$ and $^{79}\text{Se}(n,n)$ not included and also suppressed with i-TED

i-TED



C6D6

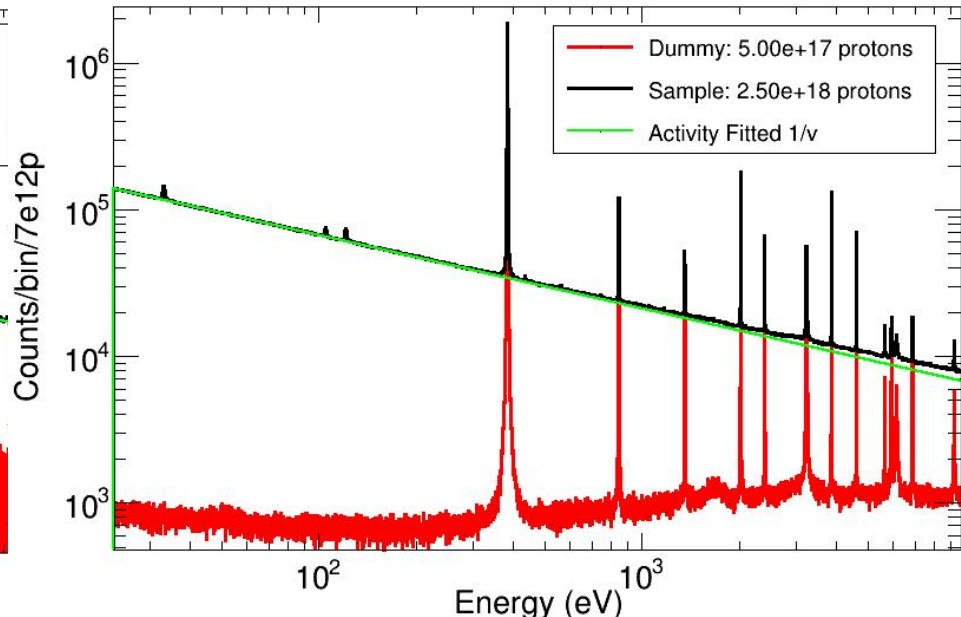
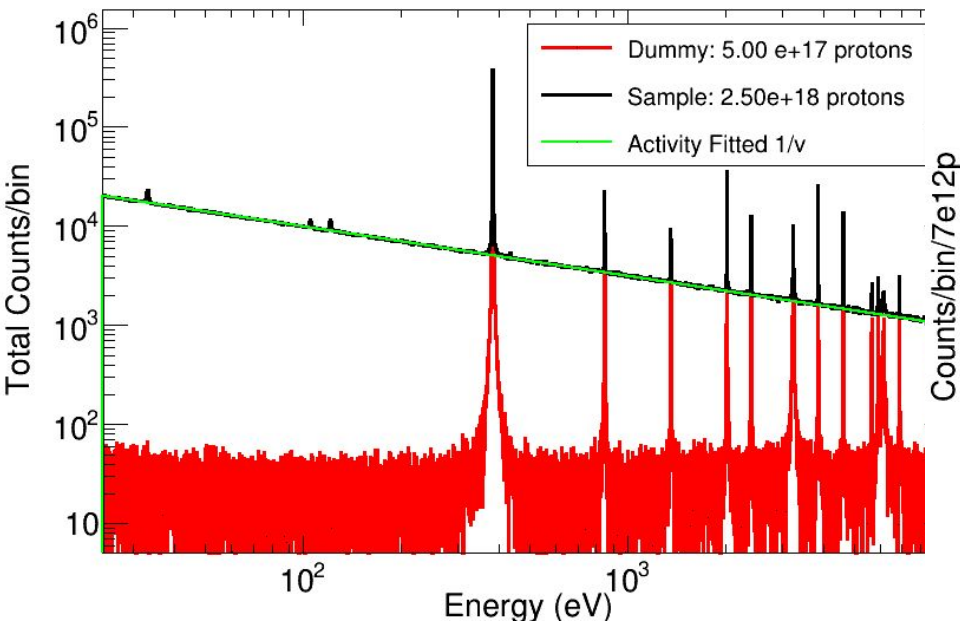


Theoretical estimation: After $1/v$ activity subtracted \rightarrow Total counts vs “dummy” sample
Reduction of the background in i-TED seems critical to observe ^{79}Se resonances,
Strength and level density may change (BASED IN TALYS)

PbSe sample: 2.5×10^{18} protons
Dummy: 0.5×10^{18} protons

i-TED

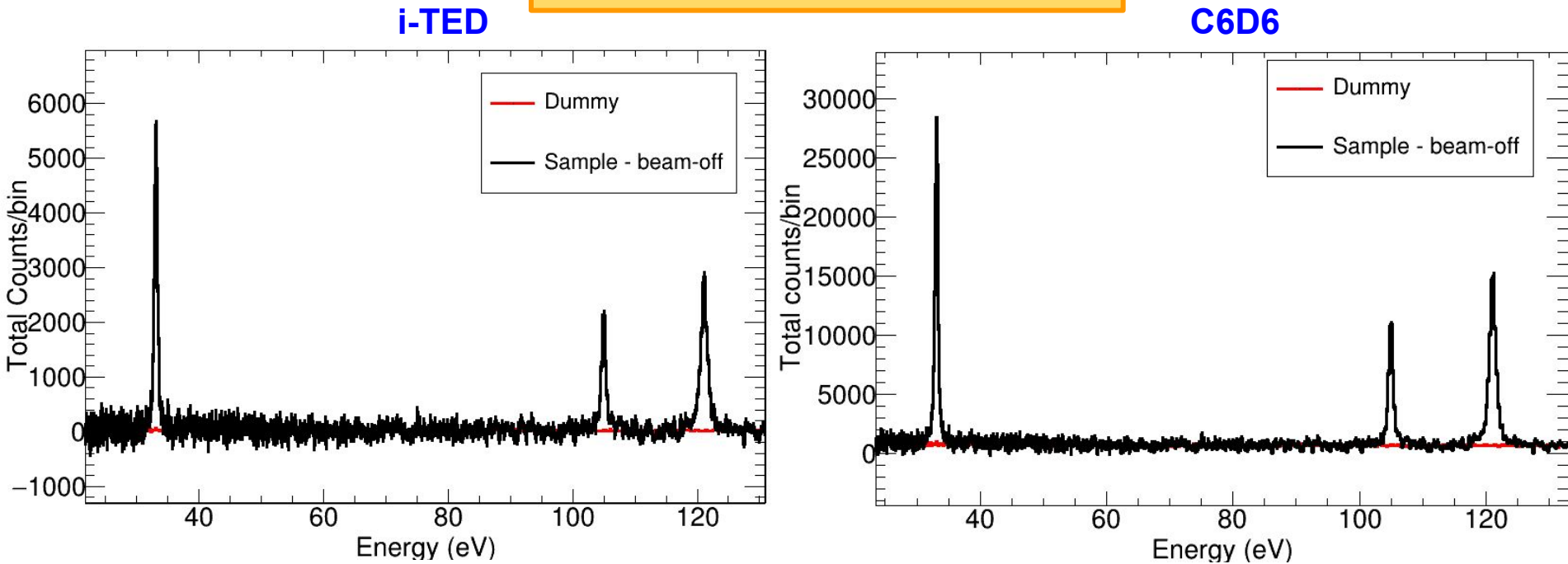
C6D6



MC simulation of the experiment: Realistic counts and statistical uncertainties

i-TED vs C6D6: reduction of activity background in 50% and the dummy in a factor ~ 5 relative to capture

PbSe sample: 2.5e18 protons
Dummy: 0.5e18 protons



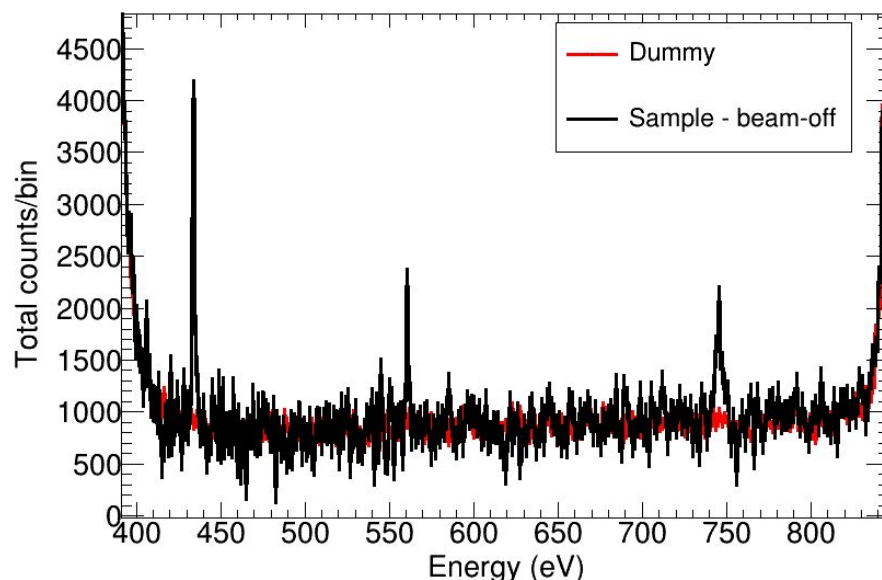
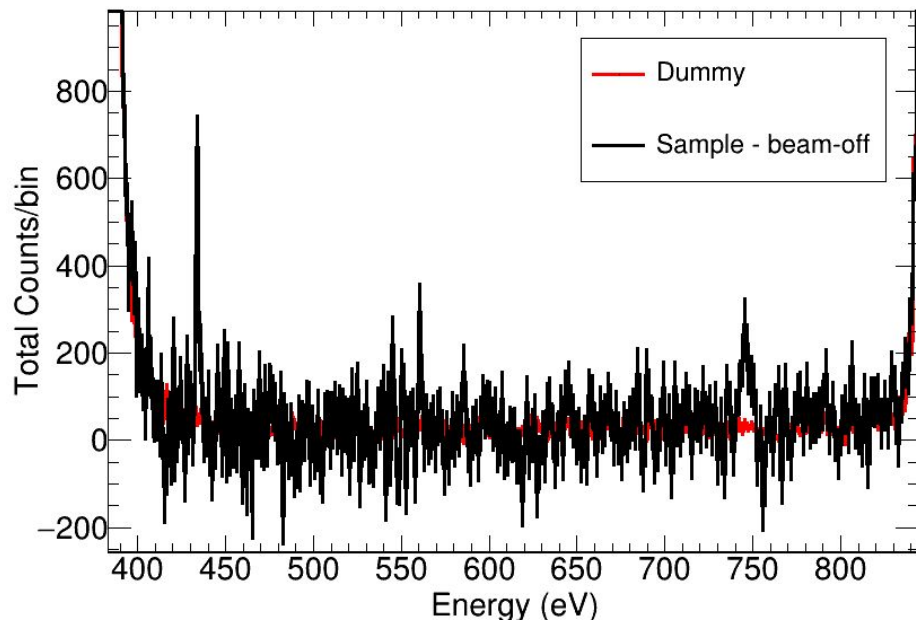
Largest resonances of ^{79}Se below 200 eV clearly observed

$^{79}\text{Se}(n,\gamma)$ @ EAR1 i-TED vs C6D6: RRR

PbSe sample: 2.5×10^{18} protons
Dummy: 0.5×10^{18} protons

i-TED

C6D6

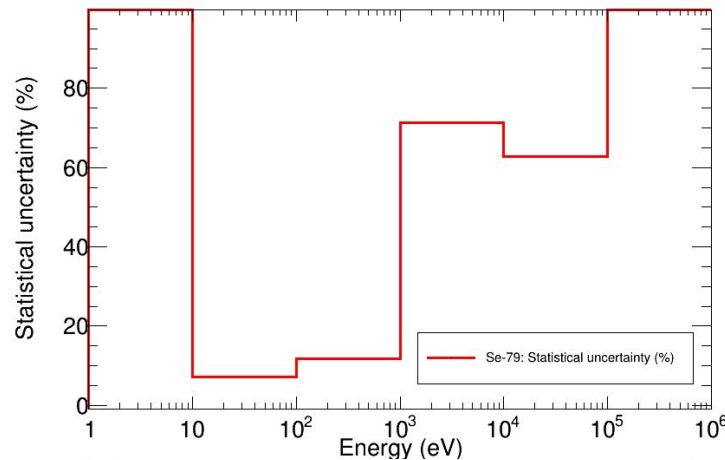


Possible to measure @ EAR1 the RRR below 1-2 keV
URR: complementary measurement at EAR2

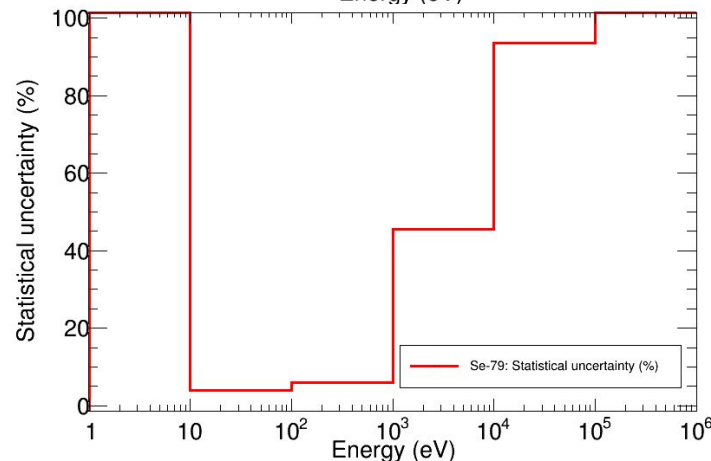
PbSe sample: 2.5×10^{18}
protons
Dummy: 0.5×10^{18}
protons

Statistical uncertainties in the $^{79}\text{Se}(n,\gamma)$ integral yield (1 bpd)

- Below 15% up to 1 keV (both setups)
- At higher energies: Uncertainty 50-70%. Very challenging to extract any cross section
- i-TED provides better uncertainty in above 10 keV \rightarrow better $^{79}\text{Se}(n,\gamma)$ /background



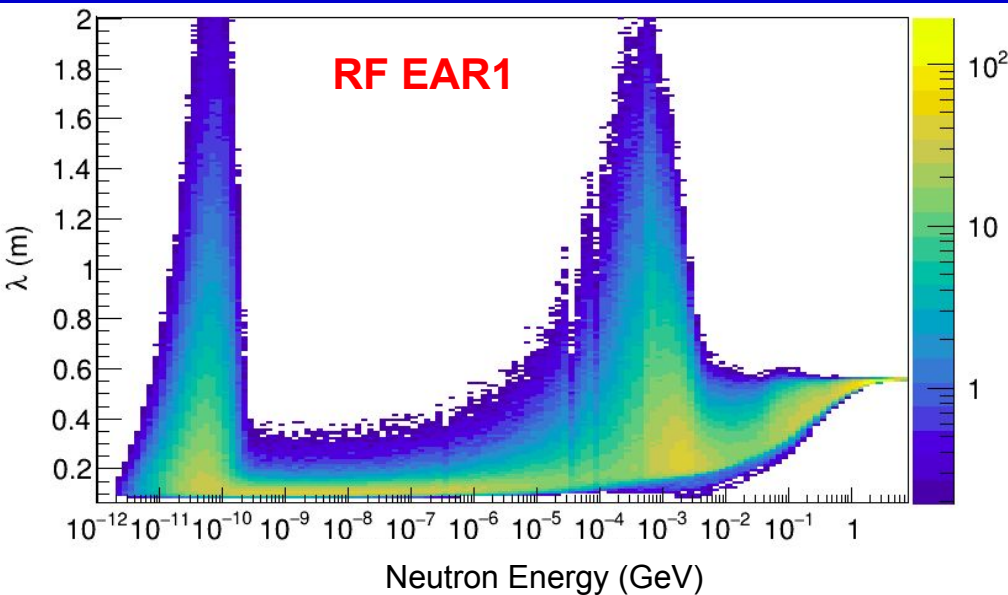
i-TED



C6D6

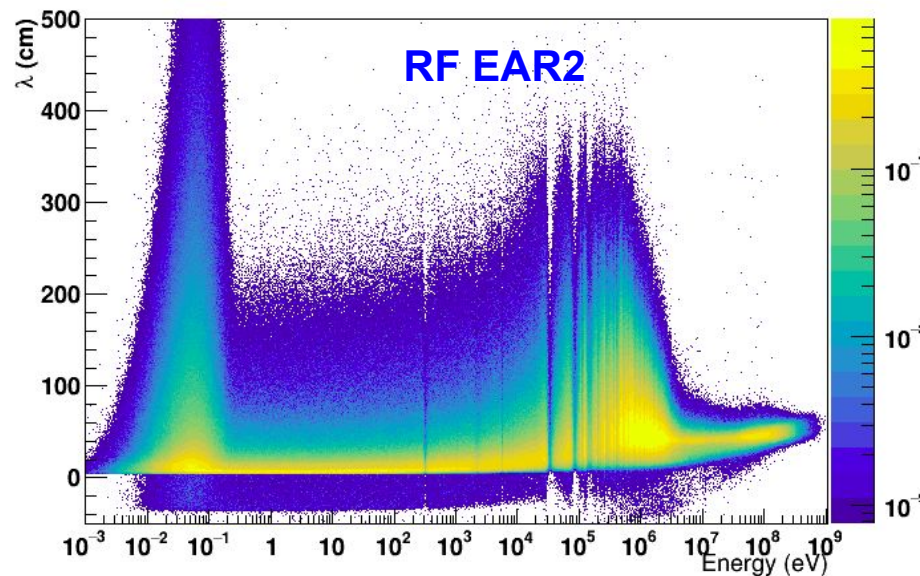
$^{79}\text{Se}(n,\gamma)$ @ n_TOF: Including RF

Resolution Function

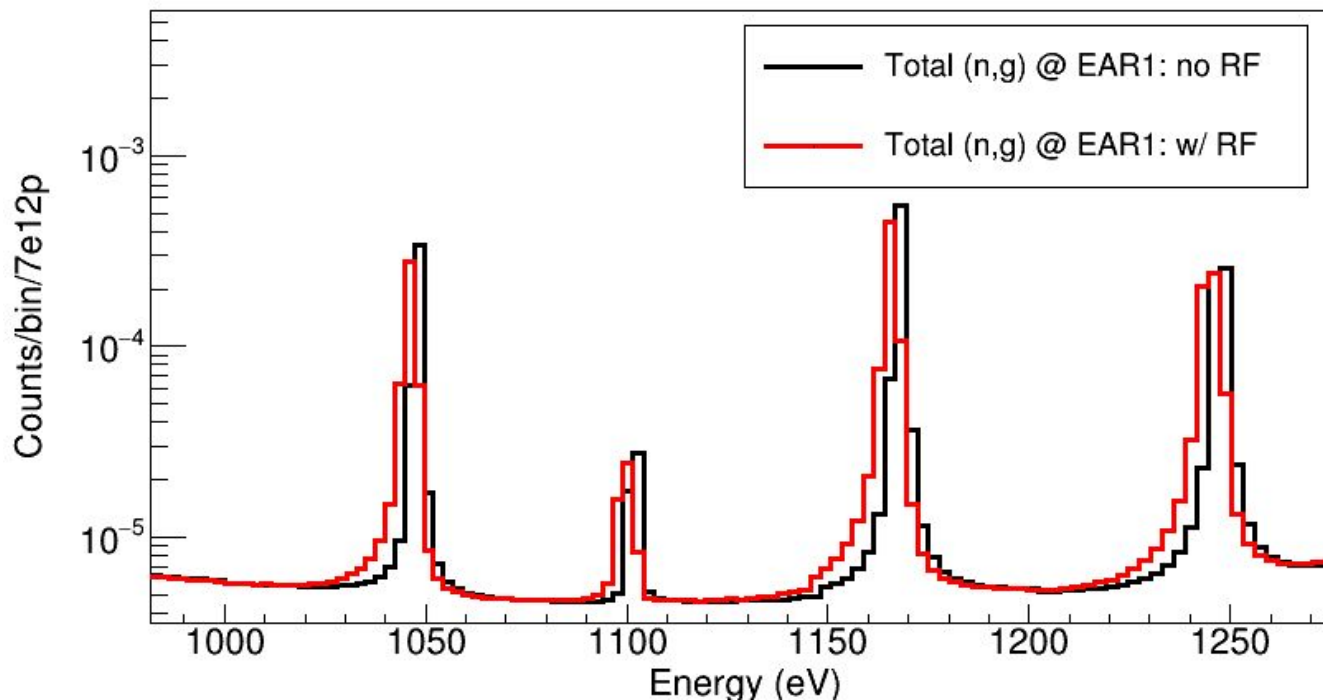


For a given real neutron Energy (E_n):

1. $L(E_n) = L_0 + \lambda(E_n) \rightarrow$ Flight path distribution
2. $TOF(E_n) = TOF(L(E_n)) \rightarrow$ TOF distribution
3. $E'(E_n) = E'(TOF(E_n)) \rightarrow$ Exp. Energy distribution



$^{79}\text{Se}(n,\gamma)$: Resolution Function



Shift resonance energy + broadening + asymmetry (low energy tail)

$^{79}\text{Se}(n,\gamma)$ thermal XS: Expected results

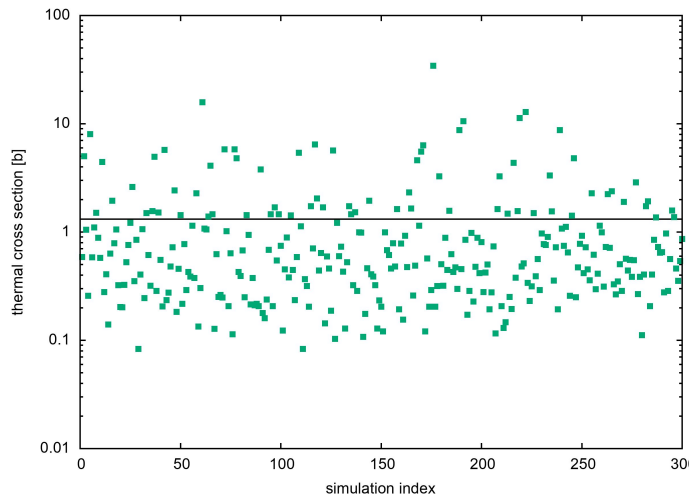
A. Mengoni's calculations:

300 sets of resonance using
average parameters in
TALYS:

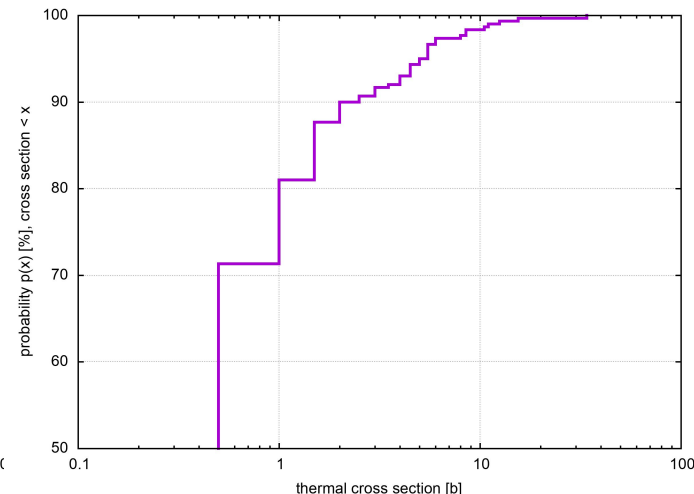
- $\langle D0 \rangle = 56.8 \text{ eV}$
- $S0 = 0.98 \times 10^{-4}$
- $\langle \text{Gamma}_g(0) \rangle = 0.078$
(+10%)

JEFF-3.3 (TENDL 2019)
uses $\langle \text{Gamma}_g(0) \rangle =$
0.100 meV

CALCULATED THERMAL XS



PROBABILITY SIGMA_TH



Calculation at thermal shows remarkable differences with evaluations

- Calculation: $P(\text{sigma_th} < 1\text{b}) = 80\%$ + $P(\text{sigma_th} < 10 \text{ b}) = 98\%$
- $\text{sigma_th} = 50 \text{ b}$ in ENDF/B-VIII.0
- $\text{sigma_th} = 11.8 \text{ b}$ in TENDL-2019

Realistic value thermal XS

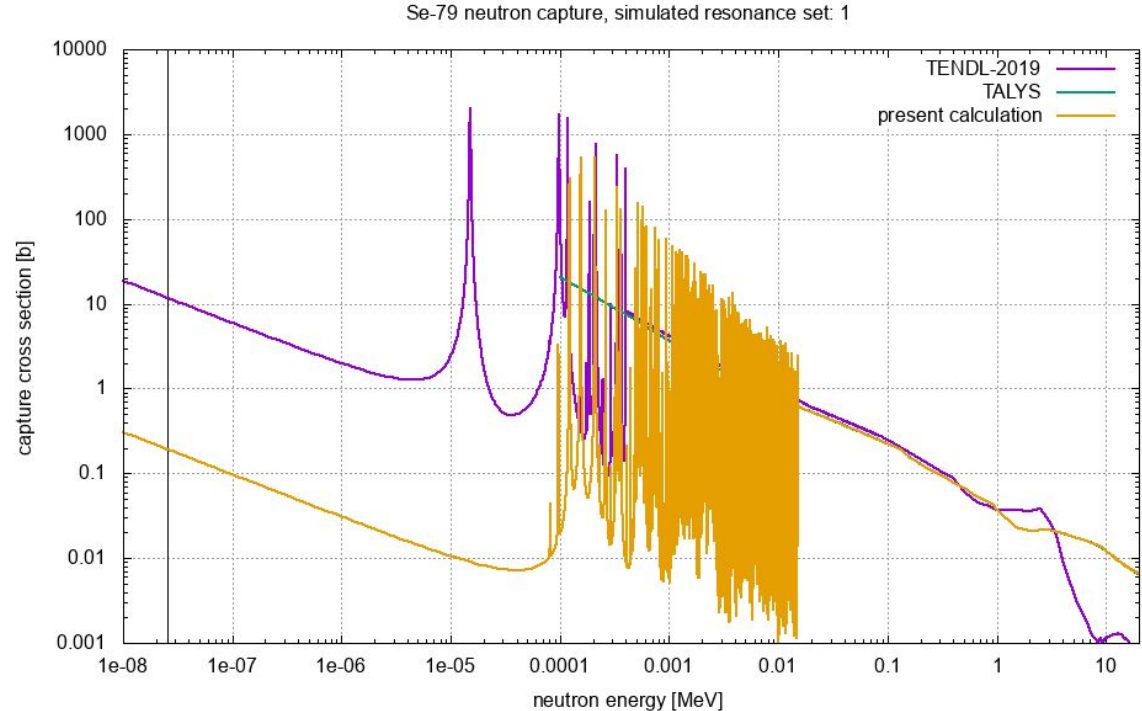
Calculation at thermal

shows remarkable differences with evaluations

- Calculation: $P(\sigma_{th} < 1b) = 80\% + P(\sigma_{th} < 10 b) = 98\%$
- $\sigma_{th} = 50 b$ In ENDF/B-VIII.0
 $\sigma_{th} = 11.8 b$ in TENDL-2019

Two scenarios:

- Thermal XS follows systematics \rightarrow Measurable
- Much smaller \rightarrow Lower limit constrained from RRR



Realistic value thermal XS

Systematics:

- Odd-Even isotopes in that mass range:
 - Se-77: 42(4) b
 - Br-79: 10.32(13) b

**THERMAL NEUTRON CAPTURE CROSS SECTIONS
RESONANCE INTEGRALS AND G-FACTORS**
<https://www.osti.gov/etdeweb/servlets/purl/20332542>

Evaluations:

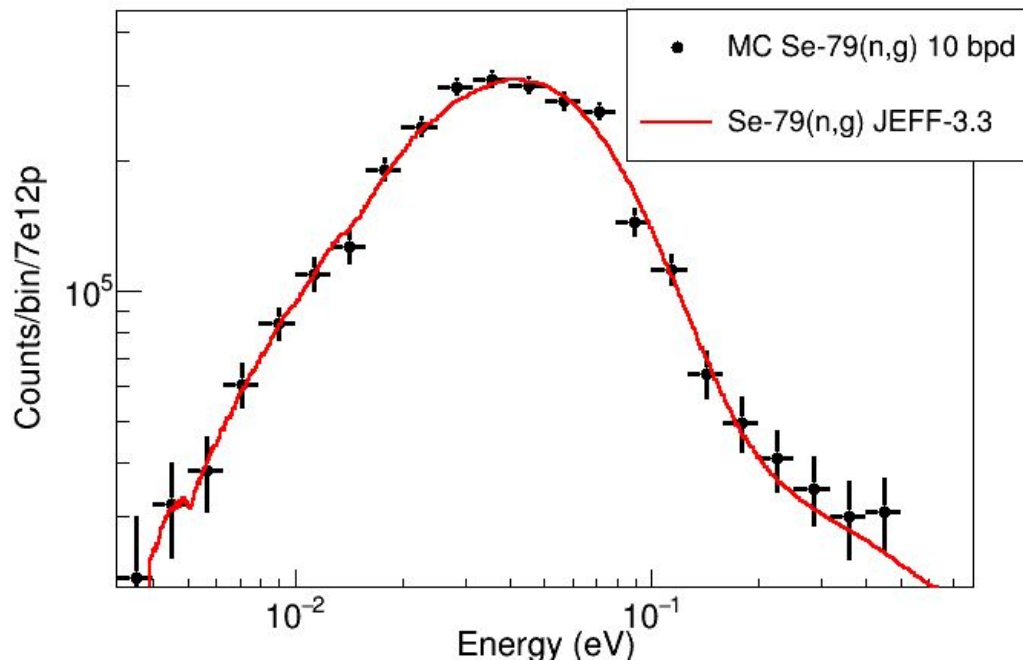
- **sigma_th = 50 b in ENDF/B-VIII.0**
(THE THERMAL CAPTURE CROSS SECTION WAS DETERMINED BY THE SYSTEMATICS FROM THE NEIGHBORING SE ISOTOPES)
- **sigma_th = 10.97 b in JEFF-3.3 (TENDL-2015)**
NO INFORMATION IS GIVEN

Contribution of direct capture and/or negative resonances seems to be much larger than the 100 mb - 1b expected from the tails of the positive resonances

Thermal XS: statistical & systematic unc

- **Input cross sections:**
 - JEFF-3.3
 - ENDF/B-VIII.0
- **MC Resampling: proton distribution**
 - S: 1.5e18 p+ D: 0.5e18p
 - S: 1e18p + D: 1e18p
- **Experimental Approaches**
 - **Method A: Sample:** Se-78 + ⁷⁹Se + **Dummy** (Al + Pb) → Syst unc in dummy (0.5%) + Syst unc in Se-78 thermal XS (5%)
 - **Method B:** Se-78 + ⁷⁹Se + **Dummy (Al + Pb + Se-78)** → Syst unc in dummy (0.5%)

Thermal XS: statistical uncertainty



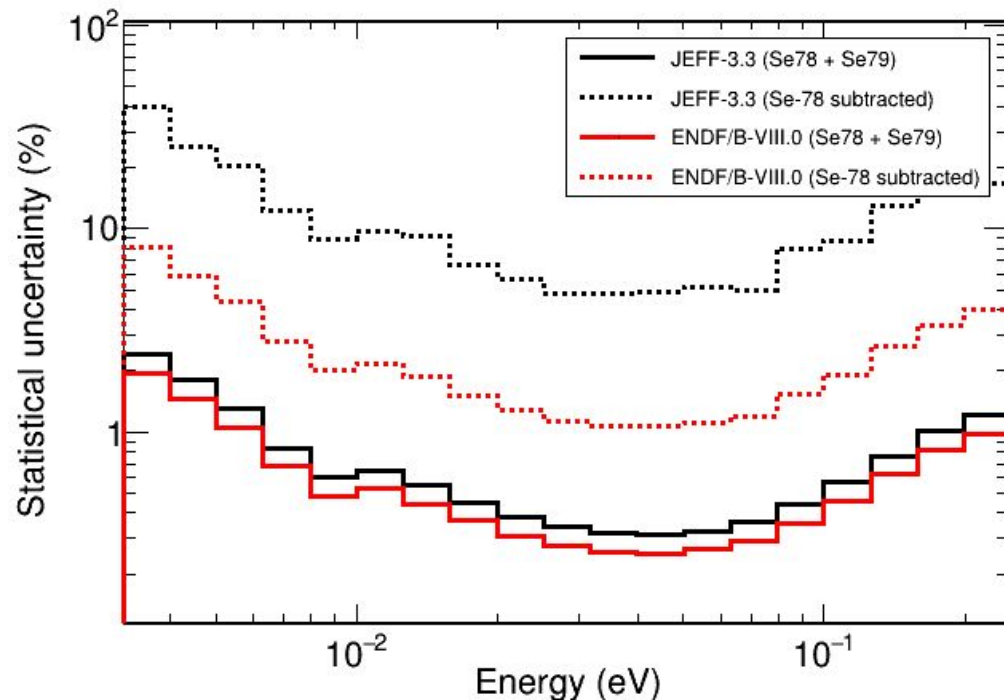
Method B:

Se-78 measured as part of the dummy and subtracted.

Thermal XS extracted as the integral of the Se-79 contribution in the bin containing $E_n = 25.3$ meV

Statistical uncertainty of Se-79 after Se-78 contribution is subtracted depends on the final XS and the binning → LET's evaluate it for the different evaluations

Thermal XS: statistical uncertainty



MC experiment @ EAR2:

10 bpd

Sample: 1.5×10^{18} p

Dummy : 0.5×10^{18} p

Statistical uncertainty per bin

- **Se-78+79Se (i.e. Al+ Pb Dummy) :**
< 1% (dominated by Se-78)
- **79Se (Se-78 + Al + Pb dummy subtracted):**
2-10% depending on the value of the thermal XS

Thermal XS: systematic unc.

Contribution of the different (n,g) and background components at thermal

MOST CHALLENGING FOR THE THERMAL CROSS SECTION: SYSTEMATIC UNC. IN THE DUMMY

OPTIONS FOR THE THERMAL XS:

OPTION A) Dummy and Se-78 measured alone

Se-78 measured alone + normalized to resonances + subtracted: NO systematic unc. in mass & XS

Subtract dummy: more difficult to subtract with negligible syst. Uncertainty : Same Al and lead mass + shape of sample.

OPTION B) Produce and measure a full dummy

Make a full dummy (with Se-78 with exactly the same Al casing and PbSe mass → normalization to Se-78 resonances should apply for the full dummy)

Dummy ~ 90% of the counts →
Could be reduced with i-TED

$^{78}\text{Se} + ^{79}\text{Se}$ ~10 % counts of which ^{79}Se :
7% (JEFF-3.3) - 30% (ENDF)

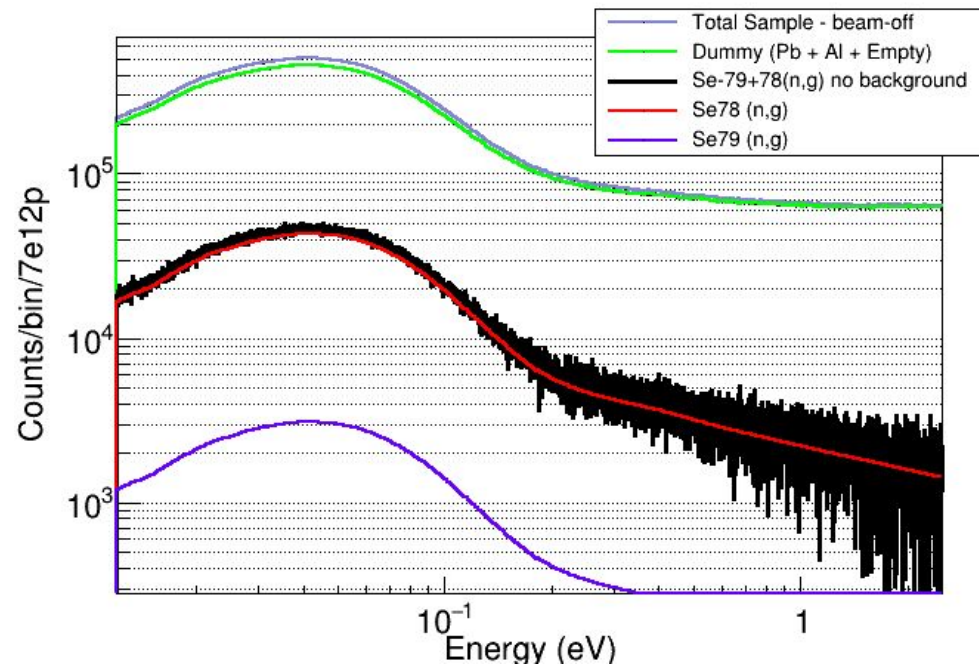
^{79}Se ~ 1 - 3 % of the total counts → 0.5%
syst unc in the dummy → 17 to 50 % syst
unc in the ^{79}Se thermal XS.

The level of the syst. Unc will depend on:

- Degree of background rejection
- Syst. unc in the dummy
- Both are uncertain → we can do a rough estimate

Thermal XS: systematic unc.

EXAMPLE : JEFF-3.3



MC experiment:

10 bpd

Sample: 1.5×10^{18} p

Dummy : 0.5×10^{18} p

Dummy $\sim 90\%$ of the counts \rightarrow
Could be reduced with i-TED

$^{78}\text{Se} + ^{79}\text{Se} \sim 10\%$ counts of which ^{79}Se :
7% (JEFF-3.3) - 30% (ENDF)

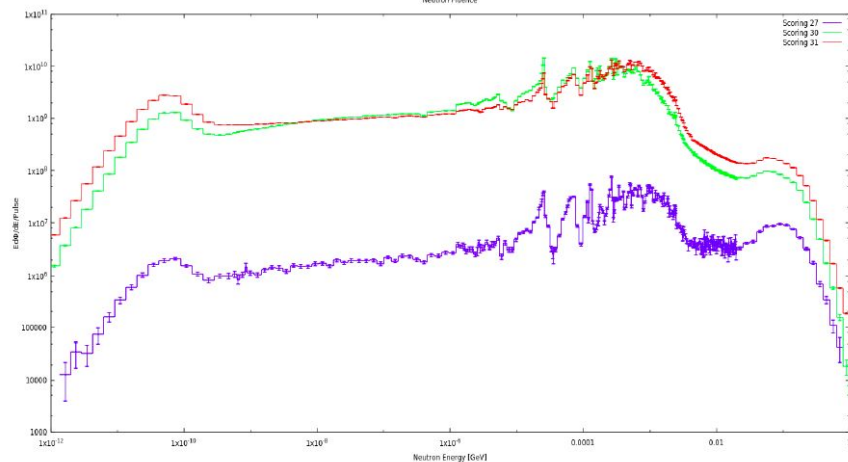
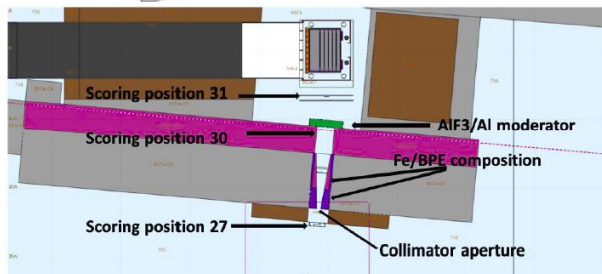
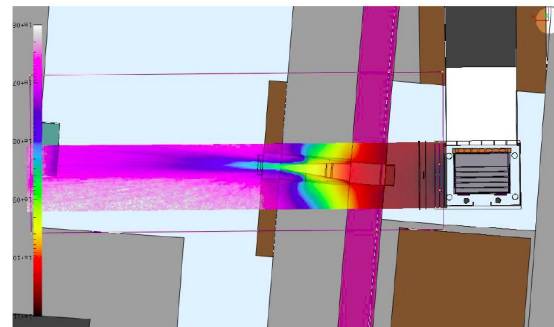
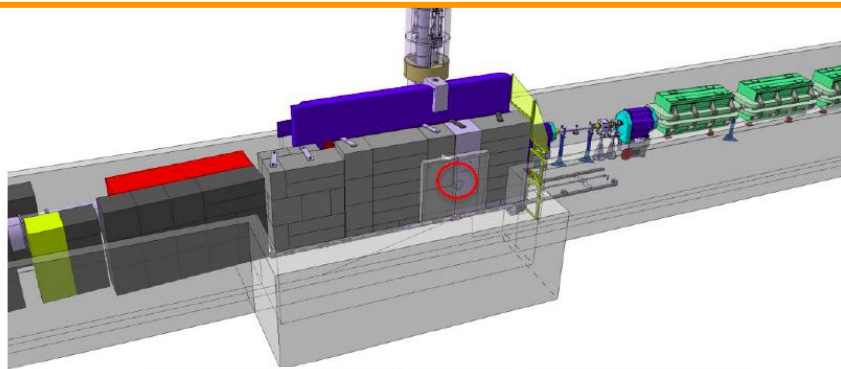
$^{79}\text{Se} \sim 1 - 3\%$ of the total counts $\rightarrow 0.5\%$
syst unc in the dummy $\rightarrow 17$ to 50% syst
unc in the ^{79}Se thermal XS.

The level of the syst. Unc will depend on:

- Degree of background rejection
- Syst. unc in the dummy
- Both are uncertain \rightarrow we can do a rough estimate

Future plans: Measuring the MACS @ n_TOF-NEAR

This new station (NEAR Station) at less than 3 meters from the target module, with **strongly enhanced neutron fluence**



New record in neutron fluence
(10^2 (27) - 10^4 (31) higher than to n_TOF-EAR2)

First step: Commission flux

^{94}Nb , ^{79}Se RADIOACTIVE ISOTOPES:
DIFFICULT TO PRODUCE ENOUGH MASS

SAMPLES PRODUCED @ ILL/PSI and (n,g) TOF
measurements at n_TOF Proposed for 2022



**FUTURE PLANS: MEASURE THESE UNIQUE
SAMPLES IN THE FUTURE NEAR FACILITY**

^{94}Nb

Activation
(^{95}Nb unstable)

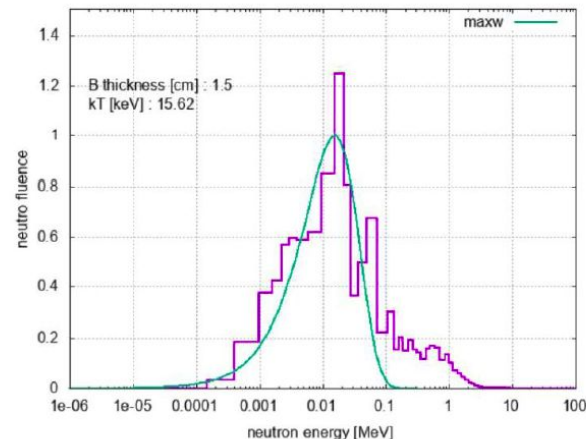
^{79}Se

ICP-MS/AMS
(^{80}Se stable)

GOALS:

- 1) Direct measurements of the MACS at different kT
- 2) Complementary to measurement of the resonances at n_TOF
- 3) Validation of the empirical method to determine the MACS from Resonances.

**Shape
the flux
to stellar
maxwell.**



**Challenging
becomes
feasible
with short
beam times**

